

DESIGN AND PERFORMANCE EVALUATION OF A  
SOLAR CONCENTRATOR AND RECEIVER SYSTEM  
AND ITS APPLICATIONS

THESIS

Submitted in partial fulfilment  
of the requirement for the degree of  
DOCTOR OF PHILOSOPHY

BY

NIRANJAN KUMAR MANDAL

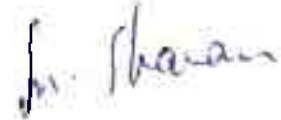
BIRLA INSTITUTE OF TECHNOLOGY AND SCIENCE  
PILANI (RAJASTHAN) INDIA

1993

BIRLA INSTITUTE OF TECHNOLOGY AND SCIENCE  
PILANI RAJASTHAN

CERTIFICATE

This is to certify that the thesis entitled "DESIGN AND PERFORMANCE EVALUATION OF A . SOLAR CONCENTRATOR AND RECEIVER SYSTEM AND ITS APPLICATIONS" submitted by NIRANJAN KUMAR MANDAL ID No. 88 PHXF405 for award of Ph.D. Degree of the Institute, embodies original work done by him under my supervision.



Date: 28.7.93

Dr. SHIVENDRA NATH SHARAN  
Asstt. Prof.,  
Department of Electrical and  
Electronics Engineering

## A C K N O W L E D G E M E N T S

The author expresses his gratitude to Dr. S.N. Sharan for his efficient guidance and encouragement during the whole work of the Ph.D Thesis.

The author sincerely thanks to Dr. S. Venkateswaran, the Director of the Institute for permitting him to persue Ph.D. and providing the necessary facilities for the work.

The author expresses his thank to Dr. G.P. Avasthi, the Dean FD-I for his continuous encouragement and permission to perform some experimental works on the roof in C - Block. He also expresses his sincere thanks to Dr. L.K. Maheshwari, Dean, Research and consultancy, for his continuous encouragement and evaluation of the progress in his Ph.D. work.

The author is thankful to Dr. PSVSK Raju, Chief, IPC, for providing computer facilities for the work. He is also thankful to prof. K.E. Raman, Chief Instrumentation, for permitting him to get the word processing done for the work in the Reprography Section.

The author is thankful to Mr. S.D. Dewan for neat tracing and to Mr. Rohitash Kumar for excellent word processing of this thesis.

The author also takes this opportunity to express his sincere thanks to his parents in law and elder brothers and other relatives for their continuous encouragements during the whole work.

Lastly, the author puts on record the help and co-operation in each step by his wife Mrs. Tanusri and the pleasant atmosphere provided by his two beloved daughters Ranjusri and Srayasri.

Engineering Technology Group

3/9/93  
Date:

  
(N.K. Mandal)

## C O N T E N T S

|   | Page<br>No. |
|---|-------------|
| <u>CHAPTER-I</u> : Review on solar concentrator and receiver system and its applications. | 1           |
| 1.1 Introduction  | 2           |
| 1.2 Solar Concentrators   | 3           |
| 1.2.1 Classification of Solar Concentrators   | 7           |
| 1.2.2 Point focussing concentrators   | 8           |
| 1.2.2.1 Dish type concentrator  | 8           |
| 1.2.2.2 Compound Parabolic concentrator   | 9           |
| 1.2.2.3 Circular Fresnel Lens   | 10          |
| 1.2.2.4 Segmented mirror Reflectors   | 10          |
| 1.2.2.5 Central Tower Receiver system   | 11          |
| 1.2.3 Line Focussing Concentrators:   | 13          |
| 1.2.3.1 Cylindrical Parabolic trough  | 13          |
| 1.2.3.2 Composite parabolic trough  | 14          |
| 1.2.3.3 Linear Fresnel Reflector  | 15          |
| 1.2.4 Line focussing with limited extent:   | 15          |
| 1.2.4.1 Conical concentrator  | 15          |
| 1.2.4.2 Hemi - spherical Bowl.  | 16          |
| 1.3 Solar Steam generators - Case studies.  | 16          |
| 1.3.1 Experimental setup of solar boiler developed in Austria (1854-1873)                 | 16          |
| 1.3.2 Solar boiler developed in France (1860-1878)  | 17          |
| 1.3.3 Solar steam generating system, developed in Bombay, India (1876-1878).              | 18          |

|  | Page No. |
|--|----------|
| 1.3.4 Eneas solar steam generating system developed in California (1901)                               | 18       |
| 1.3.5 Solar steam generating system developed by C. Abbot in 1936.                                     | 19       |
| 1.3.6 Solar steam generator developed in C.S. Draper Laboratory (1970)                                 | 19       |
| 1.3.7 Solar concentrator/cavity receiver system developed by James A. Harris and Terry G. Lenz (1985). | 19       |
| 1.3.8 Solar steam generating system installed in a silk weaving factory, Bangalore, India (1992)       | 20       |
| Application of solar steam generator to produce electric power-case studies.                           | 20       |
| 1.4.1 Goddard's solar-electric power plant (1919)  | 20       |
| 1.4.2 Francia's solar powered plant at St. Ilario-Nervi, Genoa, Italy (1956-68)                        | 21       |
| 1.4.3 Sunshine project in Japan (1974-81)  | 21       |
| 1.4.4 Solar thermal electric power plants for Iran (1985)  | 21       |
| 1.4.5 100 $KW_e$ /700 $KW_{th}$ Co-generation solar power plant in Kuwait (1986)                       | 22       |

|  | Page<br>No. |
|--|-------------|
| 1.4.6 5 KW Solar thermal power plant developed in Sardar Patel Renewable Energy centre, Gujrat, India, for electric power generation and water pumping for irrigation (1987) | 23          |
| 1.4.7 Solar thermal electric power plant installed in Gurgaon, Haryana (1989-92).  | 23          |
| 1.5 Application of solar steam generating system to lift water for irrigation.   | 23          |
| 1.5.1 Solar steam engine developed by Ericsson in Newyork (1870-86).   | 23          |
| 1.5.2 Sun-power plant to run a printing press and a rotary water pump developed in France (1878).  | 24          |
| 1.5.3 Solar powered water pumping system in Auteulli, France (1885).   | 24          |
| 1.5.4 Solar steam generating plants developed between 1905 and 1908 in California, to drive irrigation pump.   | 25          |
| 1.5.5 Shuman's solar steam engines for irrigation (1906 to 1911)   | 25          |
| 1.5.6 A large solar powered-irrigation plant developed in 1913 in Meadi, Egypt.  | 26          |
| 1.5.7 Solar steam engine developed in New Mexico for pumping water (1920).   | 27          |
| 1.5.8 Solar steam generating system for solar engine developed by Molero of Soviet Union (1941-46).  | 27          |

|   | Page<br>No. |
|---|-------------|
| 1.5.9 Solar installation developed in National Physical Laboratory, Israel (1967)                                     | 27          |
| 1.5.10 Solar steam engine developed by Masson and Giradier in Dakar, Senegal (1962-1966)                              | 28          |
| 1.5.11 Sofrete's solar-powered water pumping plant in Guanajuato, Mexico (1969)                                       | 28          |
| 1.5.12 Battelle Memorial Institute Built solar powered pumping plant, Gilla Bend, Arizona (1977).                     | 28          |
| 1.5.13 Sandia Laboratories built solar-powered pumping installation (Willard, New Mexico, 1985).                      | 29          |
| 1.5.14 An Autonomous Combined Solar System for heating, cooling and Water supply developed in Odessa, Ukraine (1992). | 29          |
| <u>CHAPTER-II</u> : Analysis and modelling of a solar concentrator-receiver system.                                   | 35          |
| 2.1 Introduction  | 36          |
| 2.2 Analysis  | 37          |
| 2.2.1 Mathematical modelling  | 37          |
| 2.3 Results and Discussion.   | 44          |
| <u>CHAPTER-III</u> : Analysis of a solar thermal electric power generating system.                                    | 51          |
| 3.1 Introduction  | 52          |
| 3.2 Analysis and modelling  | 53          |
| 3.3 Economic analysis of a solar thermal electric power generating system.  | 55          |
| 3.4 Results and Discussions.  | 58          |



|  |     |
|--|-----|
| <u>CHAPTER-IV</u> : Analysis of a combined system consisting of a solar steam generator and a water pumping system for irrigation. | 65  |
| 4.1 Introduction   | 66  |
| 4.2 Analysis and modelling   | 67  |
| 4.3 Econometric model  | 69  |
| 4.4 Results and Discussion.  | 71  |
| <u>CHAPTER-V</u> : Experiments on a solar thermal concentrator-receiver system.  | 78  |
| 5.1 Introduction   | 79  |
| 5.2 Test setup   | 79  |
| 5.2.1 Linear composite parabolic concentrator  | 79  |
| 5.2.2 Receiver   | 80  |
| 5.2.3 Arrangement for circulating water through the receiver   | 80  |
| 5.2.4 Measuring Instruments  | 81  |
| 5.3 Test Procedure   | 81  |
| 5.4 Results and Discussions  | 83  |
| <u>CHAPTER - VI</u> : Conclusion   | 99  |
| References   | 103 |
| List of publications   | 107 |
| APPENDIX :   | 109 |

|   | Page<br>No. |
|---|-------------|
| A1 : Evaluation of overall heat transfer coefficient ( U )                    | 110         |
| A2 : Linearized heat transfer coefficient for convection and radiation ( C ). | 111         |
| A3 : Computer Programming and results for the Chpters II - V.                 | 113         |

CHAPTER -I  
-----

Review on solar concentrator and receiver system and its  
application

## CHAPTER - I

### 1.1 INTRODUCTION:

Solar concentrator and receiver systems, using linear solar concentrators, have been given importance for the last many years. Some important applications of solar concentrator - receiver systems already reported in some research papers [1-6] are - production of electricity by an electrical generator coupled to a steam turbine, driving of steam turbine or steam engine along with a centrifugal pump to lift water for irrigation and driving of a steam engine to run a printing press, etc. In the above systems, fluids with low boiling point, such as ammonia, ether etc. have been taken as primary fluid and water as secondary heat transfer fluid. However, water may also be used as primary heat transfer fluid if steam is required to be produced. Steam can be produced using highly concentrated solar radiation which can easily be achieved using solar-concentrator receiver system. Two common ways of developing concentrated radiation have been explored viz. the glass lens and the reflectors. These devices concentrate the solar radiation to focal plane. If a receiver is placed on the focal plane which receives concentrated radiation, then the temperature of the receiver is increased considerably. The temperature of the receiver can easily be controlled by the concentration factor and the mass flow rate of the working fluid passing through the receiver.

In this chapter, a rigorous effort has been made to review the works done on various aspects of concentrator - their geometries and performances, applications of the concentrators for producing super saturated steam and then the application of super saturated steam, thus produced in generating electricity and driving water pumps, etc.

## 1.2 SOLAR CONCENTRATORS:

Solar concentrators are the collectors which are designed to condense the large amount of solar radiation upon a relatively small absorber area. Solar energy collection at high temperature can be achieved with the help of concentrator which focusses the solar radiation collected over a large area to a much smaller area, where it is absorbed. Not only high temperature of energy collection is possible by this method, but also the heat loss from the absorber is reduced considerably due to small heat transfer area of the receiver in contact with the ambient air. Since, a solar concentrator is an optical system, it is necessary that it faces the sun at all times in order to focus the maximum solar flux on the absorber surface. The essential components of a solar concentration receiver system therefore, are:

i) an optical device to focus solar radiation, and ii) an absorber. However, in case of a concentrator-receiver system designed for normal incident of flux on the aperture plane of the concentrator, the system is also provided with a tracking system. In the recent years, many developments in design and use of solar concentrators have been reported [5-7]. The conventional imaging reflecting and/ or refracting devices have found applications in

both the line focus and the point focus geometries.

A concentrator is characterized by the following parameters:

i) Aperture area: It is the plane area through which the incident solar flux is accepted and is defined by the physical extremities of the concentrator.

ii) Absorber area: The total area that receives the concentrated solar flux. It is the area from which the useful energy can be obtained.

iii) Acceptance angle: The limit to which the incident ray path may deviate from the normal drawn to the aperture plane and still reach the absorber, is defined as the acceptance angle.

iv) Local concentration ratio: It is defined as the ratio of the flux arriving at any point of the receiver to the incidence flux at the aperture of the concentrator.

v) Geometrical concentration ratio: It is defined as the ratio of the aperture area ( $A_a$ ) of the concentrator to the area of its absorbing surface ( $A_{abs}$ ) ie.

$$R = A_a / A_{abs} \quad (1.1)$$

It represents the maximum factor by which solar radiation can be increased on the receiver surface.

vi) Intercept factor: It is <sup>the</sup> fraction of the total available radiation energy received by the absorber. For the line focussing concentrator it is defined as

$$\frac{\int_{-W/2}^{W/2} I(x) dx}{\int_{-r}^{r} I(x) dx} \quad (1.2)$$

Where,  $I(x)$  is the intensity of radiation received at a distance ' $x$ ' from the focal line of the concentrator in the focal plane and ' $W$ ' is the width of the receiver.

vii) Optical efficiency: The optical efficiency ( $\eta_0$ ) of the system is defined as the ratio of the energy absorbed by the receiver to the energy incident at the collector aperture. It depends on reflection or refraction loss, inaccuracy in tracking the sun, shading of the aperture by the absorber and mounting systems, intercept factor, transmittance of cover (for the absorber) material and emittance of the absorber.

viii) Thermal efficiency: The thermal efficiency ( $\eta_{th}$ ) of a concentrator is defined as the fraction of the incident beam energy effectively delivered by the concentrator, i.e.

$$\begin{aligned} \eta_{th} &= \frac{q_u}{I_b A_a} \frac{T_{abs} - T_a}{T_{abs} - T_a} \\ &= \eta_0 - \frac{U_L}{I_b (A_a / A_{abs})} \frac{T_{abs} - T_a}{T_{abs} - T_a} \\ &= \eta_0 - \frac{U_L}{I_b C} \frac{T_{abs} - T_a}{T_{abs} - T_a} \end{aligned} \quad (1.3)$$

Where,

- $q_u$  = Useful energy
- $I_b$  = Solar beam flux
- $U_L$  = Overall heat loss coefficient
- $T_{abs}$  = Average temperature of the absorber

$T_a$  = Ambient temperature  
 $\eta_o$  = Optical efficiency

Limit of concentration:

The maximum geometrical concentration ratio that can be achieved by a concentrator depends upon the angle of acceptance for which it is designed. It is given by:

$$C_{\max} = \frac{1}{\sin^2 \theta_m}, \text{ for a point focussing system} \quad (1.4)$$

$$\text{and } C_{\max} = \frac{1}{\sin \theta_m}, \text{ for a line focussing system} \quad (1.5)$$

However, because of finite size of the sun, every concentrator must have a minimum acceptance angle of 16' which is half the subtense angle of the sun on the earth. The limiting concentration possible for the two types of concentrators are about 45,000 and 200 respectively.

Concentration ratio and operating temperature:

Concentrators are usually used for high temperature collection of solar energy. Under this condition, radiation loss is most dominant. For sake of simplicity, the heat loss ( $q_{\text{loss}}$ ) can be written as

$$q_{\text{loss}} = U_L (T_{\text{abs}}^4 - T_a^4) A_{\text{abs}} \quad (1.6)$$

Where,  $U_L$  = Effective heat loss coefficient

If  $T_{\text{abs}}^4 \gg T_a^4$ , then the equation (1.6) becomes

$$q_{\text{loss}} = U_L T_{\text{abs}}^4 A_{\text{abs}} \quad (1.7)$$



If  $\epsilon$  be the emissivity of the absorber and  $\sigma$  be the Stefan's constant, then the heat loss ( $q_{loss}$ ) can be written as,

$$q_{loss} = \sigma \epsilon T_{abs}^4 A_{abs} \quad (1.8)$$

### 1.2.1 CLASSIFICATION OF SOLAR CONCENTRATORS:

Solar concentrators may be broadly classified into three categories, namely,

- i) point focussing,
- ii) line focussing, and
- iii) line focussing of limited extent.

Each category, may be i) a reflecting or refracting type ii) single piece or composite optical surface type, iii) tracking or non-tracking iv) imaging or non-imaging and v) single stage or two stage type solar concentrators.

Practically, all point focussing concentrators require two-axis tracking. They have circular symmetry and are generally used when high concentration ratio is required. A circular fresnel lens, paraboloid of revolution and the central tower receiver system are the examples of this category. Line focussing linear concentrators have cylindrical symmetry and are generally used when the concentration ratio is sufficient in the intermediate range. A cylindrical parabolic trough, etc. belong to this category.

A third type of the solar concentrators also exist which produce a line focus of limited extent. The truncated cone or axicon, the hemi-spherical bowl mirror belong to this class of concentrators. There are some other miscellaneous concentrator designs which

can<sup>not</sup> be grouped into either of the categories of concentrators earlier described. These designs include a catchall type collector, chromatic dispersion concentrator, dispersive concentrating systems based on transmission phase holograms, a quasi cylindrical array of plane mirrors and an array of independently steered mirrors on a single frame, etc.

Among the various designs of solar concentrators, the commonly used concentrators in the generation of solar steam to produce electric power and other applications, include parabolic trough [8], dish type concentrators such as parabolic dish or paraboloid of revolution or by a spherical dish [9], Fresnel lens, segmented mirrors and heliostat used in central tower receiver system, etc.

#### 1.2.2 POINT FOCUSING CONCENTRATORS:

##### 1.2.2.1 DISH TYPE CONCENTRATOR:

Dish type concentrators have the advantage of higher concentration of solar intensity at off noon hours (Fig.1.1 ). Two-dimensional tracking is required to obtain high performance.

An intriguing approach has been proposed by J. Reichert of Texas Tech. University, in which large dish of about 200 ft. diameter is built into the ground to resemble a football stadium. Unlike the smaller dishes, which are paraboloids of revolution, the large dish has been proposed as a spherical mirror. The paraboloid has theoretical property that it will focus parallel light into single focal point. However, the paraboloid must be rotated to make it co-axial with the solar rays. The dish proposed by Reichert utilizes a fixed spherical lens and

movable receiver and has been called the FMDF (fixed mirror/diffuse focus) collector. In principle, the optics of a paraboloid is far superior to the optics of a spherical lens.

The concentration ratio for a paraboloid can be determined easily from the basic geometry but depends on the shape of the absorber. For a spherical absorber, it is given by

$$C_{\text{sph}} = \frac{\sin^2 \phi}{4 \sin^2 \frac{\phi}{2}} \quad (1.9)$$

Maximum concentration is achieved for  $\phi = \pi/2$ , which is one fourth of the ideal limit. Wide studies are going on various types of dish concentrators to find their thermal and optical performance and their application in the field of solar steam generation [9].

#### 1.2.2.2 COMPOUND PARABOLIC CONCENTRATOR:

A two - dimensional compound parabolic concentrator consists of two similar parabolic segments placed in such a manner that the focus of one parabola falls at the lower end of the other. The axes of the parabolic segments are inclined to the compound parabolic concentrator axis, on the either side, by the acceptable angle. The slope of reflector surface at the aperture is parallel to the optical axis of the above concentrator. Thus the rays entering the collector at the maximum acceptance angle, are reflected tangentially to the surface of the absorber (fig.1.2), so that

$$\tan \phi_{\text{max}} = \frac{D + d}{2H} \quad (1.10)$$

Where, H = Height of the concentrator

D = Width of the aperture of the concentrator

d = Width of the absorber

$\theta_{\max}$  = Acceptance angle.

The geometrical concentration ratio of the above concentrator is the ratio D/d. It can be written as  $1/\sin^2 \theta_{\max}$  by the relation.

$$H = \frac{D (1 + \sin \theta_{\max})}{2 \tan \theta_{\max}} \quad (1.11)$$

Work on this type of concentrator is being carried out currently to find the thermal and optical performance in many research centres, throughout the world [10].

#### 1.2.2.3 CIRCULAR FRESNEL LENS

The principle of operation of a circular Fresnel lens is similar to that of linear fresnel lens. Such lenses are used to generate high concentration of light rays. The aperture of circular Fresnel lens is divided into zones, the spacing of which ranges from a few lengths of millimeter to several centimeters. Within each aperture zone the surface of the lens is tilted such that its optical behaviour is similar to that of conventional spherical lens of same focal length (Fig.1.4).

#### 1.2.2.4. SEGMENTED MIRROR REFLECTORS:

An alternative to the parabolic trough is a segmented

mirror system, which replaces the large curve surface to approximate the surface angles of a trough (Fig. 1.5). The principal hope of this design is that the sum total of costs of narrow mirror segments can be fabricated for less than a large curved trough. The mirror segments can be fabricated flat so that the concentration is simply the number of stats (less one for receiver shadow). The receiver for a segmented mirror reflector system with flat stats can be similar to an ordinary flat plate collector which faces downward. Recent studies show that using about 6-8 stats, it is possible to achieve the elevated temperatures required for solar cooling. For additional concentration, the individual stat can be curved as circular cylindrical surface to concentrate the reflected light on the receivers. Use of 10 mirror segments and a secondary concentration ratio of 3 should produce an overall theoretical concentration ratio of about 30.

The advantages of the segmented mirror reflector are that the receiver is fixed and the mirror stats are small and presumably relatively inexpensive. Efforts are <sup>CT</sup> ~~being~~ made for further improvement of the above concentrator, so that these concentrators ~~may~~ be used in solar steam generating system [11-12].

#### 1.2.2.5 CENTRAL TOWER RECEIVER SYSTEM:

In the central tower receiver system, solar radiation is reflected from a large number of independently steered mirrors, called heliostats, to a central tower receiver as shown in Fig.1.6 The arrangement overcomes, namely, the need to

plumbing, carrying the working fluid over a long distance, rotating joints and heat loss from large number of receivers. Concentration ratio of about 3000 can be achieved from such a system. It however, depends upon the shape of the receiver, the fraction ( $\psi$ ) of ground area covered by the mirrors, and the angle  $\theta_r$ , subtended by the heliostat field at the receiver (corresponding to the rim angle). It can be expressed as

$$C_{\text{sph.}} = \frac{\psi \sin^2 \theta_r}{4 \sin^2 \frac{\theta_c}{2}} \quad (1.12)$$

$$\text{and } C_{\text{flat}} = \frac{\psi \cos(\theta_r + \frac{\theta_c}{2}) \sin \theta_r}{\sin^2 \frac{\theta_c}{2}} \quad (1.13)$$

The value of  $\psi$  varies between 0.3 to 0.5. A typical heliostat from M.B.B. consists of 16 square mirror elements each of 1.3 m x 1.2 m. Its reflecting surface has an area of about 23m<sup>2</sup> and the mirror elements are of 3mm<sup>thick</sup> float glass spherically shaped and back silvered, designed to form the solar image at a distance of 200mm. Another typical heliostat manufactured by CETHEL has an area of 51.8 m<sup>2</sup> built up of 8 modules of 6 rectangular mirrors each of 1.8m x 0.6m. The mirrors are 6mm thick and are made of back silvered float glass.

Considerable research efforts have been made in last 15 to 20 years to develop a central receiver heliostat system which utilizes a large number of large size heliostat in the system and it has been directed towards high temperature applications [13-17].

### 1.2.3 LINE FOCUSING CONCENTRATORS:

#### 1.2.3.1 CYLINDRICAL PARABOLIC TROUGH:

A cylindrical parabolic trough [18-19] as shown in Fig 1.7 is an optical imaging device used to focus a parallel beam into a line image. The concentrator is rotated about an axis to track the sun. Such a concentrator may be decided in terms of its aperture diameter (D), rim angle ( $\phi_r$ ) and absorber shape and size. The focal length (f) of the system is given by

$$D = 4 f \tan \phi_r/2 \quad (1.14)$$

The geometrical concentration ratio for a flat horizontal absorber can be expressed as

$$C_{\text{flat, horizontal}} = \frac{\sin \phi \cos(\phi + \xi)}{\sin \xi} - 1 \quad (1.15)$$

where,  $\xi$  = Angle of inclination.

For a cylindrical absorber, the geometrical concentration ratio has different form, namely

$$C_{\text{cylindrical}} = \frac{\sin \phi}{\sin \xi} \quad (1.16)$$

The geometrical concentration ratio has the maximum value for  $\phi = 45^\circ$ , in case of flat, horizontal absorber and for  $\phi = 90^\circ$  in case of cylindrical absorber.

A parabolic trough may be put in any of the three orientations,

viz., E-W, N-S or polar. The polar mount, however, collects more radiation than others. An interesting configuration of a parabolic trough is the one in which the receiver is cylindrical or flat plate, placed on the focal plane and along the geometrical axis of the parabola.

Work on this class of concentrators is being carried out in many centres of solar energy research throughout the world and some of the findings have already been published in the form of research papers. Efforts have been made to explore the possibility of using the above concentrator and its derivatives to produce solar steam.

#### 1.2.3.2 COMPOSITE PARABOLIC TROUGH:

Large parabolic troughs are generally built up using mirror strips because of ease of fabrication. Such concentrators give relatively smaller concentration than single piece reflector. They are symmetrically arranged on either side of the optic centre and the other in which the optic centre lies in the middle of the central element (Fig.8).

The concentration of a composite parabolic trough depends upon the shape of the receiver, as well as, the width of the mirror element used to built up the parabolic surface. Larger the size of the mirror element, smaller is the concentration produced. Some recent studies on the geometrical optical performance characteristics of such composite parabolic trough have been done which reveal that the above type of concentrator can be advantageously used for moderate concentration applications [20-21].



### 1.2.3.3 LINEAR FRESNEL REFLECTOR:

A linear Fresnel reflector is a concentrating device which is made of smaller flat or curved component. It consists of a large number of long narrow mirror elements mounted on a flat arrangement (Fig. 1.3). Each mirror element is placed such that all incident parallel rays of light intercepted by the concentrator are reflected to a common focus. Various design and performance aspects of linear Fresnel reflector have been studied in some detail [10].

### 1.2.4. LINE FOCUSING WITH LIMITED EXTENT:

#### 1.2.4.1 Conical concentrator:

Conical concentrators [22] are distinguished by their simplicity of construction. The basic geometry of the conical concentrator is the mirror surface (which may be single piece or composite type), inclined at a desired angle to the incoming radiations. The radiations incident at the mirror surface are directed to its axis (Fig.1.9). All the incident rays at the mirror surface after reflection cross the axis, thus forming a line focal image on its axis. The receivers can be placed on the axis of the conical concentrator which may either be conical or cylindrical in shape. It has, however, been found that the distribution of local concentration ratio will be more uniform on the conical receiver as compared to the cylindrical absorber. According to recent studies on the axicon concentrators, the shape of the concentrator may deviate from its conventional conical shape so as to produce more or less uniform illumination on both conical as well as cylindrical absorber. The maximum

theoretically achievable concentration ratio by the conical concentrator is 214 in case of conical absorber, where as in the case of cylindrical absorber is 188.4.

#### 1.2.4.2 Hemi-spherical Bowl:

The major components of this type of concentrator are: a fixed mirror (spherical or dish shape), a tracking linear absorber, directed parallel to the sun's rays, a support structure and a tracking device. The proto type of hemi-spherical bowl (Fig.10 ) concentrator have been designed, fabricated and tested at several R & D laboratories of the world [22]. The distribution of local concentration ratio along a finite size absorber has also been studied. Attempts have been made to calculate the area of the absorber which may be illuminated during part of the day.

### 1.3 SOLAR STEAM GENERATORS-CASE STUDIES:

This section presents an overall picture of past efforts made towards building solar steam generators.

#### 1.3.1 EXPERIMENTAL SETUP OF SOLAR BOILER DEVELOPED IN AUSTRIA (1854-1873):

The experiment, with solar boilers to generate steam using reflectors was apparently done by C. Gunter of Laibach, Austria from 1854 to 1873. He used series of long, narrow mirrors lying parallel to one another on the ground, each revolving about its own axis. Each mirror was tilted so that it reflected the sun rays on to a long boiler placed above the mirrors and parallel to them. Linkages between the mirrors caused them all to turn

simultaneously to follow the sun. He found that  $18.6 \text{ m}^2$  of mirror surface could generate steam sufficient to produce 1 h.p. of mechanical power.

### 1.3.2 SOLAR BOILER DEVELOPED IN FRANCE (1860 - 1878):

A. Mouchot did research on solar energy conversion in France from 1860 to 1878. He used a conical mirror ( $45^\circ$  cones) to focus solar radiation on a copper boiler located along the axis of the cone. The boiler was blackened to enhance absorbtivity and covered with glass to reduce heat losses. The entire apparatus was tracked manually to follow the sun.

Mouchot demonstrated his first solar engine in Paris in 1866. He constructed a second engine in 1875 with financial assistance from the French government. This engine has a reflecting surface area of  $4 \text{ m}^2$  and an axial boiler  $0.8 \text{ m}$  long. It produced steam at  $50.7 \times 10^4 \text{ N/m}^2$  and  $426^\circ \text{K}$ . The pressure was reduced to  $20.3 \times 10^2 \text{ N/M}^2$  and the steam was used to operate a small reciprocating engine at 80 strokes per min. Later, it was used to power a rotary engine driving a water pump. The inventor claimed that this arrangement was capable of producing 0.5 H.P of mechanical power.

In 1878, Mouchot built a third engine whose boiler consisted of many tubes placed side by side. The reflector area was  $5.2 \text{ m}^2$ . It was tested by two commissions appointed by the French Government. During a period of 176 days the apparatus distilled  $2.7 \text{ m}^3$  of water. The commission eventually concluded that the device was too expensive to be employed economically.

1.3.3 Solar steam generating system, developed in Bombay, India (1876-1878):

From 1876 to 1878 W. Adame in Bombay, India, experimented with small plane mirrors arranged to approximate a segment of a spherical surface of 12.2 m in diameter, focussing the solar radiation on a thick copper boiler. This arrangement said to have continuously produced steam at a pressure of  $20.7 \times 10^4 \text{ N/m}^2$ , running a 2.5 h.p pump for 20 consecutive days.

1.3.4. Eneas solar steam generating system developed in California (1901):

The most famous solar installations built by Eneas was the one erected at the Ostrich farm in Pasadena, California in 1901. According to a report published in 1901, the reflector was a truncated cone 10.2 m in diameter with a central opening of 4.6 m in bottom. The inner surface was composed of 1788 small and flat mirrors, arranged to approximate the conical surface. The mirrors reflected solar radiation on to the central tube boiler 4 m in length which held  $0.38 \text{ m}^3$  of water, leaving  $0.20 \text{ m}^3$  for steam. The entire boiler and reflector system was mounted on an equatorial axis, automatically clock-driven to follow the sun. The steam at a pressure of  $10.3 \times 10^5 \text{ N/m}^2$  drove an 11 h.p compound condensing engine belted to a centrifugal pump. At a pumping rate of  $5.3 \text{ m}^3 / \text{min}$ . against a 3.6 m head, the system produced a peak power of about 10 h.p. Eneas also built another plant at Mesa, Arizona in 1904 which was moved to Tempe in 1904 and subsequently moved to Willcox, and Cochise, in south-eastern Arizona. The plant used about  $65 \text{ m}^2$  of collecting surface to

produce steam at a pressure of  $10.3 \times 10^5 \text{ N/m}^2$ . About  $2.5 \times 10^3$  KJ of solar radiation was collected by every  $\text{m}^2$  of collector.

1.3.5 Solar steam generating system developed by C. Abbot in 1936:

In 1936 C. Abbot converted solar energy into mechanical power via. 05 h.p steam engine. The autho claimed an overall system efficiency of 15.5 percent. Solar radiation was intercepted by a parabolic trough collector whose focal axis was mounted parallel to the earth's axis of rotation to produce the familiar equatorial mounting used by astronomers. Along the focal axis was a single tube flash boiler encased in a long, double-walled, evacuated glass sleeve to reduce heat losses. Water was fed to the boiler automatically, The system was designed to raise full steam pressure within five minutes of exposure to the sun's rays, producing saturated steam at  $547^\circ \text{K}$ .

1.3.6 Solar steam generator developed in the C.S. Draper Laboratory (1970):

A thermal hydraulic model of once through subcritical steam generator has been developed for predicting dynamic characteristics of solar thermal power plant as well as for control system design. The purpose of the model is to evaluate the overall performance and component interaction with sufficient accuracy for controller design rather than microscopic occurring within the steam generator.

1.3.7 Solar concentrator /cavity receiver system developed by James A. Harris and Terry G. Lenz (1985):

James A. Harris and Terry G. Lenz worked on various configurations of solar concentrator /cavity receiver system. They

studied the thermal performance of paraboloid dish/cavity receiver system operated at temperatures between 550 and 900°C to produce saturated steam.

1.3.8 Solar steam generating system installed in a silk weaving factory, Bangalore, India (1992):

A solar steam generating system, which generates steam at a rate of 100Kg/hr, and a temperature of 150°C has been installed in a silk weaving factory in India. Parabolic trough concentrator modules have been used in this system to heat pressurized water which flashes to steam in a flash boiler.

1.4 Application of solar steam generator to produce electrical power-Case studies:

This section presents an overall picture of the past efforts made towards designing solar steam generators for production of electrical power.

1.4.1 Goddard's solar- electric power plant (1919):

In 1919, R.H. Goddard described the first large scale solar electric power plant. In his paper he stated that the system would produce thirty useful horse power when operating under a clear sky between the hours of ten in the morning and three in the afternoon, the time when sunlight is at its maximum power in the United states. The amount of power converted into electrical energy would far exceed the requirements of a large farm; the unused current could be employed to charge batteries.

#### 1.4.2 Francia's solar-powered plant at St. Ilario-Nervi, Genoa, Italy (1956-68):

The generation of steam at high temperature and pressure using heliostat and special multi-cellular solar radiation receivers was achieved in Italy. One such plant built by G. Francia in 1956 at St. Ilario-Nervi, Genoa produced 18.9 Kg/h of steam at  $152 \times 10^5$  N/m<sup>2</sup> pressure and 773 °K average temperature for a 5-6 hour period. The collector area was 30 m<sup>2</sup>. Francia increased the collector surface area in 1966 which resulted in a doubling of the average output of the steam from 18.9 Kg/h to 37.8 Kg/h at a pressure of  $152 \times 10^5$  N/m<sup>2</sup> and a temperature of 773 °K. The last power plant built in 1968 used 200m<sup>2</sup> of heliostats area producing 149.7 Kg of steam per hour at  $152 \times 10^5$  N/m<sup>2</sup> pressure and 823 °K temperature. The bell-shaped boiler of 0.91 m diameter was about 0.9 m high and absorbed 95 percent incident solar energy. Although the plant has been used to pump water, this type of system is now being investigated for this purpose.

#### 1.4.3 Sun-shine Project in Japan (1974-1981):

In this project, a solar thermal electric power system was being developed. This project was initiated in 1974 to develop the utilization of the systems of new energy resources. Two pilot plants of solar thermal electric power system of capacity 1000 KWe were constructed on the basis of conceptual and detailed design in 1981.

#### 1.4.4 Solar thermal electric power plants for Iran (1985):

The production of electricity by solar thermal technique is

evaluated for Iran. A simple economic analysis of solar thermal electric power plant shows that due to the low domestic fossil fuel cost and the present high installation cost of solar thermal power plants, most of the conventional methods of producing electricity are more economical than solar thermal electric power plant and will remain so even by 1994, when nuclear power generation becomes economically attractive for peak and intermediate loads in Iran provided that the installation costs of the solar plant is about 2000 sterling/KW.

1.4.5 100 KWe/700 KWth co-generation solar power plant in kuwait (1986):

A 100 KWe/ 700 KWth distributed receiver, solar thermal power plant was installed in a remote desert location 35 Km South-West of kuwait city in the country of kuwait. The co-generation solar power plant was designed to supply the electric power and fresh <sup>water</sup> needs of a small agricultural desert settlement. The power plant utilizes 56 point focussing parabolic collectors, each five meter in diameter and equipped with a two-axis tracking system. A synthetic fuel is circulated in the collector field via a pipe line network, where it was heated to 400°C. In the energy conversion system, the heat transfer fluid enters a series of heat exchangers where it heats up and vaporizes another organic fluid (Tolune). The vapour under high pressure, operates a radial flow turbine, producing mechanical and subsequently electrical energy. The rejected heat was ultimately used for powering multistage flash desalination system to provide the fresh water needs for the integrated food-water power complex.



1.4.6 5 KW Solar thermal power plant developed in Sardar Patel Renewable Energy centre, Gujrat, India, for electric power generation and water pumping for irrigation(1987):

A solar powered steam engine system of 5KW capacity for pumping water or generating electricity has been installed in Sardar Patel Renewable Energy Research centre. It used 25 parabolic trough concentrator (Vulcan concentrator imported from Austrilla) each with dimensions 1.7m x3.6m. It is designed for an operating temperature of steam at 200oC with a pressure of 10Kg/cm<sup>2</sup>.

1.4.7 Solar thermal electric power plant installed in Gurgaon, Haryana (1989-92):

An experimental setup of 50KW solar thermal power plant was commissioned in 1989 in solar energy centre at Gurgaon near Delhi. The plant has been operated for 3 years to characterize energy performance, determine equipment short comings and quantify operating and maintenance requirements.

1.5 Application of solar steam generating system to lift water for irrigation - case studies

This section presents an overall picture of the past efforts made towards designing solar steam generating system intregated with a steam turbine or a steam engine and a centrifugal pump to lift water for irrigation.

1.5.1 Solar steam engine developed by Ericsson in New York (1870-86):

Ericsson constructed a solar steam engine in 1870 using long boiler tubes located at the foci of parabolic troughs. This boiler-reflector arrangement could extract, on an average, during

9 hours a day,  $40\text{KJ}$  per minute for each  $\text{m}^2$  of area, presented perpendicularly to the sun's rays.

In 1883, Ericsson, built a large 'Sun motor' which was demonstrated in New York. It consists of a shallow parabolic trough 3.3m long and 4.9m wide focussing solar radiation on a 3.5m diameter boiler tube. Steam from the boiler was fed to steam engine. The entire aperture was turned manually to follow the sun. He indicated that summer trials allowed operation at a steam pressure of  $24 \times 10^4 \text{ N/m}^2$  driving a reciprocating engine at 120 rpm. With a concentration ration 9, he claimed to generate 1 H.P. with  $9.3\text{m}^2$  of reflecting surface. In 1886, he experimented with a 2.5 H.P. solar engine.

1.5.2 Sun-power plant, to run a printing press and a rotary water pump developed in France (1878):

A. Pifre experimented with concentrating reflectors and boilers. Unlike Mouchot, he used parabolic reflectors rather than truncated cones. Pifre demonstrated his sun - power plant at the Paris Exposition 1878. It drove a small steam engine which then ran a printing press. In a report published in 1880, he described a  $9.3\text{m}^2$  reflector which drove a rotary pump raising about  $0.1\text{m}^3$  of water in 14 minutes against a 3m pumping head.

1.5.3 Solar powered water pumping system in Auteuli, France (1885):

In 1885 an experiment was performed in Auteuli, France, during which over  $1\text{m}^3$  of water was pumped over one hour using a solar vapour engine. Sunlight falling on metal roof top collectors, warmed an ammonia solution driving off ammonia vapour. This

vapour displaced the water inside a submerged iron sphere thus providing a pumping action. A flexible rubber membrane acted as a bellow, keeping the ammonia physically separated from the water. When the water was pumped out, the ammonia was condensed and recycled, and the cycle began. The inventor claimed that in a warmer climate this type of solar pump could pump about  $3 \text{ m}^3$  of water per hour against a 19.8 m head.

1.5.4 Solar steam generating plants developed between 1905 and 1908 in California, to drive irrigation pump:

In 1905, a plant was built using sulphur di-oxide as the working fluid at Needles, California. Heat from the collectors generated vapour pressure of working fluid over  $13.8 \times 10^5 \text{ N/m}^2$ , corresponding to temperature above  $344^\circ \text{K}$ . This vapour drove a 20 h.p slide - valve engine which operated a centrifugal pump, a compressor and two circulating pumps. A second and final plant at Needles built in 1908 used a series of single and double glazed collectors (total area  $9.3 \text{ m}^2$ ) to produce water temperature of  $355^\circ \text{K}$ . The solar engine attained 15 h.p at a pressure of  $14.8 \times 10^5 \text{ N/m}^2$ .

1.5.5 Shuman's solar steam engines for irrigation (1906 to 1911) :

In the period between 1906 and world war-I, F. Shuman built a number of solar engines, some of which were used for pumping irrigation water. In 1907, he used solar energy in Tacony, Pennsylvania to drive a 3.5 h.p vapour engine using ether as working fluid. In his plant, a pond of  $11.2 \times 10^3 \text{ m}^2$  covered by glass was used to heat ether which circulated in a heat

exchanger immersed in the water. Ether vapour generation in this way ran an engine connected to a small centrifugal pump.

In 1910, Shuman built a second type of absorber, basically a boiler made of two sheets of copper, each 1.8 m, separated by a space of 0.05. The boiler was enclosed in wooden box covered with two sheets of ordinary window glass. The upper boiler plate was painted black. His object was to produce saturated steam at a pressure of  $10^5 \text{ N/m}^2$  and at a temperature of 473°K. The result was a peak production of 0.4 Kg of steam during one hour of system operation on 27th August 1910. The 1000KJ of heat needed to produce steam meant that the absorption rate for this small collector was 672 KJ/h-m<sup>2</sup>.

Shuman concluded from this modest performance that a concentration of the sun's rays would be necessary. In 1911, he made a system to pump 11.3 m<sup>3</sup> of water per min. to a height of 10 m, equivalent to a peak power output of 24 h.p. Shuman especially designed the engine for this irrigation plant to run on low pressure steam at 150 rpm. The single piston had a diameter of 0.9 m and a stroke of 0.9m..

1.5.6. A large solar-powered irrigation plant developed in 1913 in Meadi, Egypt:

A large and important irrigation plant, installed by Shuman and Boys in 1913 in Meadi, Egypt, consisted of a glass-covered boiler tubes and placed along the focusing axis of trough-shaped parabolic cylinders. Each parabolic concentrator ( five in total) used to generate steam in the Shuman and Boy's irrigation plant, was 62.5 m long and 4 m wide, providing a total solar radiation

collecting surface of 1280.8 m<sup>2</sup>. The concentration ratio of 40 resulted in a over all peak absorber efficiency of 40.7 percent. The plant developed upto 73 h.p.

1.5.7. Solar steam engine developed in New Mexico for pumping water (1920):

In 1920, in New Mexico, J. Harrington focused sunlight into a boiler to run a steam engine that pumped water upto 6 m into a tank with capacity of 18.9 m<sup>3</sup>. The system was used to supply power to a water turbine driven generator.

1.5.8. Solar steam generating system for solar engine developed by Molero of Soviet Union [1941-46]:

From 1941 to 1946, F. Molero of soviet union, used 10 m diameter parabolic dish reflectors to produce steam at a pressure of 20.3 x 10<sup>4</sup> N/m<sup>2</sup> for solar engines which can be used to pump water for irrigation.

1.5.9. Solar installation developed in National Physical Laboratory, Israel (1965):

H. Tabor built a 5 h.p solar installation for pumping water in 1961. The system used a binary rankine cycle with monchlorobenzene (C<sub>6</sub>H<sub>5</sub>Cl) vaporized by superheated steam from solar collectors. The vapour ran through a turbine to generate mechanical power. The national Physical Laboratory of Israel commercially developed this concept and produced what are known as ORMAT Rankine power units. Power units of this type are currently available, ranging from a few hundred watt to 15 kW. Such a solar irrigation plant was used for pumping water in 1965 in Mali, Africa. This plant lifted 11.3m<sup>3</sup> of water per day from a 45.7 m well.

1.5.10 Solar steam engine developed by Masson and Girardier in Dakar, Senegal [1962-66]:

In Dakar, Senegal from 1962 to 1966, H. Mascon and J. Girardier operated a small solar engine which pumped 7.9 - 9.8 m<sup>3</sup> of water per min. from a depth of 13 m, using a collection area of 6 m<sup>2</sup>. The operation of this prototype leads to the design and construction of a larger and relatively efficient pump. This new installation, with a collection area of 300 m<sup>2</sup> was capable of pumping 37.8 m<sup>3</sup> water. The water was used to vaporize secondary fluid which expanded through a turbine to generate electricity. The electricity in turn drove the pump via. an electric motor.

1.5.11. SOFRETES solar - powered water pumping plant in Guanajuato, Mexico (1976):

A solar water pumping station built by the French company SOFRETES began operation in Guanajuato, Mexico in 1976. The installation employs 2499 m<sup>2</sup> of flat- plate collectors. Water was used as the primary heat transfer fluid. The heat was transferred from water to the working fluid (Refrigrant- 11). A vapour turbine and an electric generator produced 30KW of electric power which drove two pumps. This system, capable of producing 25 KW and 50 KW power output was also available from SOFRETES.

1.5.12 Battelle Memorial Institute built solar- powered pumping plant. Gilla Bend + Arizona (1977):

In April 1977, a large installation for pumping irrigation water was put into operation on Gila River Ranch, Phonix, Arizona. The system is equipped with parabolic tracking collectors having total area 564 m<sup>2</sup>. The collector design

efficiency was 55 percent, while actual field efficiency is 44.5 percent. The Rankine cycle power unit consists of a radial-inflow turbine/ gear box, boiler, condenser, regenerator and pre-heater, and is capable of delivering 50 h.p output and pumping about 38 m<sup>3</sup> irrigation water per min. at peak operation. Water heated to 433 K was used as primary heat transfer fluid. Refrigerant 113 was used as the working fluid. The radial inflow turbine develops 30,500 rpm which was reduced by gear box to an output shaft speed of 1760 rpm.

1.5.13 Sandia Laboratories built solar-powered pumping installation (Willard, New Mexico, 1988):

A solar-powered irrigation plant near Willard, New Mexico began operation in June 1988. Parabolic trough collectors oriented north-south with a total area of 622.4m<sup>2</sup> were used to provide energy for immediate operation and for storage. The Rankine cycle operates at a peak temperature of 436 K of the secondary fluid in a 22.7 m<sup>3</sup> tank. The specially built vapour turbine runs at 36,300 rpm developing 1760 rpm at the output shaft of gear box. The system developed 25 h.p. with a Rankine cycle efficiency of 15 percent. The water output of 2.6 m<sup>3</sup> per min. from a 34m deep well can provide irrigation for up to 404.6 m<sup>2</sup> collectors.

1.5.14 An Autonomous Combined Solar System for heating, cooling and water supply developed in Odessa, Ukraine (1992).  
A small-scale combined solar system for simultaneous heating, cooling and water supply has been designed and tested by V.A. Petrenko and V.A. Goubanov in Odessa, Ukraine. It consists of a Freon vapour ejection refrigerator, a heat pump and solar heater.

## 1.6 THE LIST OF THE FIGURE CAPTIONS:

Fig.1.1 : Dish type concentrator.

Fig.1.2 : The compound parabolic concentrator

Fig.1.3 : Linear Fresnel Reflector.

Fig.1.4 : Circular Fresnel lens.

Fig.1.5 : Segmented mirror.

Fig.1.6 : Central tower receiver system.

Fig.1.7 : Cylindrical parabolic trough.

Fig.1.8 : Composite parabolic trough.

Fig.1.9 : Conical concentrator.

Fig.1.10 : Hemi-spherical bowl.



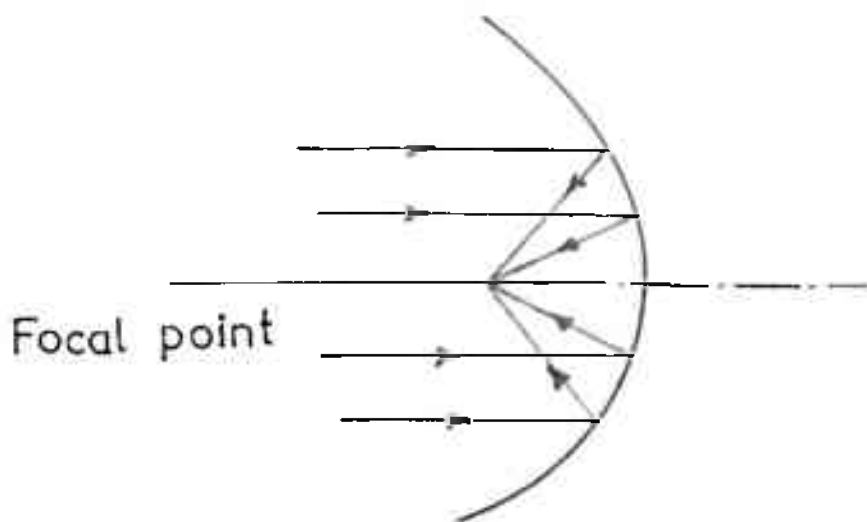


Fig. 1.1: Dish type Concentrator

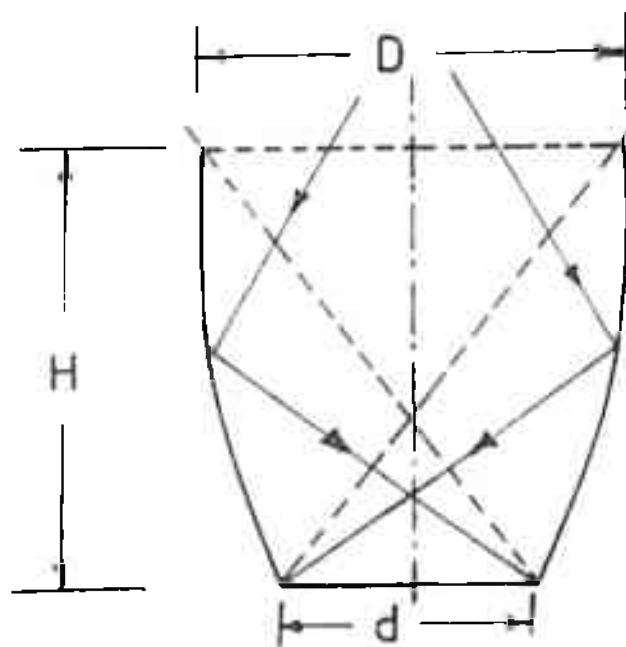


Fig. 1.2: Section of the compound parabolic concentrator.

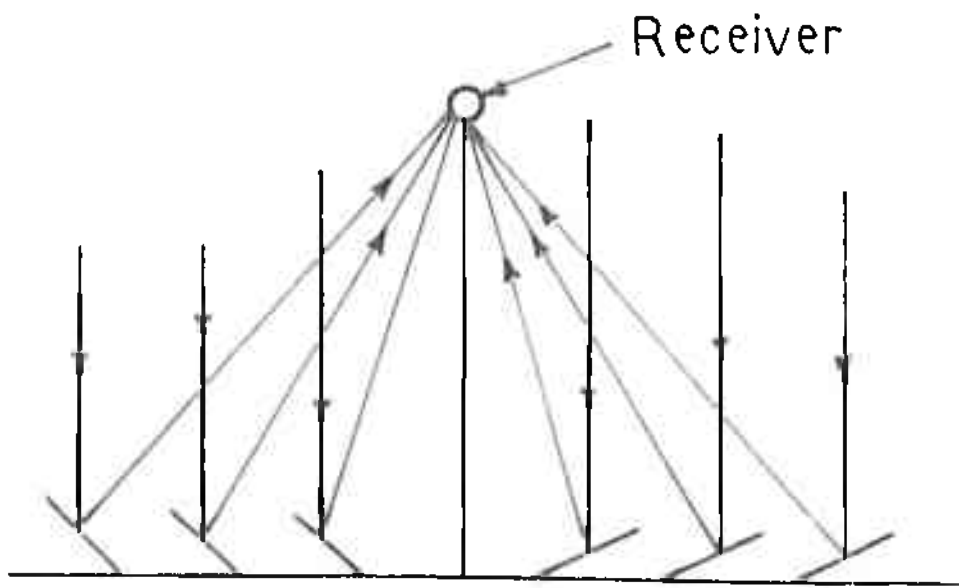


Fig.1.3 : Linear Fresnel Reflector

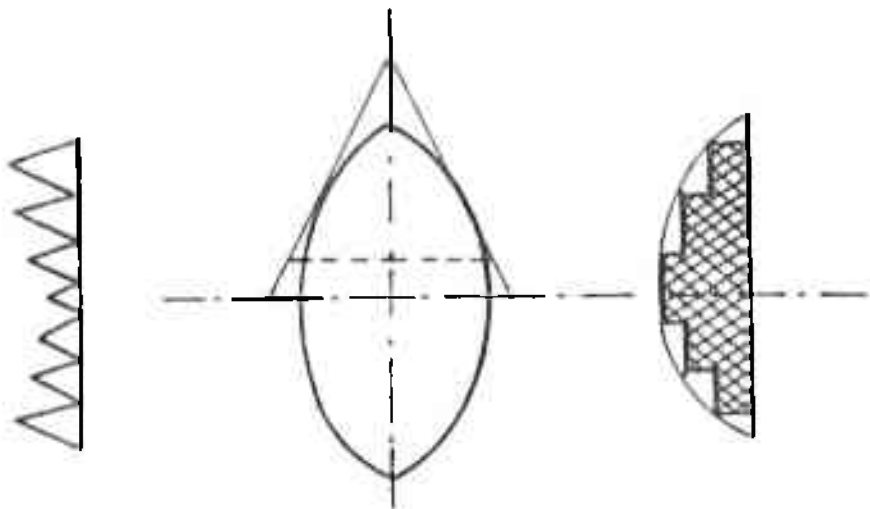


Fig.1.4 : Circular Fresnel Lens

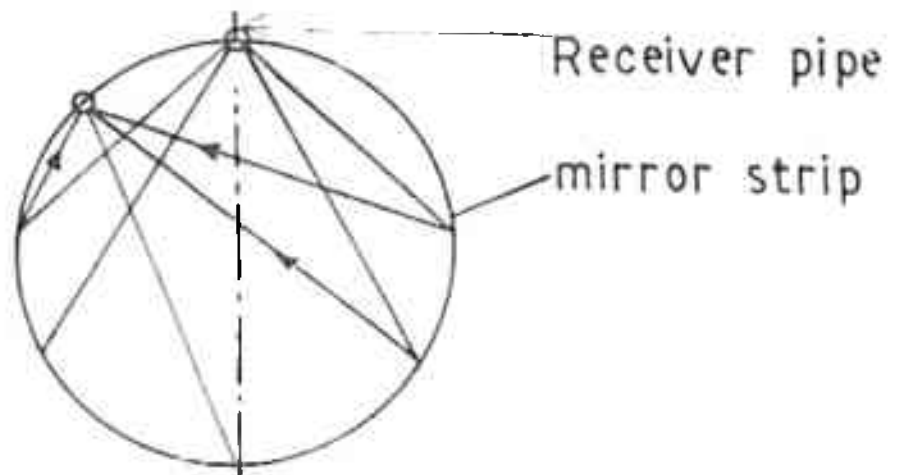


Fig.1.5 : Segmented mirror

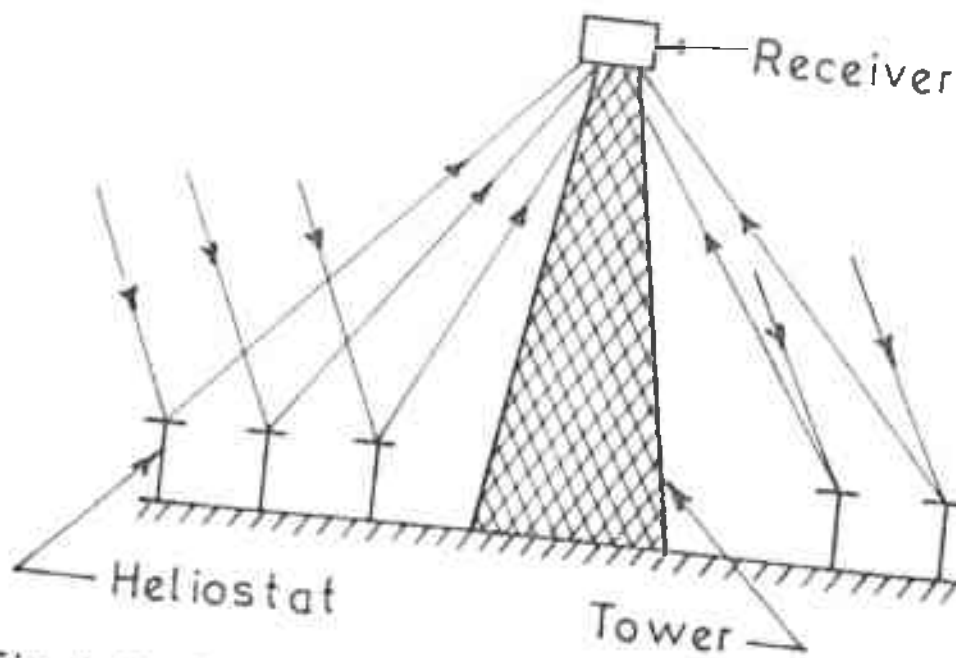


Fig.1.6: Central Receiver System

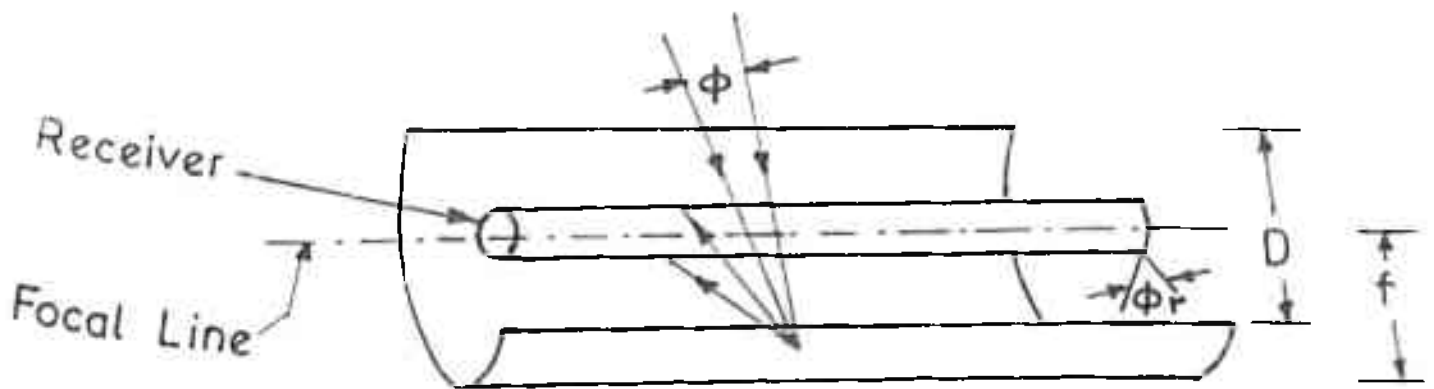


Fig.1.7: Cylindrical parabolic trough

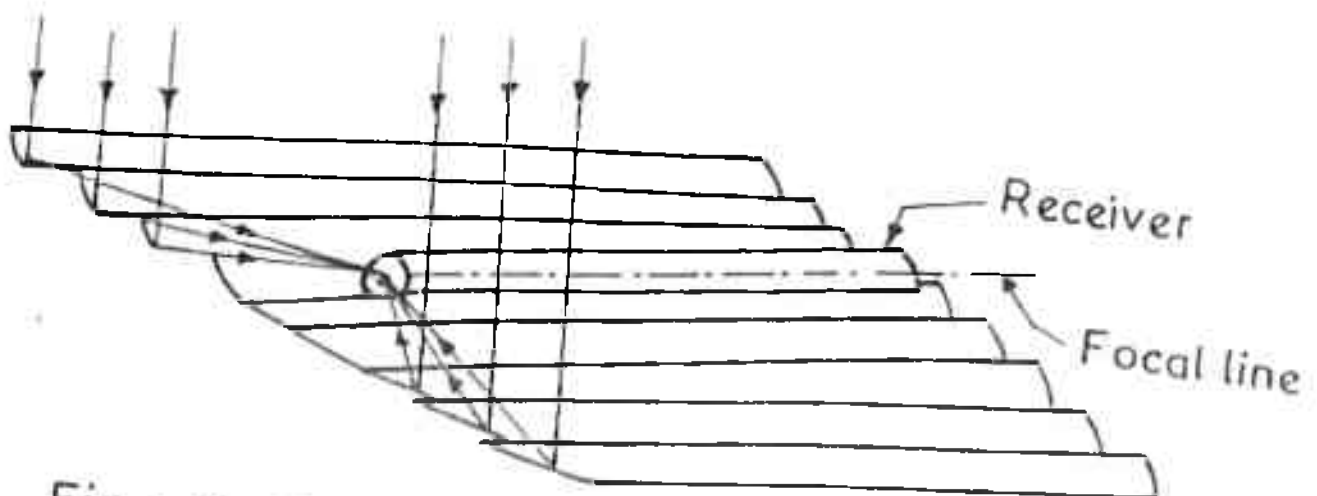


Fig.1.8: Composite parabolic trough

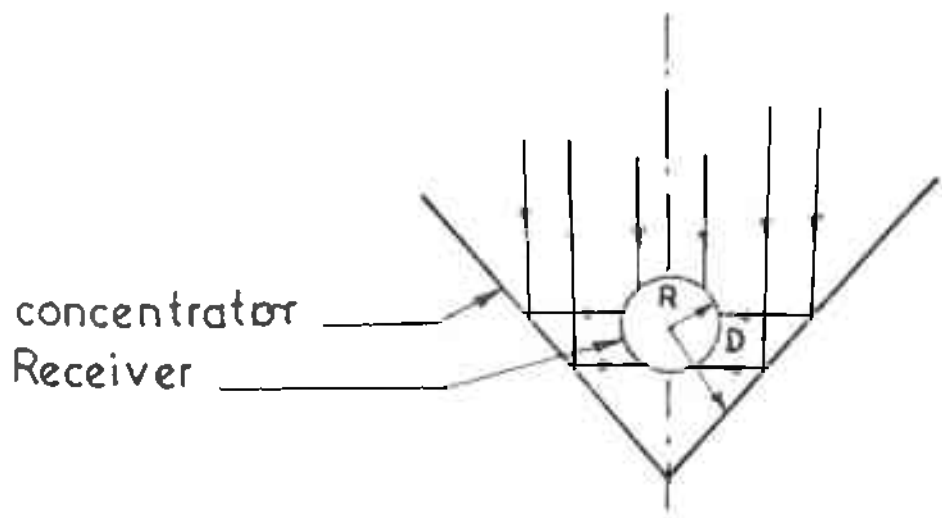


Fig. 1.9: Conical concentrator

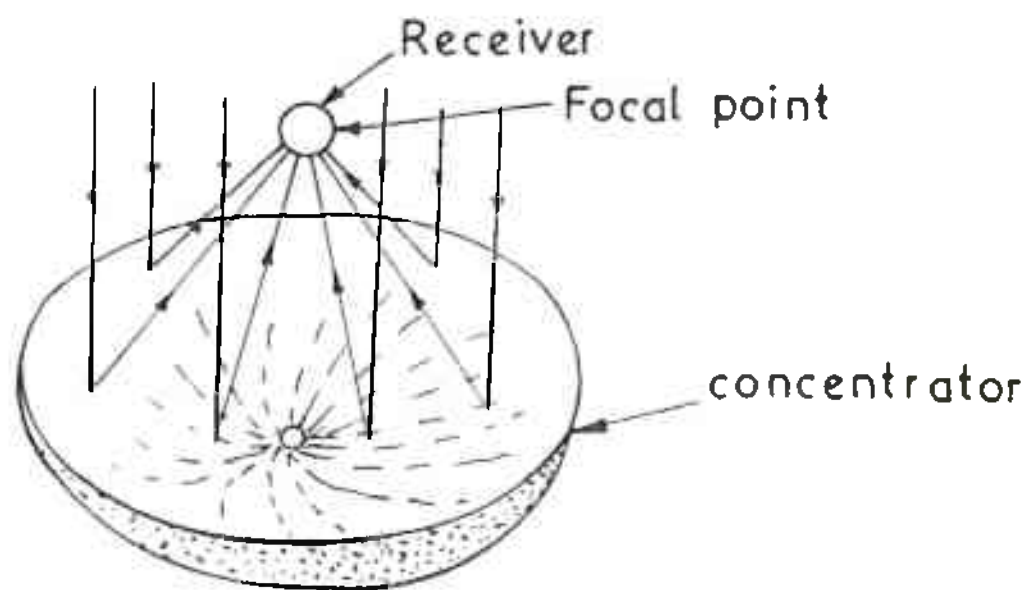


Fig. 1.10: Hemi - spherical Bowl.

CHAPTER -II

Analysis and modelling of a solar concentrator and receiver  
system

2.1 INTRODUCTION:

Solar thermal systems, consisting of a linear concentrator and a receiver placed on the focal plane of the concentrator, have been given due importance for the last few years. This is because of the fact that such a system is not only capable of conserving fossil fuels, nuclear fuels, etc. but can also produce thermal energy without polluting environment. The above solar thermal systems may be used to produce hot water at high temperature and also steam at supersaturated temperature. When the above system is used to produce steam, then the receiver acts as a steam generator. An appropriate tracking system may be used so that solar radiations are always normally incident on the aperture plane of the concentrator and the reflected rays are always focussed on the plane of the receiver.

In this chapter, an attempt has been made to model a concentrator-receiver system (shown in Fig 2.1) which consists of a linear parabolic concentrator. Such a system, in fact, may be useful for producing steam at the temperature range of  $200^{\circ}\text{C}$  to  $300^{\circ}\text{C}$ . Some typical numerical calculations have been made to find the variation of the temperature along the length of the receiver for the different values of solar concentration ratio and also the amount of the hot water / steam that may be produced for the different length of the receiver. The results are shown graphically and discussed.

## 2.2 ANALYSIS:

For the analysis of the above system, the following simplifying assumptions have been made.

- i) The linear concentrator is fully tracked.
- ii) The whole outer surface of the receiver is uniformly illuminated.
- iii) The temperature of the fluid at any cross-section is uniform.

### 2.2.1 MATHEMATICAL MODELLING

For the mathematical analysis, the total length of the receiver is assumed to be divided into three sections, namely AB, BC and CD of lengths  $x_1$ ,  $x_2$  and  $x_3$  respectively, as shown in Fig. 2.2.

In the section AB the working fluid is considered to be in purely liquid state, in the section BC the fluid is in mixed state (ie, liquid and vapour) and in the section CD, the fluid is in purely vapour state.

#### Expression for the temperature of the water and the length AB of the receiver:

To find the expressions for the temperature of water and length AB (ie,  $x_1$ ) as a function of mass flow rate of working fluid (ie, water/steam) and solar concentration ratio, let us consider the elemental length  $dx_1$  of the receiver as shown in fig. 2.3.

The heat balance equation for the elemental length  $dx_1$  of the section AB, may be written as

$$I(2\pi r_0) R_n dx_1 = \dot{m}_w c_w dT_w + 2\pi r_0 C_s (T_s - T_a) dx_1 \quad (2.1)$$

Where,  $I$  = Intensity of solar radiation . ( KW/m<sup>2</sup> )

$\eta_0$  = Optical efficiency of the solar concentrator

$R$  = Solar concentration ratio.

$\dot{m}_w$  = Mass flow rate of water ..(Kg/sec)

$c_w$  = Specific heat of water = (KJ/Kg°C)

$r_0$  = Outer radius of the receiver ( m )

$C$  = Linearized heat transfer coefficient for convection and radiation ( KW/m<sup>2</sup> °C )

$$C = h_a + h_r$$

$h_a$  = Convective heat transfer coefficient ( KW/m<sup>2</sup> °C )

$$h_a = h_{an} \left( \frac{T_s - T_a}{T_s^* - T_a^*} \right)^{0.33} + h_{af} \left( \frac{V_a}{V_a^*} \right)^{0.66}$$

$h_{an}$  = Natural convective heat transfer coefficient ( KW/m<sup>2</sup> °C )

$h_{af}$  = Forced convective heat transfer coefficient ( KW/m<sup>2</sup> °C )

$T_a$  = Ambient temperature ( °C )

$T_a^*$  = Design ambient temperature ( °C )

$T_b$  = Boiling temperature of water ( °C )

$T_i$  = Initial temperature of water ( °C )

$T_s$  = Surface temperature of the receiver ( °C )

$T_s^*$  = Design surface temperature ( °C )

$T_w$  = Temperature of water ( °C )

$V_a$  = Velocity of wind ( Km/hr )

$V_a^*$  = Design velocity of wind ( Km/hr )

If we assume,  $U$  as over all heat transfer coefficient of the above section , then the heat received by the water in the receiver,  $\dot{m}_w$  be written as

$$2\pi r_0 \int_0^L U (T_s - T_w) dx = \dot{m}_w c_w dT_w \quad (2.2)$$



The equations (2.1) and (2.2) may be written in combined form, after eliminating the term  $T_s$ , as

$$\dot{m}_w c_w [1 + C/U] dT_w = 2\pi r_o [I\eta R + CT_w] dx - 2\pi r_o C T_w dx \quad (2.3)$$

Now, integrating the equation (2.3) over the length AB of the receiver and applying boundary conditions,

- i)  $x = 0, T_w = T_i$  and ii)  $x = x_1, T_w = T_{w1}$

the expression for the temperature of the water along the length AB of the receiver may be expressed as

$$T_w(x_1) = (P/C) - [(P/C) - T_i] \exp(-Acx_1) \quad (2.4)$$

Where,  $P = I\eta R + C T_i$

$$A = 2\pi r_o / [\dot{m}_w c_w (1 + C/U)]$$

Further extension of this analysis leads to the expression for surface temperature of the receiver along the length AB, as

$$T_s(x_1) = T_w(x_1) + [(m_w c_w) / (2\pi r_o)] \exp(-Acx_1) \quad (2.5)$$

From the equation (2.4) the length of the receiver required to raise the temperature of water to its boiling point, may be written as

$$x_1 = \frac{1}{Ac} \ln \left[ \frac{(P/C) - T_i}{(P/C) - T_{w1}} \right] \quad (2.6)$$

Expression for the length of the receiver in the section BC.

To find the expression for the length  $x_2$  of the receiver for the section BC, let us consider an elemental length  $dx$  of this section as shown in Fig. 2.4.

The heat balance equation for the above length  $\frac{dx}{2}$  of the receiver may be written as

$$\dot{m} C (T_s - T_a) \frac{dx}{2} = 2\pi r_o C (T_s - T_a) \frac{dx}{2} \quad (2.7)$$

$$\text{or, } 2\pi r_o \eta_o I R \frac{dx}{2} = \dot{m} dH + 2\pi r_o C (T_s - T_a) \frac{dx}{2} \quad (2.8)$$

Where,  $I$  = Intensity of solar radiation ( $\text{KW/m}^2$ )

$\eta_o$  = Optical efficiency of the solar concentrator

$R$  = Solar concentration ratio

$r_o$  = Outer radius of the receiver (m)

$\dot{m}$  = Mass flow rate of working (water / steam) ( $\text{Kg/s}$ )

$dH$  = Enthalpy for the section  $\frac{dx}{2}$  ( $\text{KJ/Kg}$ )

$T_a$  = Ambient temperature ( $^{\circ}\text{C}$ )

$T_s$  = Surface temperature ( $^{\circ}\text{C}$ )

$C = h_a + h_r$  = Linearized heat transfer coefficient for convection and radiation (APPENDIX)

$h_a$  = Convective heat transfer coefficient ( $\text{KW/m}^2\text{ }^{\circ}\text{C}$ )

$h_r$  = Radiative heat transfer coefficient ( $\text{KW/m}^2\text{ }^{\circ}\text{C}$ )

If we assume  $U$  as over all heat transfer coefficient of the section BC of the receiver and  $T_b$  as the boiling temperature of the water which remains constant in the section BC, then the heat received by the working fluid of the length  $\frac{dx}{2}$  of the above section may be written as

$$2\pi r_o U (T_s - T_b) \frac{dx}{2} = \dot{m} dH \quad (2.9)$$

Combining the equations (2.8) and (2.9) after eliminating

$T_s$  we get,

$$2\pi r_o \left[ \eta_o R + C (T_b - T_a) \right] \frac{dx}{2}$$

$$= \dot{m} \left[ 1 + C/U \right] dH \quad (2.10)$$

Now, integrating the equation (2.10) over the length BC of the receiver and applying boundary conditions

$$\begin{aligned} \text{i) } x &= 0, & H &= H_1 \text{ and} \\ \text{ii) } x &= x_2, & H &= H_g \end{aligned}$$

the expression for the length  $x_2$  of the section BC of the receiver may be written as

$$x_2 = \alpha (H_g - H_1) \quad (2.11)$$

$$\text{Where, } \alpha = m[1 + C/U]$$

$$\text{and } \alpha = 2\pi r_0 [I_0 R + C(T_b - T_a)]$$

$$\text{or, } x_2 = [\alpha (H_g - H_1)] / \beta$$

Where,  $H_g$  = Enthalpy of the steam (KJ/Kg)

$H_1$  = Enthalpy of the liquid (KJ/Kg)

The values of  $H_g$  and  $H_1$  may be obtained from steam Table.

The expression for the surface temperature of the receiver for the section BC, can be written as

$$T_s(x_2) = T_b + (1 - \alpha) I_0 R + C(T_b - T_a) \quad (2.13)$$

Expression for the temperature of the steam and the length of the receiver for the section CD :

To find the expressions for the superheated steam temperature along the length CD and the length  $x_3$  of the receiver, let us consider an elemental length  $dx_3$  of the length CD of the receiver as shown in Fig 2.5.

The heat balance equation for the above elemental length may be written as

$$2\pi r_0 I_0 R dx_3 + m_s c_s dT_s + 2\pi r_0 C (T_s - T_a) dx_3 \quad (2.14)$$

Where,  $I_0$  = Intensity of solar radiation (KW/m<sup>2</sup>)

$R$  = Solar concentration ratio

$\eta$  = optical efficiency of the concentrator

$r_o$  = Outer radius of the receiver (m)

$\dot{m}_s$  = Mass flow rate of steam (Kg/sec)

$c_s$  = Specific heat of steam (KJ/Kg)

$T_s$  = Temperature of steam ( $^{\circ}\text{C}$ )

$T_v$  = Surface temperature of the receiver in  $^{\circ}\text{C}$

$T_a$  = Ambient temperature ( $^{\circ}\text{C}$ )

$C = h_a + h_r$  = Linearized heat transfer coefficient for convection and radiation (APPENDIX).

$h_a$  = Convective heat transfer coefficient ( $\text{KW/m}^2 \text{ } ^{\circ}\text{C}$ )

$h_r$  = Radiative heat transfer coefficient ( $\text{KW/m}^2 \text{ } ^{\circ}\text{C}$ )

If, 'U' is assumed as overall heat transfer coefficient

for the section CD of the receiver, then the heat received by the

water vapour in the elemental length  $dx_3$ , may be written as

$$2\pi r_o U (T_s - T_a) dx_3 = \dot{m}_s c_s dT_v \quad (2.15)$$

Combining the equations (2.14) and (2.15), after eliminating  $T_s$

we get .

$$\dot{m}_s c_s [1 + \epsilon/U] dT_v = 2\pi r_o [\eta R + \epsilon T_a] dx_3 - 2\pi r_o \epsilon T_v dx_3 \quad (2.16)$$

Now integrating the equation (2.16) and applying the boundary

conditions

i)  $x = 0$ ,  $T_v = T_b$ , and

ii)  $x = x_3$ ,  $T_v = T_v(x_3)$

the temperature of the steam along the length CD may

be written as

$$T_v(x_3) = (P/C) - [(P/C) - T_b] \exp(-ACx_3) \quad (2.17)$$

Where,  $P = \dot{m}_o \eta_o + C T_a$

$$A = \frac{2\pi r_o}{\dot{m}_s c_s} (1 + C/U)$$

Further extension of this analysis leads to the expression for the surface temperature of the receiver along the length CD can be given as

$$T_s(x_3) = T_v(x_3) + \left[ \frac{\dot{m}_s c_s}{2\pi r_o U} \right] \left\{ \frac{P}{C} - T_b \right\} \exp(-ACx_3) \quad (2.18)$$

Now, from the equation (2.17) the expression for the length  $x_3$  of receiver, can be written as

$$x_3 = \frac{\ln \left\{ \frac{P/C - T_b}{P/C - T_v(x_3)} \right\}}{AC} \quad (2.19)$$

The expression for the total length of the receiver

The expression for the total length,  $x$  of the receiver may be obtained by adding the equations (2.6), (2.12) and (1.19), as

$$x = x_1 + x_2 + x_3 \quad (2.20)$$

The expression for the mass flow rate of the steam:

If we assume that there is no transport delay of the working fluid and overall heat transfer coefficient is same for all the three section AB, BC and CD, then mass of the steam produced per unit time may be obtained from the equation (2.20) assuming  $\dot{m}_w = \dot{m}_s = \dot{m}$  and expressed as

$$\dot{m} = \frac{2\pi r_o K x}{c_w \ln \left[ \frac{P - C T_i}{P - C T_b} \right] + \frac{C (H - H_1)}{P - C (T_b - 2T_a)} + c_s \ln \left[ \frac{P - C T_b}{P - C T_v} \right]}$$

Where,  $K = 1 / \left( \frac{1}{c} + \frac{1}{U} \right)$

(2.21)

### 2.3 RESULTS AND DISCUSSIONS:

The analysis presented in the above section, may be used to study the performance of a solar thermal system consisting of a linear concentrator and a receiver, to produce hot water and steam. Some numerical calculations have been made for a typical system in which a parabolic trough is used to as a concentrator and water as working fluid. Figure 2.6 shows the variation of temperature of the working fluid with the distance along the length of the receiver. In the section of length  $X_1$ , the temperature of water rises exponentially from its initial temperature to the boiling point. In the section of length  $X_2$ , the temperature of two phase fluid remains constant at boiling point. In the section of length  $X_3$ , the temperature of the steam rises exponentially to produce saturated steam. It may be noted that the total length of the receiver required to produce hot water or steam decreases with the increase in the solar concentration ratio. It is observed that the length of the third section ( $X_3$ ) length of the first section ( $X_1$ ) length of the second section ( $X_2$ ). This is due to the fact that the heat received by the receiver at higher concentration ratio is more than that of at lower concentration ratio. Again the length of the receiver for the second section ( $X_2$ ) is higher than other sections because the enthalpy of the two-phase fluid is higher than that of the fluids in the other two sections. Figure 2.7, shows the variation of the rate of the mass of the hot water or steam produced with solar concentration ratio for different lengths of the receiver considering the effect of wind. It may be observed that the mass of the steam/ hot water produced by the

receiver is slightly lower with the effect of wind taken into consideration than that of the same without the effect of the wind. This may be attributed to the fact that the wind gives rise to an increased heat loss.

## 2.4 : LIST OF THE FIGURE CAPTIONS:

- Fig.2.1 : Schematic diagram of a steam generating system using linear solar concentrator.
- Fig.2.2 : Cross sectional view of the receiver.
- Fig.2.3 : First section of the receiver to raise temperature of the water from its initial temperature to the boiling point.
- Fig.2.4 : Second section of the receiver where the temperature of the fluid remains constant.
- Fig.2.5 : Third section of the receiver to produce super - heated steam.
- Fig. 2.6 : Variation of the temperature of the fluid along the length of the receiver.
- Fig.2.7 : Variation of the steam production rate with solar concentration ratio.



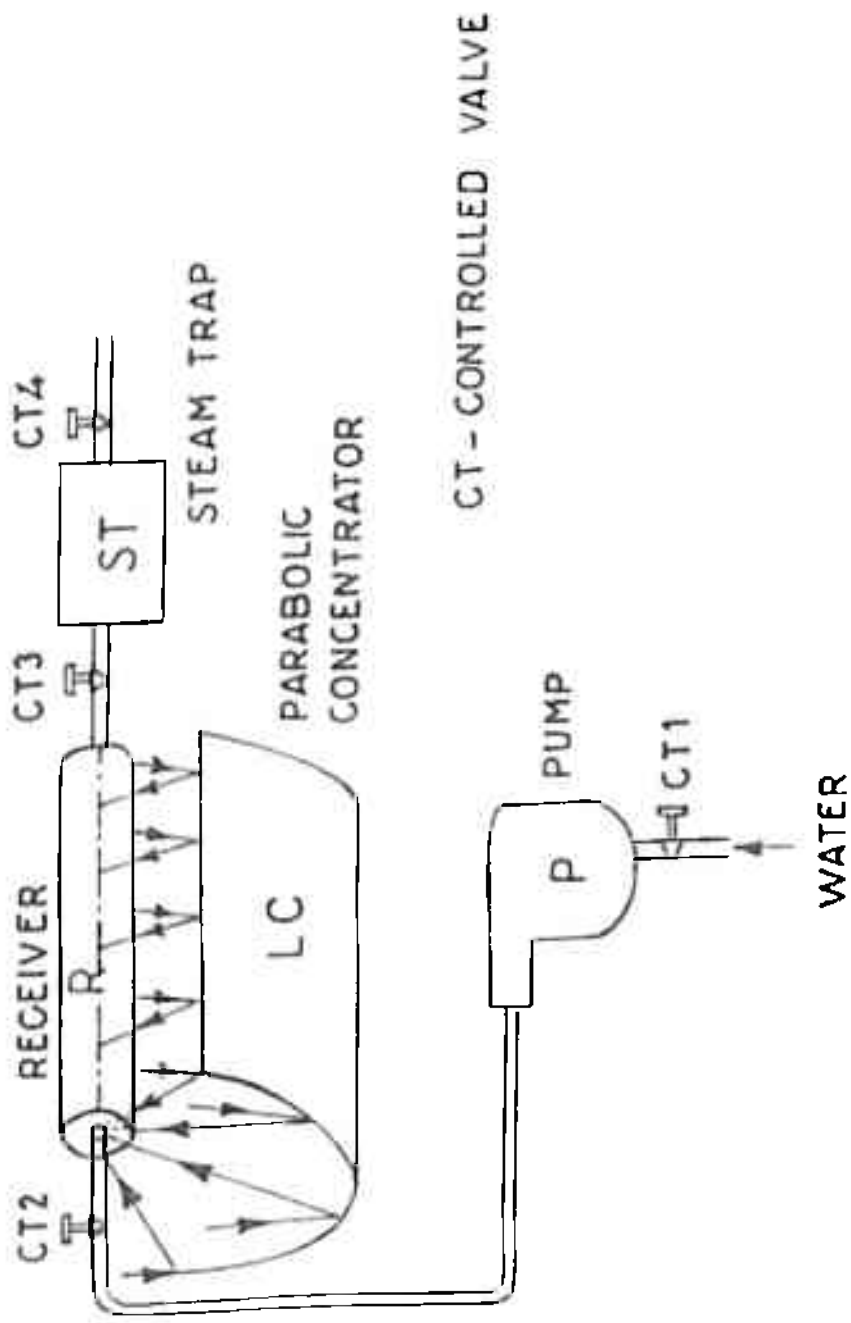


Fig.2.1: Schematic diagram of a steam generating system using linear solar concentrator

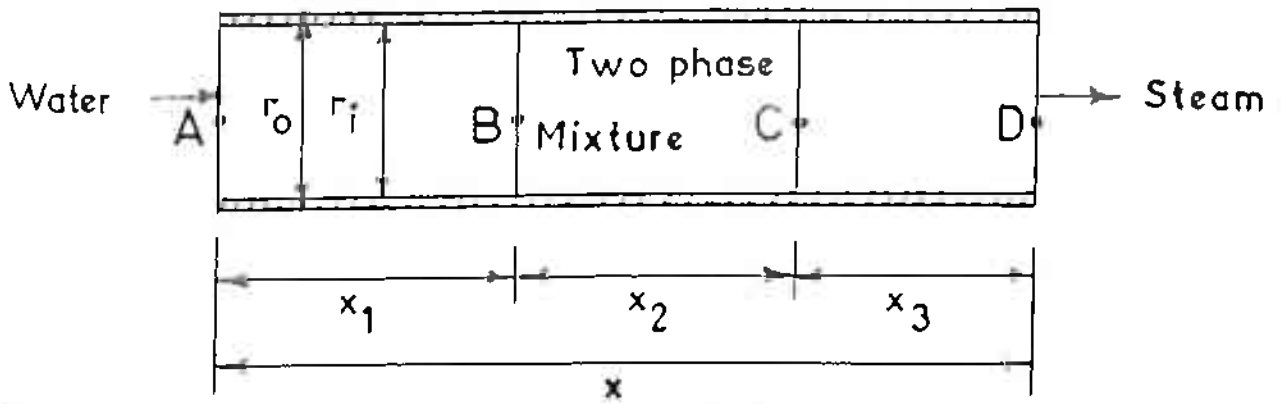


Fig.2.2.: Cross-sectional view of the receiver

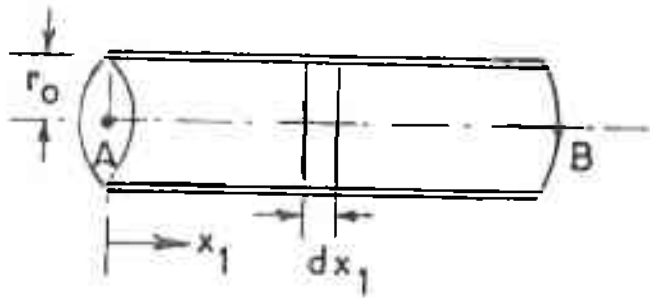


FIG. 2.3: First section

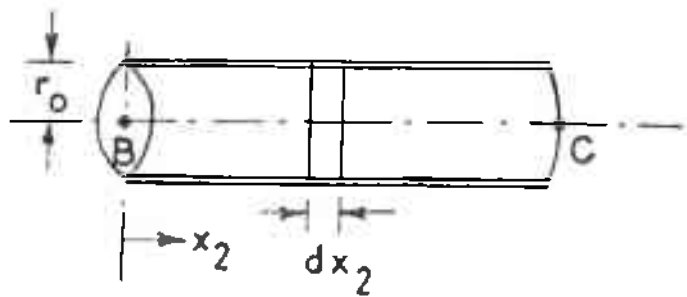


FIG. 2.4: Second section

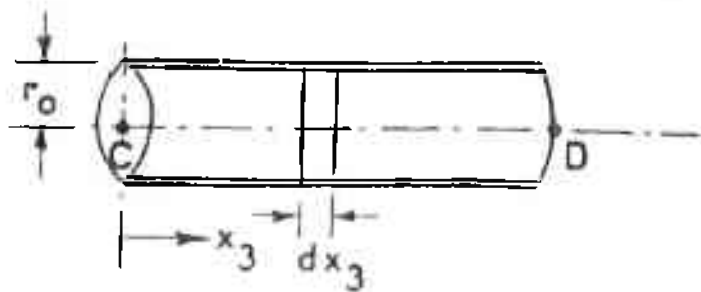
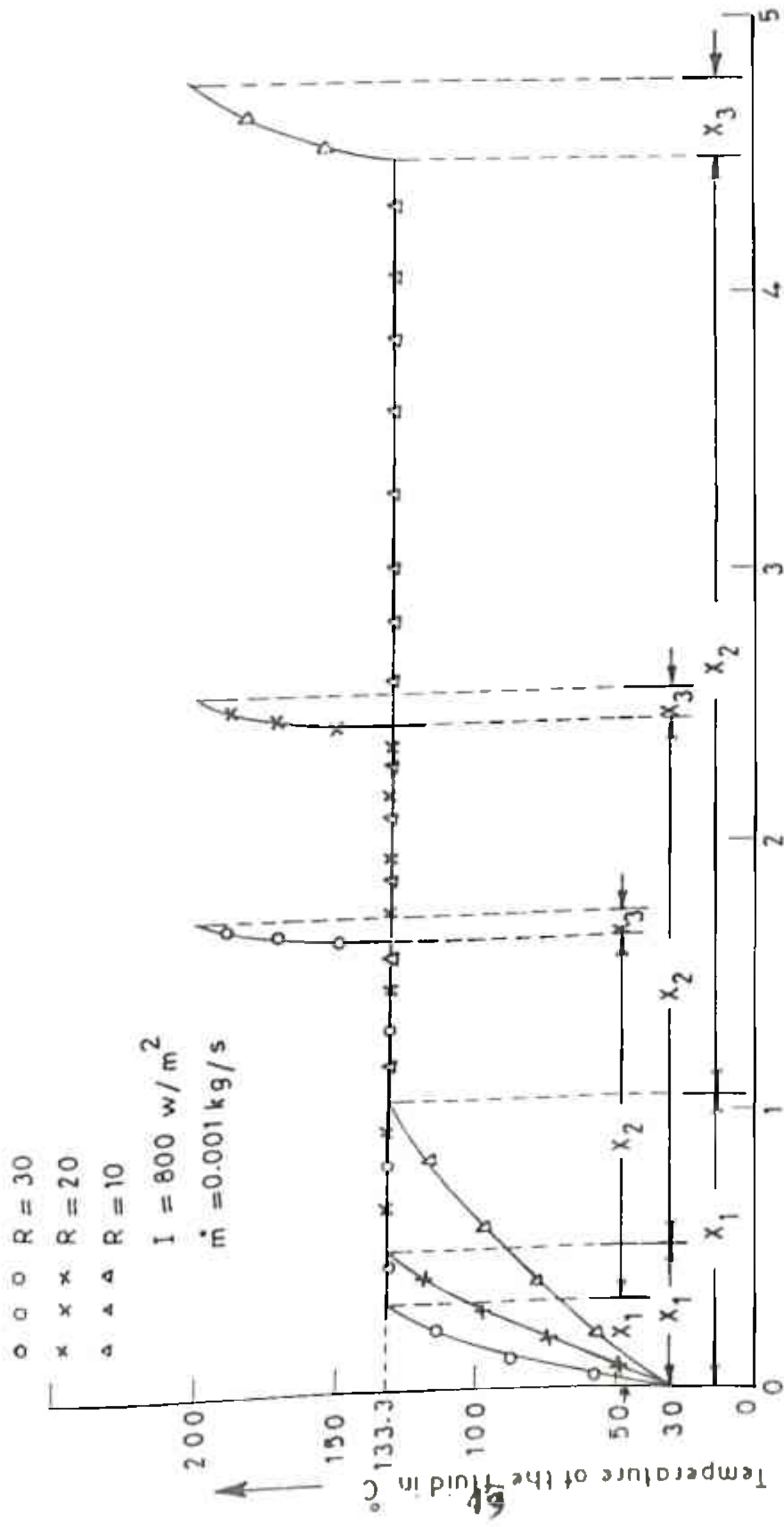


FIG. 2.5: Third section



Length of the receiver ( $x = x_1 + x_2 + x_3$ ) in meters  $\longrightarrow$

Fig.2.6: Variation of the temperature along the length of the receiver

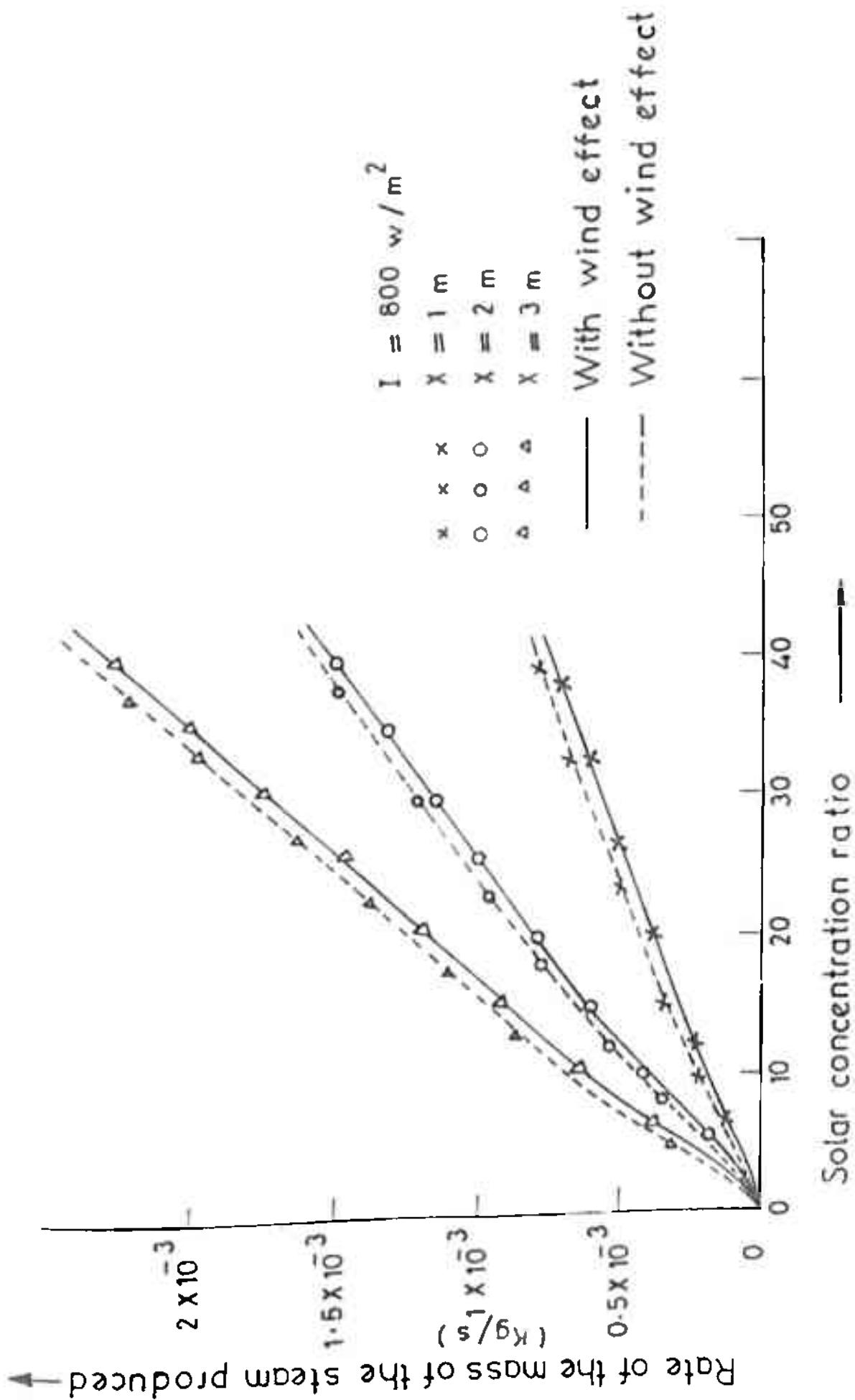


Fig.2.7: Variation of the rate of the mass of steam produced with solar concentration ratio .

CHAPTER - III

Analysis of a solar thermal electric -power generating system

## CHAPTER-III

### 3.1 INTRODUCTION :

One of the most important applications of solar concentrator - receiver system, is that it may be utilized to produce steam and hence electrical power. This can be done by coupling the solar steam generating system to an electric power generating system consisting of a steam turbine and an electric generator as shown in Fig. 3.1. The coupling is done through the nozzle. In the above combined system, the steam generated by steam generator, is allowed to pass through the nozzle by throttling action. The steam which comes out from the nozzle at high velocity, strikes on the blades of the turbine to do useful work. So, the kinetic energy of the working fluid is converted to mechanical energy by the turbine. This mechanical energy is utilized to drive the electric generator which produces electric power.

To supply mechanical force to drive a turbine, the pressure of the steam entering the turbine should be at least 6.89 bar [22]. This pressure is attained in a water system when the temperature of the water reaches  $422^{\circ}\text{K}$ . Theoretically, the steam can be raised at the above temperature and the pressure by choosing the suitable length of the receiver and the solar concentration ratio.

In this chapter, a mathematical model of a typical solar thermal electric power generating system has been presented. In this mathematical model, the expression for the mass flow rate of fluid, the net electrical power output have been obtained. Some

numerical calculation have been made to study the performance of this system. In the present study an econometric model has also been made to assess whether the above system is feasible or not. Some numerical calculations have also been done to find the cost per unit of electrical energy generated. The results, thus obtained, have been shown graphically and discussed.

### 3.2 ANALYSIS :

For mathematical analysis, following simplifying assumptions have been made :

- i) The flow of the fluid at any cross section of the receiver is uniform.
- ii) The intensity of light incident throughout the length of the receiver is uniform.
- iii) There is no transfer delay of the working fluid i.e water/steam.

The total length of the receiver,  $x (= x_1 + x_2 + x_3)$  as derived in the chapter - II can be written as

$$x = \frac{1}{A_1 C} \ln \left[ \frac{(P/C) - T_1}{(P/C) - T_b} \right] + \frac{\alpha}{\beta} [H_6 - H_1] + \frac{1}{A_3 C} \ln \left[ \frac{(P/C) - T_b}{(P/C) - T_v} \right] \quad (3.4)$$

Where,

$$P = I \eta_0 \cdot \left( \frac{r}{a} \right)^2$$

$$C = h_a \cdot h_r \cdot C$$

$$\alpha = \frac{m \cdot \pi \cdot \epsilon \cdot \sigma \cdot T^3}{4 \cdot R \cdot (b - a)}$$

$$\beta = 2\pi r_0 \cdot I \eta_0 \cdot R \cdot \left( \frac{r}{a} \right)^2$$

$$A_1 = \frac{2\pi r_0}{\left[ \dot{m} c_w (1 + \frac{C}{U}) \right]}$$

$$A_3 = \frac{2\pi r_0}{\left[ \dot{m} c_s (1 + \frac{C}{U}) \right]} \quad (3.2)$$

From the equation (3.1), the mass flow rate of the steam can be written as

$$\dot{m} = \frac{2\pi r_0 K x}{c_w \ln \frac{In_0 R + C(T_a - T_i)}{In_0 R + C(T_a - T_b)} + \frac{C(H_g - H_l)}{In_0 R + C(T_b - T_a)} + c_s \ln \frac{In_0 R + C(T_a - T_b)}{In_0 R + C(T_a - T_v)}} \quad (3.3)$$

The net mechanical power output from the solar thermal electrical power generating system may be written as

$$P_m = (H_4 - H_5) \eta_t \dot{m} \quad (3.4)$$

Where,  $\eta_t$  = Efficiency of the turbine  
 $H_4$  - The enthalpy of the steam at the inlet of the turbine at a pressure of  $P_4$  and temperature of  $T_4$ .  
 $H_5$  = The enthalpy of the turbine at the outline at a pressure of  $P_5$  and temperature of  $T_5$ .



The net electrical power output from the above system be as

$$P_e = (H_4 - H_5) \eta_t \eta_g \dot{m} \quad (3.5)$$

or

$$P_e = \frac{2\pi r_o K x (H_4 - H_5) \eta_t \eta_g}{c_w \ln \frac{In_o R + C(T_a - T_i)}{In_o R + C(T_a - T_b)} + \frac{C(H_4 - H_1)}{In_o R + C(T_b - T_a)} + c_s \ln \frac{In_o R + C(T_a - T_l)}{In_o R + C(T_a - T_v)}} \quad (3.6)$$

Where,  $\eta_g$  = The efficiency of the generator.

### 3.3 ECONOMIC ANALYSIS OF A SOLAR THERMAL ELECTRIC POWER GENERATING SYSTEM :

To determine whether a solar thermal electric power generating system is economically feasible or not, one must know the cost per unit of electric energy generated by the system.

The cost benefit analysis for determining the cost per unit of electricity produced by the above system, include the cost of the following components.

- i) Solar concentrator
- ii) Receiver
- iii) Steam trap
- iv) Steam turbine
- v) condenser
- vi) Generator
- vii) Feed water pump and
- viii) The piping system.

According to the cost estimate, the functional dependence of cost per unit aperture area of the concentrators on their concentration ratio for the small and large scale systems are -

$$C_{cu} = 11.5 (C-1)^{1/2} \quad (3.7)$$

and  $C_{cu} = 38.5 \log C$ , where,  $C$  = Concentration ratio (3.8)

The total capital cost of concentrator with aperture area  $A_c$  may be determined for small and large scale system respectively as.

$$C_c = 11.5 (C-1) A_c^{1/2} \quad (3.9)$$

$$\text{and } C_c = 38.5 \log C \cdot A_c \quad (3.10)$$

The capital cost of the receiver to be installed may be given by [ 31 ],

$$C_{ar} = C_{sr} (A_{sr} / A_{ar})^{0.6} \quad (3.11)$$

Where,  $C_{sr}$  = Cost of the standard receiver with outer surface area of  $A_{sr}$   
 $A_{ar}$  = Outer surface area of the new receiver to be installed.

The capital cost of steam trap can be given as

$$C_{st} = C_{ssp} (V_{ssp} / V_{asp})^{0.66} \quad (3.12)$$

Where,  $C_{ssp}$  = Cost of standard steam trap with volume  $V_{ssp}$   
 $V_{asp}$  = Volume of the new steam trap

The capital cost of turbine can be given as

$$C_{at} = C_{ast} (W_{st} / W_{at})^{0.53} \quad (3.13)$$

Where,  $C_{ast}$  = Cost of the standard turbine of the capacity  $W_{st}$  (H.P)  
 $W_{at}$  = H.P of new turbine.

The capital cost of the generator can be given as

$$C_{ag} = C_{sg} (W_{sg} / W_{ag})^{0.53} \quad (3.14)$$

Where,  $C_{sg}$  = Cost of standard generator of capacity  $W_{sg}$  (KW)

$W_{ag}$  = Capacity (KW) of the new generator.

The capital cost of feed water pump (Centrifugal) be given

as

$$C_{ap} = C_{sp} (W_{sp} / W_{ap})^{0.61} \quad (3.15)$$

Where,  $C_{sp}$  = Cost of standard pump of capacity  $W_{sp}$  in  $m^3$  (hour)

$C_{ap}$  = Capacity of the new pump to be installed.

The capital cost of condenser having capacity  $W_{ac}$  ( $m^3$  / hour) may

be given as,

$$C_{ac} = C_{sc} (W_{sc} / W_{ac})^{0.61} \quad (3.16)$$

Where,  $C_{sc}$  = Cost of the standard condenser of capacity  $W_{sc}$  ( $m^3$  / hour)

The cost of the metal pipe having total length of  $L$ , can be

given as

$$C_l = C_{ul} \cdot L$$

Where,  $C_{ul}$  = Cost per unit length

The capital cost of the land having total area of  $A_f$  is

$$C_f = (C_{fu} / l_f) A_f$$

Where,  $C_{fu}$  = Cost per unit area of the land

$l_f$  = land utilization factor.

Using the expressions (3.17) to (3.18), the cost per unit electricity generated by the system may be calculated as

$$C_E = \frac{[(C_c + C_{ar} + C_{st} + C_{at} + C_{ag} + C_{ap} + C_{ac} + C_l) - F] L_{in} (1+f)^n}{365 I A C \eta_D R \eta_r \eta_t \eta_g \eta_{ss}} \quad (3.19)$$

Where,  $F$  = Salvage value of the whole system at the end of  $n$ th year.

$L_{in}$  = Annual capital recovery factor.

$$\frac{i(1+i)^n}{(1+i)^n - 1}$$

$n$  = Life period of the system.

$i$  = Rate of interest of borrowed money.

$f$  = Factor annual maintenance cost, etc.

$I$   
 $I$  = Intensity of solar radiation.

$\eta_0$  = Optical efficiency of the concentrator.

$R$  = Solar concentration ratio.

$\eta_r$  = Efficiency of the receiver.

$\eta_t$  = Efficiency of the turbine.

$\eta_g$  = Efficiency of the generator.

$h_s$  = average sunshine hour per day.

ss

### 3.4 RESULTS AND DISCUSSIONS:

The analysis presented in the section 3.2 may be used to study the performance of a solar-thermal electric power generating system comprising a solar steam generator provided with a linear solar concentrator - receiver system, turbine and an electric generator. Some numerical calculations have been made for a typical system in which a combined linear solar concentrator and a receiver system is used.

Figure 3.2 shows the variation of electrical power output with solar concentration ratio. It can be seen that at the beginning, the electrical power output changes rapidly but at higher concentration ratio the gain in the electrical power output is less. It is due to the fact that at lower solar concentration ratio the loss in power is less whereas at higher concentration ratio, the power loss is high.

Figure 3.3 shows the variation of the mechanical power output with the solar concentration ratio. It is observed that there is

Increase in mechanical power output from the turbine with the increase in solar concentration ratio up to certain extent. However, further increase in solar concentration ratio leads to relatively lower mechanical power output. It may be attributed to the fact that at lower concentration ratio power loss is less where as at higher concentration ratio the power loss is high. Figure 3.4 shows the variation of the electrical power output with the length of the receiver. It is evident from this graph that there is exponential increase in the length of the receiver. The reason for this is that for same mass flow rate of working fluid, larger length of the receiver enables more absorption of thermal power during the flow of the fluid along the length of the receiver.

3.5 THE LIST OF THE FIGURE CAPTIONS:

Fig.3.1 : Schematic diagram of a solar-thermal electric power generating system using linear solar concentrator.

Fig.3.2 : Variation of electrical power output with solar concentration ratio.

Fig.3.3 : Variation of mechanical power output with solar concentration ratio.

Fig.3.4 : Variation of electrical power output with the length of the receiver.

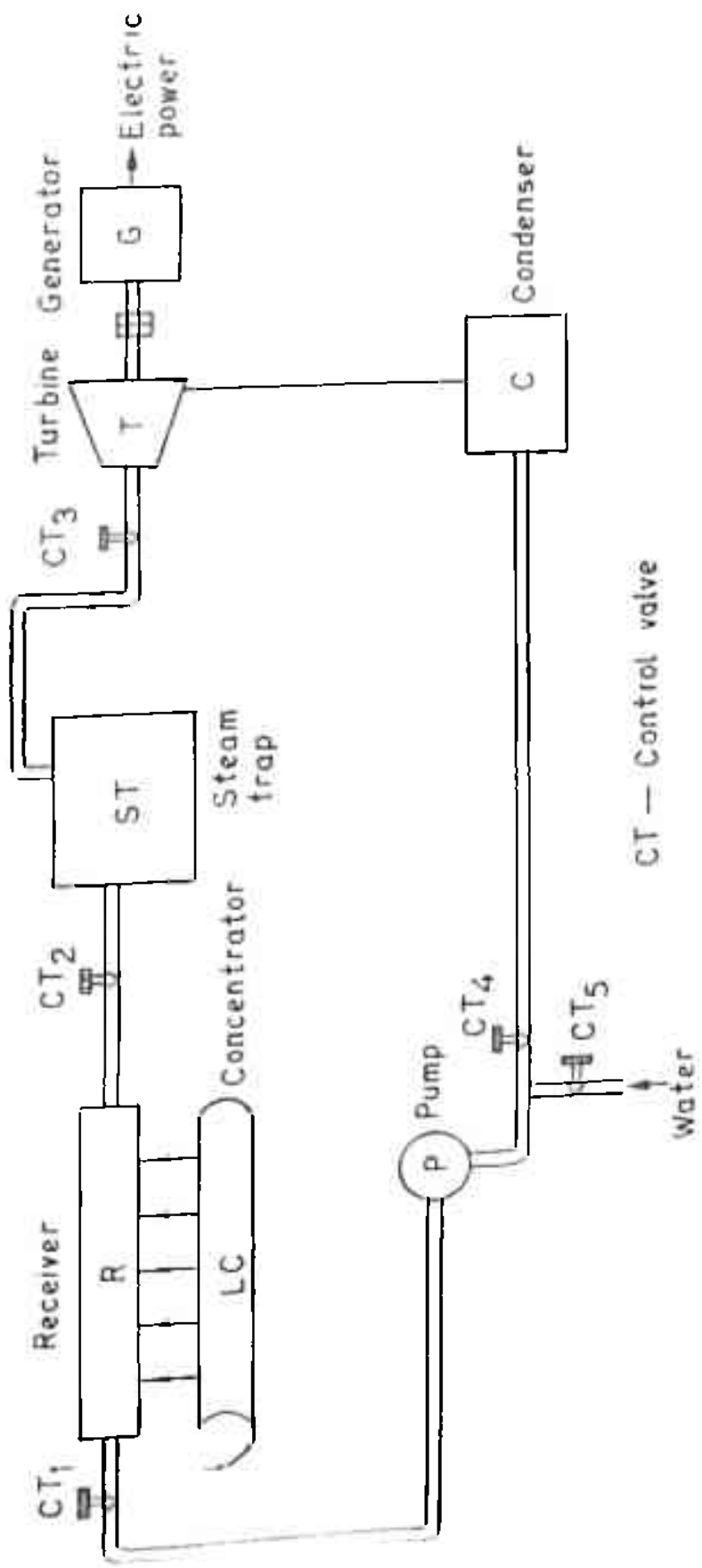


Fig. 3.1: Schematic diagram of a Solar-thermal electric power generating system using a linear concentrator.

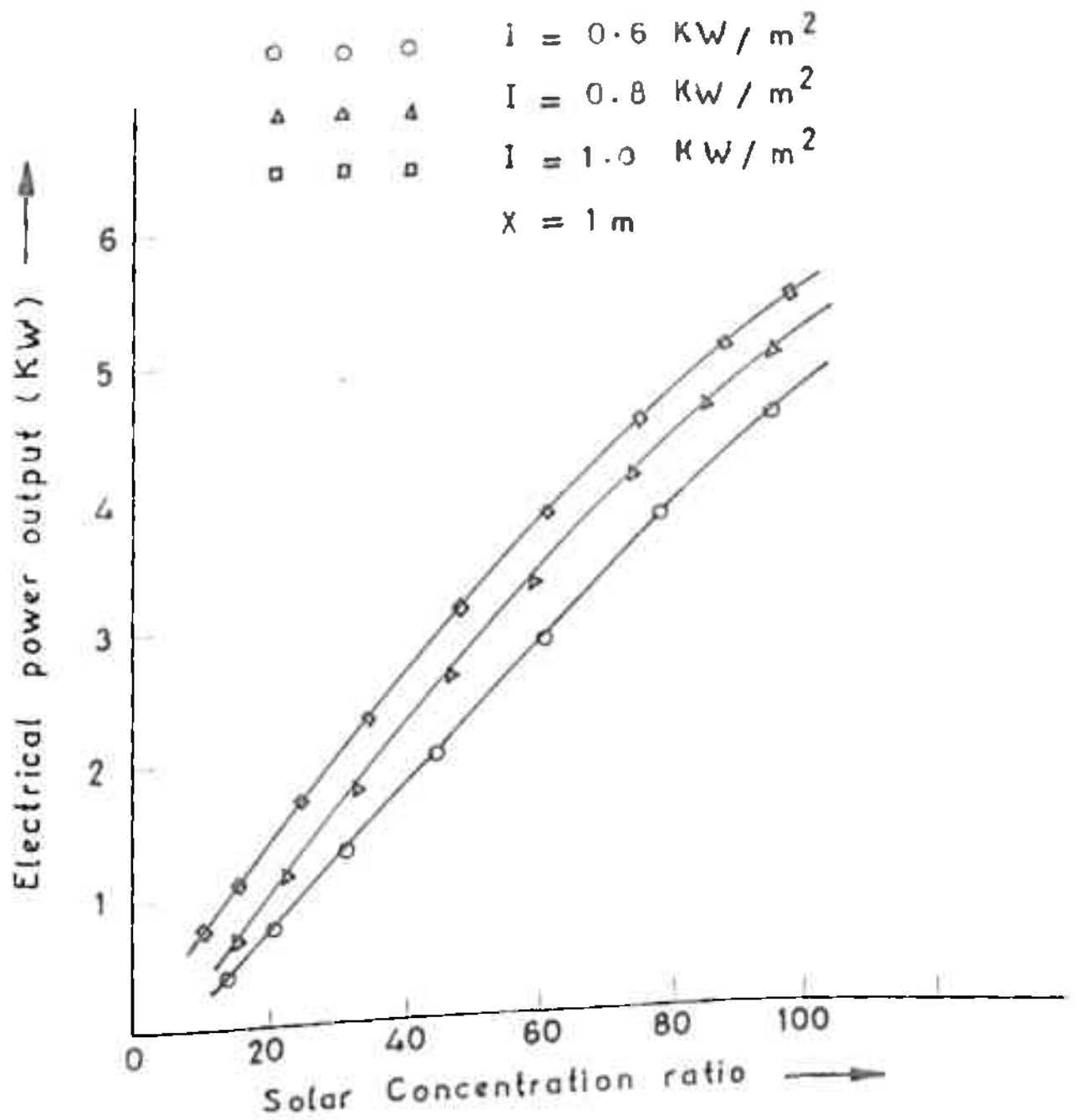


Fig. 3. 2 Variation of electrical power output with solar concentration ratio



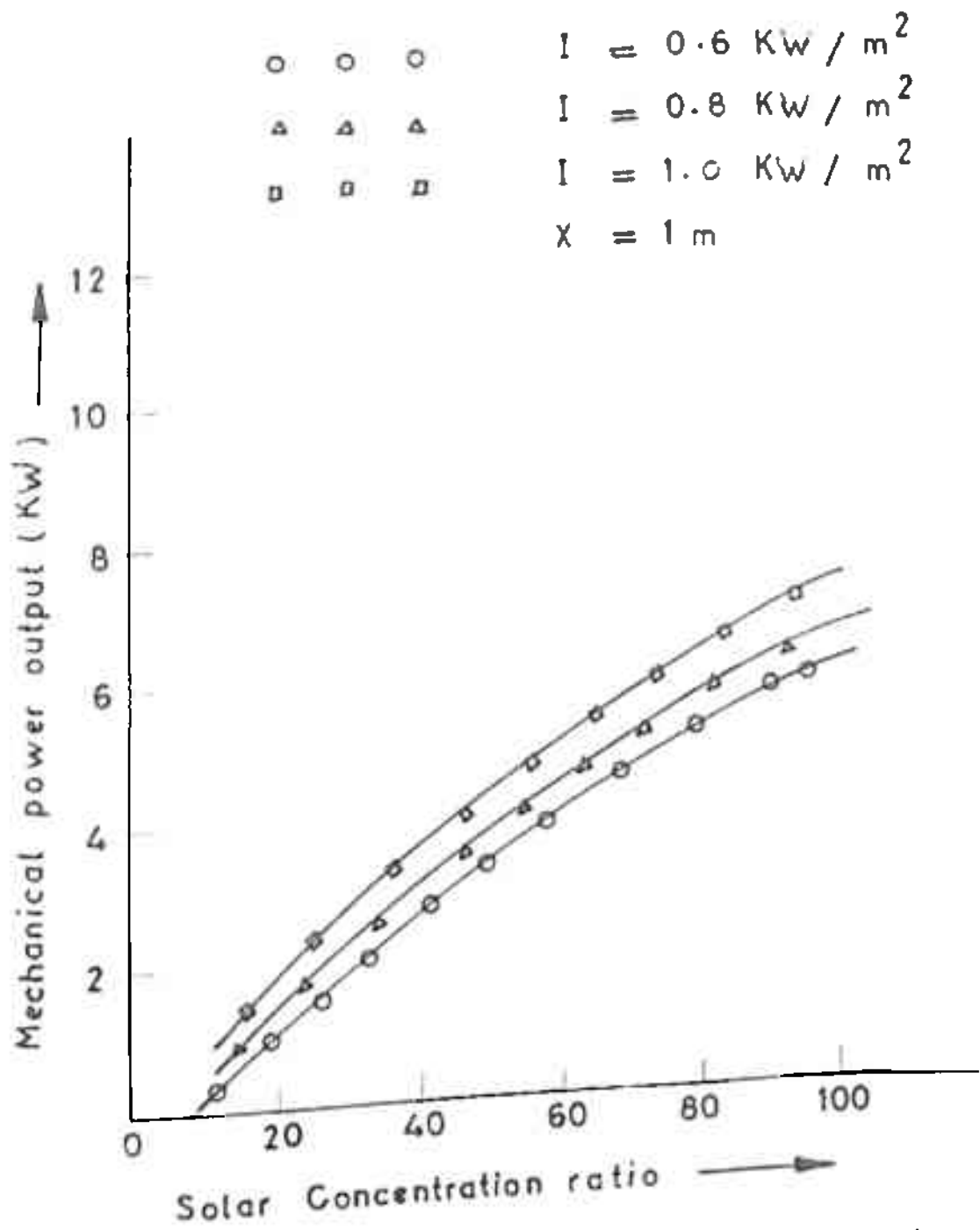


Fig. 3.3: Variation of mechanical power output with solar concentration ratio

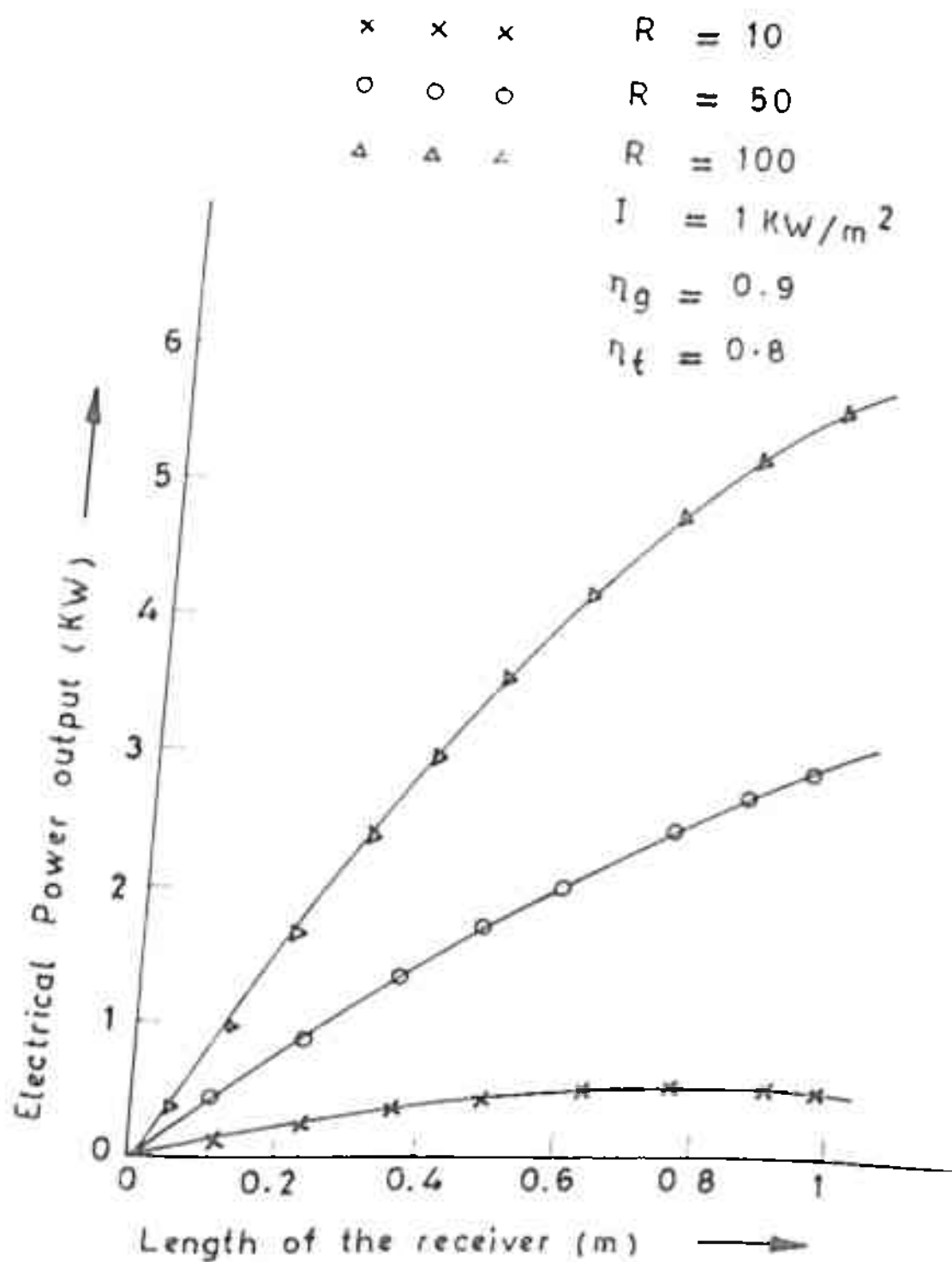


Fig 3.4: Variation of electrical power output with the length of the receiver.

CHAPTER - IV

Analysis of a combined system consisting of a solar steam generator and a water pumping system for irrigation

## CHAPTER - IV

### 4.1 INTRODUCTION

A solar steam generating system may be applied to drive a prime mover coupled to a centrifugal pump for irrigation. For this a typical solar steam generating system may be coupled to the prime movers such as steam turbine or steam engine which drives a centrifugal pump for lifting water for irrigation. The steam turbine is better of the two because of the following reasons:

- i) Steam turbine has higher thermal efficiency than steam engine.
- ii) Unlike steam engine there is no sliding or bearing member in steam turbine. Hence, the mechanical efficiency of steam turbine is higher than that of the steam engine.
- iii) The absence of reciprocating masses makes the steam turbine better balanced than the steam engine.
- iv) Higher range of speed is not possible in steam engine where as greater range of speed is possible in steam turbine.
- v) The wear, tear and the maintenance cost of steam turbine, are very low compared to that of the steam engine.

Since, a steam turbine has higher efficiency than that of the steam engine, it may be used in some specific areas like water lifting for irrigation and running printing press, etc.

In the present study, a mathematical model of a typical combined solar steam generating system coupled to a water lifting system for irrigation, has been presented. An econometric model, of the above combined system has also been included. Some numerical calculations have been done to study the performance of this system. The results, thus obtained, have been shown graphically and discussed.

#### 4.2 ANALYSIS :

For the analysis of the system, the following simplifying assumptions were made :

- i) A single stage reaction turbine is used as prime mover.
- ii) Head loss in the water lifting system is negligible.

The required pumping capacity of the pump may be given as

$$C_p = \frac{A \cdot L}{t} \text{ m}^3/\text{s} \quad (4.1)$$

Where, A = Area of the irrigation field.

L = Depth of water in the irrigation field (m.)

t = Time required (Second.)

The power required by the pump to lift water is given by,

$$P_p = \frac{K C_p h \cdot \rho}{\eta_p} \quad (4.2)$$

Where,  $\eta_p$  = The efficiency of the pump. K = Conversion factor

h = The head of water (m)

$\rho$  = Density of water (kg/m<sup>3</sup>)

Using the equations (4.1) and (4.2) the expression for the power required by the pump can be written as

$$P_p = \frac{A L h \rho}{\eta_p t} \quad (4.3)$$

Since the power required by the pump is supplied by the prime mover i.e. the steam turbine, the power supplied by the steam turbine may be written as

$$P_t = \dot{m} (H_4 - h_5) \eta_t \quad (4.4)$$

where,  $\eta_t$  = The efficiency of the turbine.

$H_4$  = The enthalpy of the steam at the inlet of the turbine (KJ/Kg)

$h_5$  = The enthalpy of the steam at the outlet (KJ/Kg)

$\dot{m}$  = Mass flow rate of steam (kg/s)

Since,  $P_p = P_t$ , then equating equations (4.3) and (4.4) we may write,

$$\dot{m} (H_4 - h_5) \eta_t = \frac{K A L h \rho}{\eta_p t}$$

$$\text{or, } \dot{m} = \frac{K A L h \rho}{(H_4 - h_5) \eta_t \eta_p} \quad K = \text{conversion factor} \quad (4.5)$$

But the expression for mass flow rate of steam, as derived in section 3.2, may be given as

$$2\pi r_o K x$$

$$\dot{m} = \frac{c_w \ln \left[ \frac{I \eta_o R + C(T_a - T_i)}{I \eta_o R + C(T_a - T_b)} \right] + \frac{C(H_g - H_l)}{I \eta_o R (T_b - T_a)} + c_s \ln \left[ \frac{I \eta_o R + C(T_a - T_b)}{I \eta_o R + C(T_a - T_v)} \right]}{(h_4 - h_5) \eta_t \eta_p} \quad (4.6)$$

#### 4.3 ECONOMETRIC MODEL :

To find whether a combined solar steam generator coupled to a water lifting system for irrigation, is economically feasible or not, it is required to find the cost per unit water pumping capacity ( $m^3$ /hour). For the econometric model of the above system, the cost of the following components have been considered;

- i) Solar concentrator
- ii) Solar steam generator
- iii) Steam trap
- iv) Steam turbine
- v) Condenser
- vi) Feed water pump
- vii) Piping system, and
- viii) Irrigation pump

The cost of concentrator per unit aperture <sup>AREA</sup><sub>A</sub> for small scale system is given by

$$C_{cu} = 11.5 (C-1)^{1/2} \frac{A}{C} \quad (4.7)$$

Total cost of solar concentrator with aperture area A can be given by

$$C_c = 11.5 (C-1)^{1/2} \frac{A}{C} \quad (4.8)$$

The capital cost of the receiver to be installed may be given

$$C_{ar} = C_{sr} \left( \frac{A_{ar}}{A_{sr}} \right)^{0.6} \quad (4.9)$$

Where,  $C_{sr}$  = Cost of standard receiver with outer surface area of  $A_{sr}$

$A_{ar}$  = Outer surface area of the new receiver to be installed.

The capital cost of steam trap may be given as

$$C_{st} = C_{ssp} \left( \frac{V_{asp}}{V_{ssp}} \right)^{0.66} \quad (4.10)$$

Where,  $C_{ssp}$  = Cost of standard steam trap with volume  $V_{ssp}$

$V_{asp}$  = Volume of new steam trap to be installed

The capital cost of turbine may be given as

$$C_{at} = C_{ast} \left( \frac{W_{at}}{W_{st}} \right)^{0.53} \quad (4.11)$$

Where,  $C_{ast}$  = Cost of standard turbine of the capacity  $W_{st}$  (H.P)

$W_{at}$  = Horse power of new turbine to be installed.

The capital cost of condenser having capacity  $W_{ac}$  ( $m^3$ /hour) may be given as

$$C_{ac} = C_{sc} \left( \frac{W_{ac}}{W_{sc}} \right)^{0.61} \quad (4.12)$$

Where,  $C_{sc}$  = Cost of the standard condenser of capacity  $W_{sc}$  ( $m^3$ /hour)

$W_{asc}$  = Capacity of the new condenser in ( $m^3$ /hour)

The capital cost of the feed water pump may be given as

$$C_{ap} = C_{sp} \left( \frac{W_{ap}}{W_{sp}} \right)^{0.61} \quad (4.13)$$

Where,  $C_{sp}$  = Cost of standard pump of capacity  $W_{sp}$  ( $m^3$ /hour)

$W_{ap}$  = Capacity of the new pump to be installed.

The total cost of piping system may be given as

$$C_l = C_{ul} \cdot L \quad (4.14)$$



Where,  $L$  = total length of the piping system in m.

$C_{ul}$  = Cost per unit length.

The capital cost of the water lifting pump may be given as

$$C_{pi} = C_{spi} (W_{api} / W_{spi})^{0.7} \quad (4.15)$$

Where,  $C_{spi}$  = Cost of standard irrigation pump with capacity  $W_{spi}$  H.P.

$W_{api}$  = Capacity in H.P of the new pump to be installed

The capital cost of the land having total area of  $A_f$  may be written as

$$C_f = (C_{fu} \cdot A_f) / l_f \quad (4.16)$$

Where,  $C_{fu}$  = Cost per unit area of the land

$l_f$  = Land utilization factor.

Using equations (4.9) to (4.16) the cost per unit volume of water, pumped by the water lifting system may be written as

$$C = \frac{[(C_a + C_{at} + C_{st} + C_{at} + C_l + C_{pi} + C_{se} + C_f) - F] L_{in} (1+i)^n}{365 C_{pss} h} \quad (4.17)$$

Where,  $L_{in}$  = Annual capital recovery factor

$$L_{in} = \frac{i(1+i)^n}{(1+i)^n - 1} \quad (4.18)$$

$i$  = Rate of interest on borrowed money

$f$  = Factor for maintenance cost, etc.

$h$  = Average sunshine hour per day

$n$  = Life period of the system

#### 4.4 RESULTS AND DISCUSSIONS:

The analysis presented in the section 4.2 has been used to study the performance of a solar steam generator coupled to a water

lifting system using centrifugal pump for irrigation. Some numerical calculations have been made considering a total area of one acre of irrigation land in which water is to be supplied by the above system.

Figure 4.2 shows the variation of pumping rate of water with the solar concentration ratio. It can be observed that at the beginning, there is very small increase in the rate of pumping of water (m<sup>3</sup>/hour) with the increase in the solar concentration ratio but at higher solar concentration ratio, increase is quite appreciable in the pumping rate of water. It is due to the fact that at lower concentration ratio the input power to the pump is very much less than that of at higher concentration ratio.

Figure 4.3 shows the variation of water head with the solar concentration ratio. It may be seen that the increase in the head of water to be pumped is more at higher concentration ratio than that of at lower concentration ratio. It may be attributed to the fact that the power supplied to the pump by the primemover is more at higher concentration ratio than that of at lower concentration ratio.

Figure 4.4 shows the variation of the depth of the water on the irrigation land with solar concentration ratio. It may be observed that at higher concentration ratio there is rapid increase in the depth of water on the irrigation land. This is due to the fact that at higher concentration ratio the pump has higher pumping capacity of water (m<sup>3</sup>/hour) than that of at lower concentration ratio.

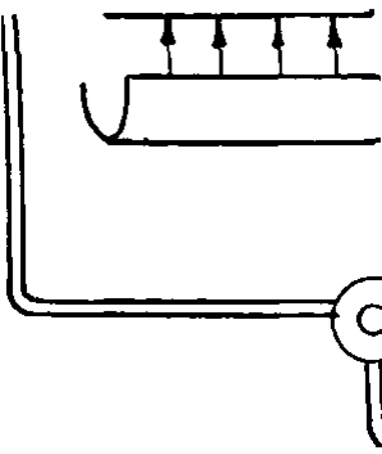
#### 4.5 THE LIST OF THE FIGURE CAPTIONS:

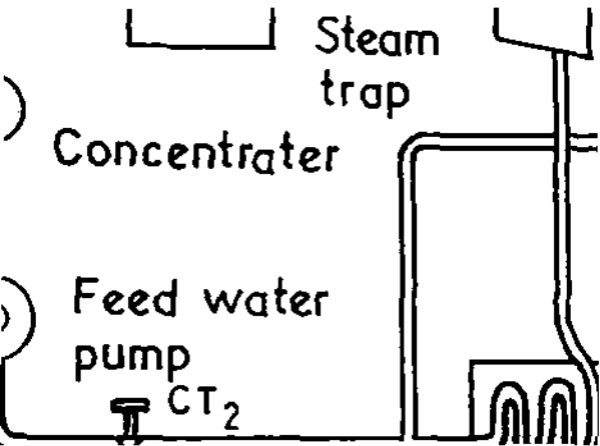
Fig. 4.1 : Schematic diagram of a solar steam generator coupled to a water lifting system for irrigation.

Fig. 4.2 : Variation of water pumping rate with solar concentration ratio.

Fig. 4.3 : Variation of water head with solar concentration ratio.

Fig. 4.4 : Variation of depth of water on the irrigation land with solar concentration ratio.





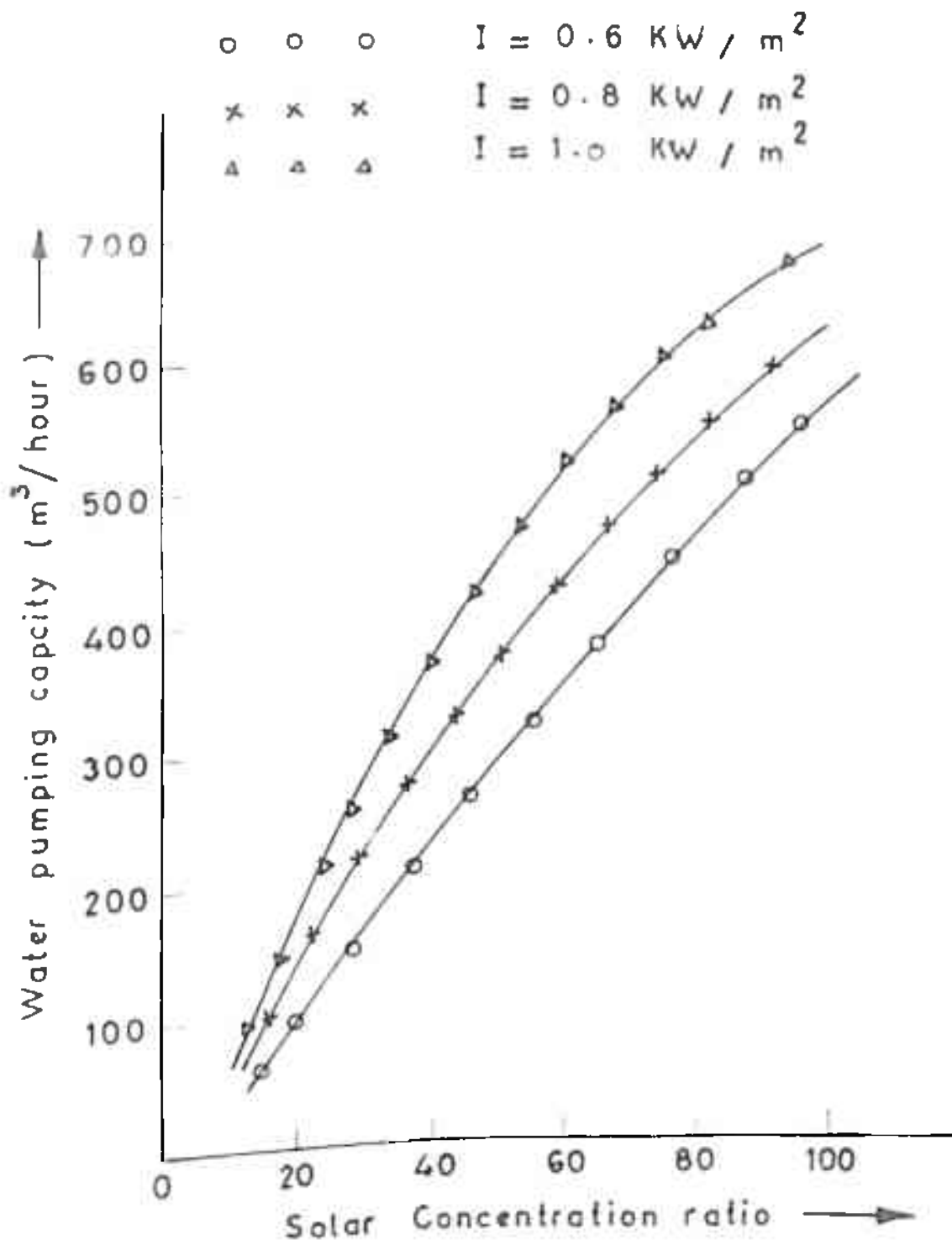


Fig. 4.2 Variation of water pumping rate with solar concentration ratio

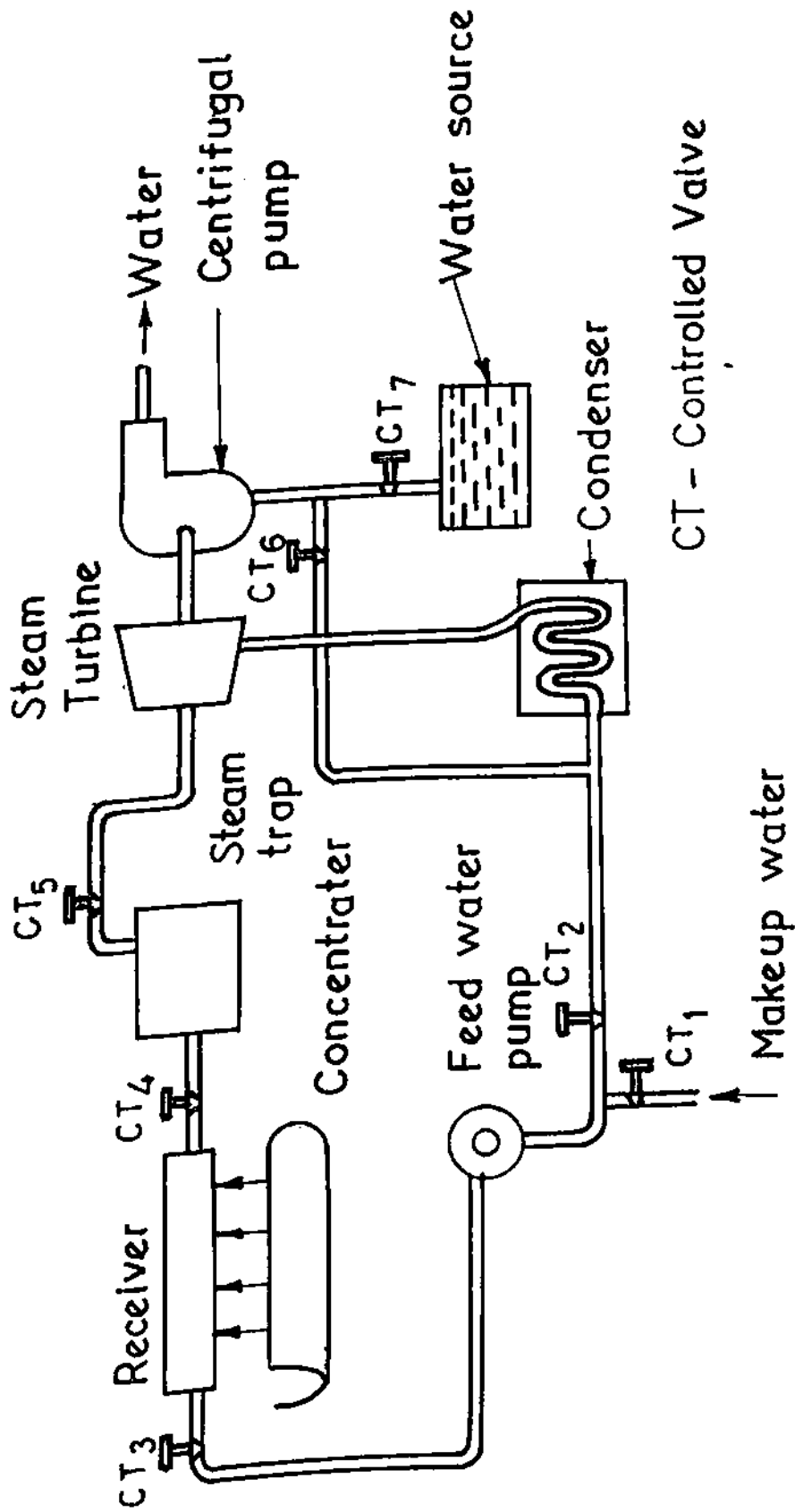


Fig.4.4: Schematic diagram of a solar - steam generator coupled <sup>to a</sup> water lifting system for irrigation .

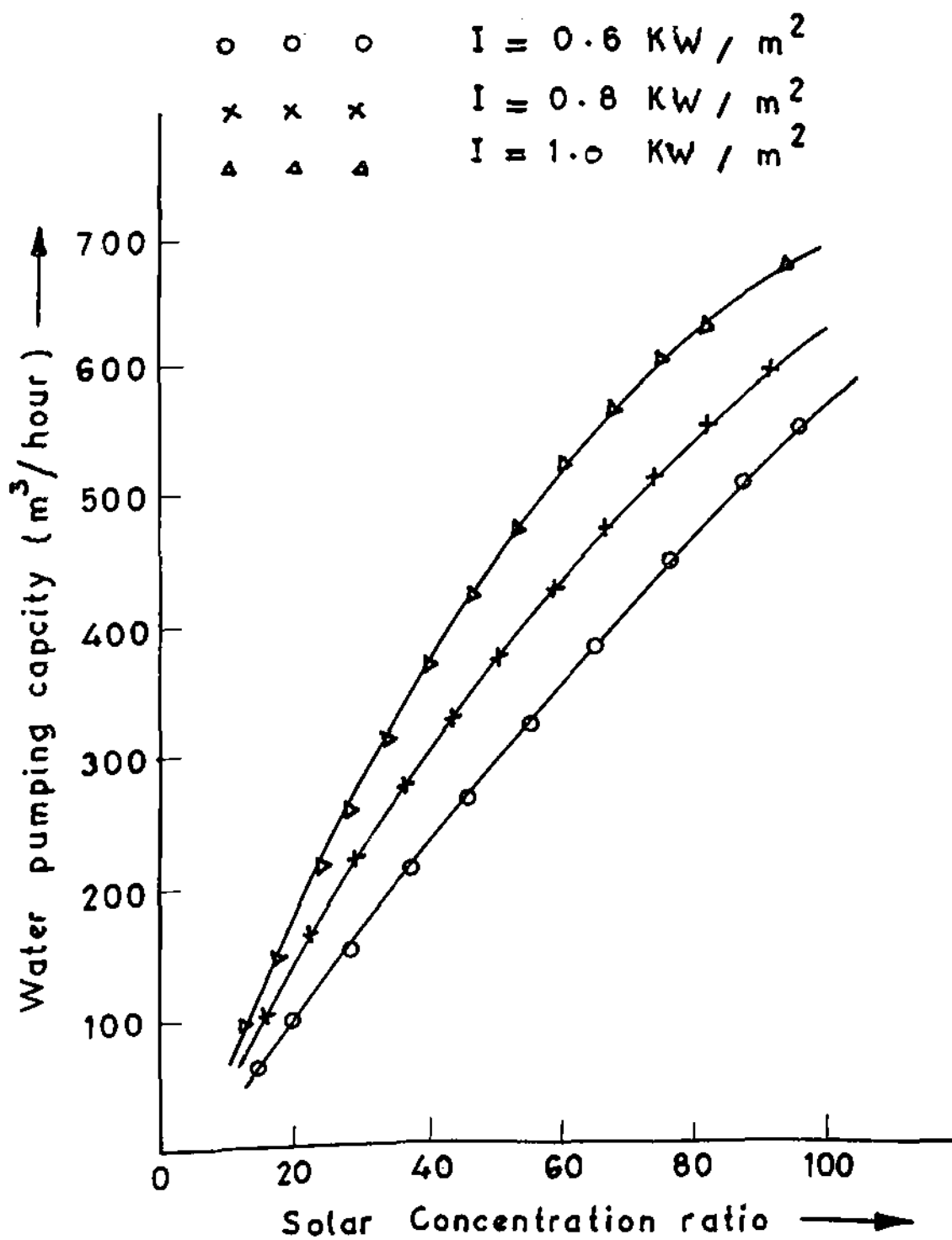


Fig. 4.2 Variation of water pumping rate with solar concentration ratio



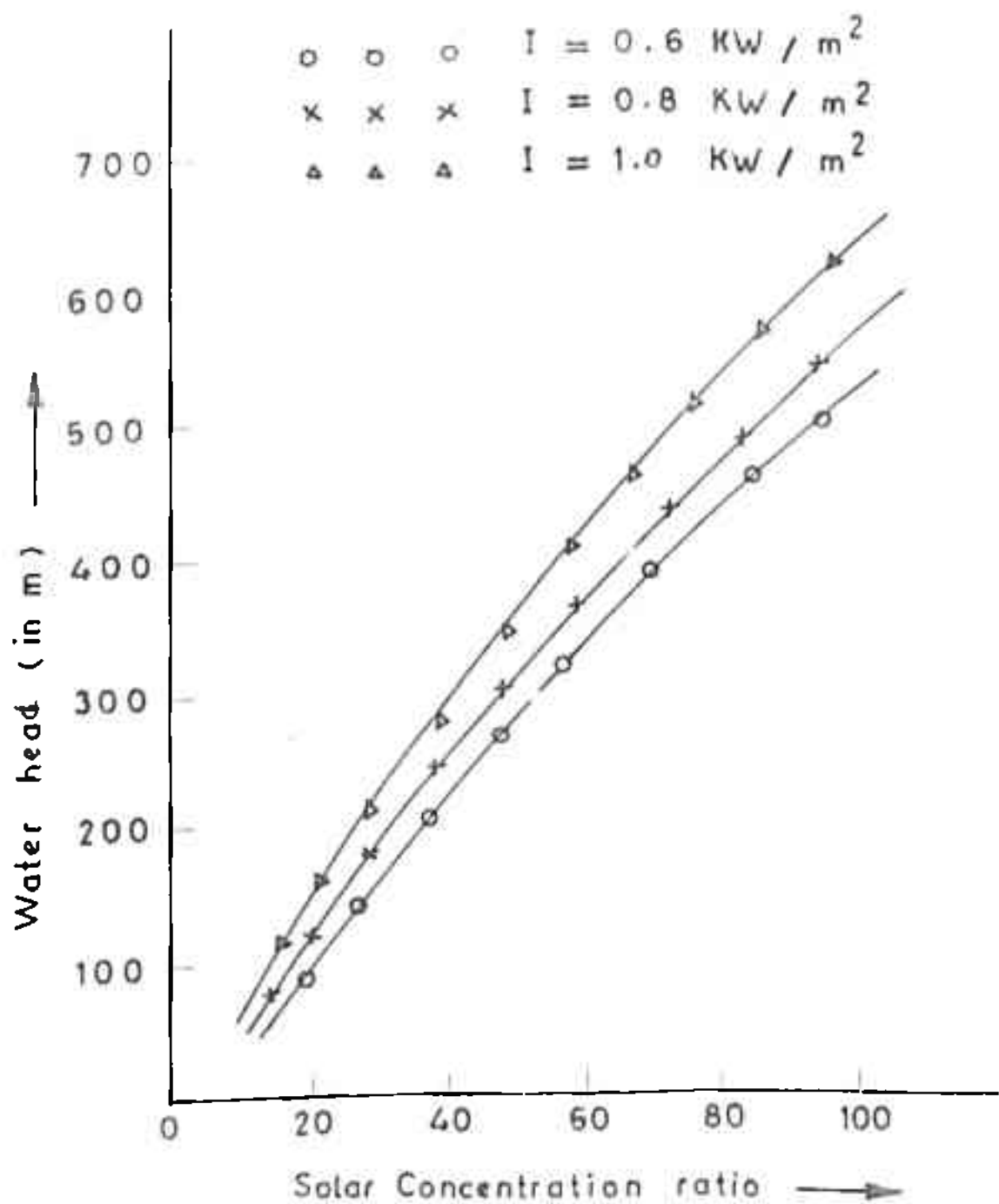
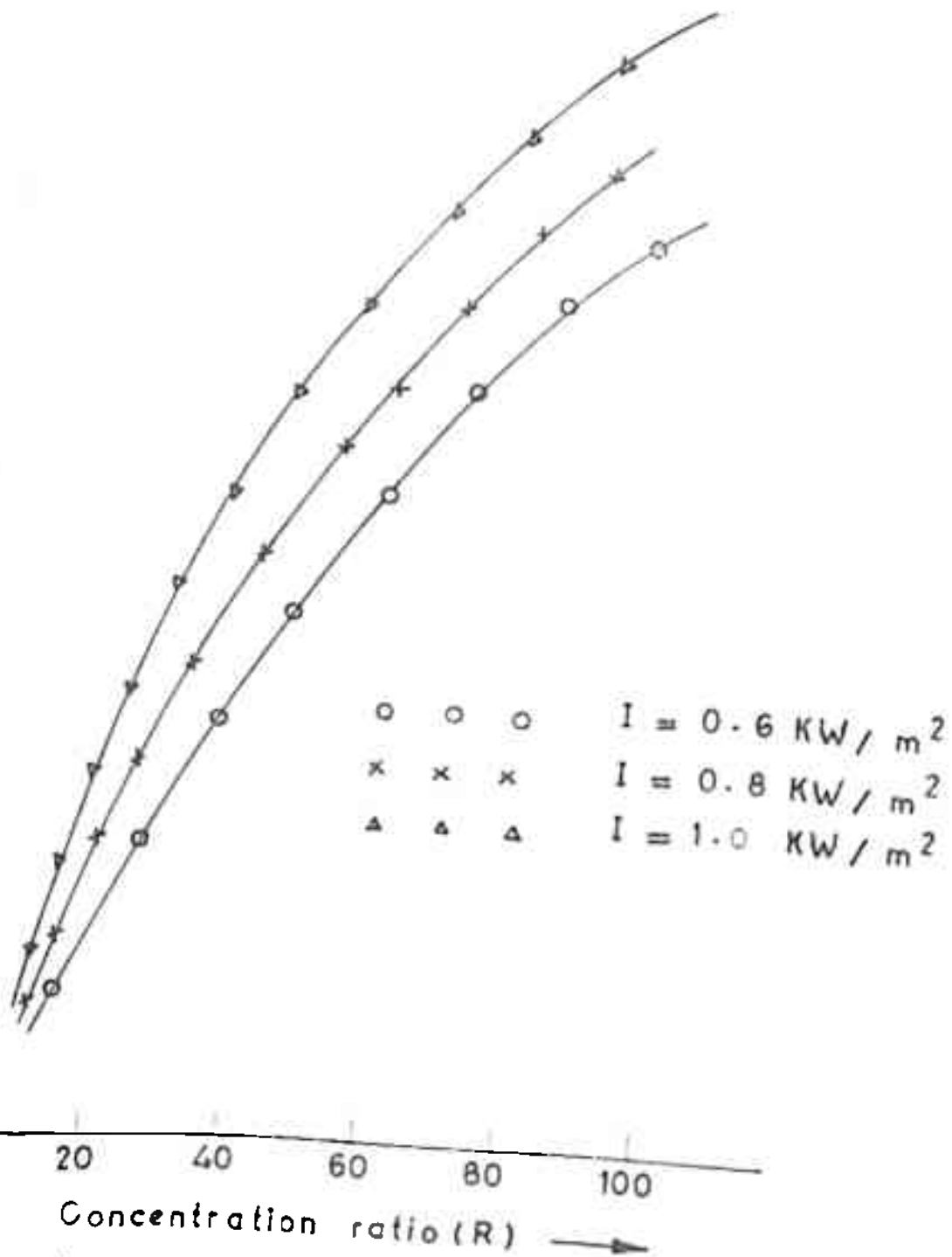


Fig. 4.3 Variation of water head with solar concentration ratio.



Variation of depth of water on the irrigation, and with solar concentration ratio

CHAPTER - V

Experiments on a solar thermal concentrator-receiver system

### 5.1 INTRODUCTION:

This chapter presents the results of some preliminary experiments conducted on a prototype combined solar thermal concentrator and receiver system. It consists of a linear composite parabolic concentrator and a copper tube receiver of circular cross section, placed on the focal plane of the concentrator.

The results presented include the studies of

- (i) variation of the temperature of the water along the length of the receiver for different concentration ratios.
- (ii) variation of the temperature of the water along the length of the receiver for different mass flow rates of water.
- (iii) variation of the temperature of the water along the length of the receiver with the time during day (ie, with the change in the intensity of the solar radiation).
- (iv) variation of the temperature of the water along the length of the receiver with the wind velocity.

### 5.2 TEST SETUP

The test setup consists of mainly following major components:

- (i) Linear composite parabolic concentrator.
- (ii) Receiver
- (iii) Arrangement for circulating water through the receiver
- (iv) Measuring instruments.

#### 5.2.1 Linear composite parabolic concentrator:

The linear composite parabolic concentrator used in the test

setup was fabricated using locally available materials. Its body is made of mica sheet bent into a parabolic shape. It has aperture breadth of 77 cm, and its length is 125 cm. The distance between the surface plane of the central mirror strip and the focal plane is 15 cm. The reflector is made of 48 mirror strips, each of 125 cm in length and of 15 mm width, placed on each half of the concentrator. The supporting structure is made of angle irons. The whole system may be tracked from east to west and also can be tilted manually with the position of the sun. The maximum geometrical concentration ratio for this concentrator is about 44.

#### 5.2.2 Receiver:

The receiver placed on the focal plane of the concentrator is used as absorber of the solar radiation reflected by the parabolic concentrator. It is made of copper tube of circular cross section. It has internal diameter of 20mm, outer diameter of 25mm and wall thickness of 2.5 mm. Its length is 125 cm. It is painted black. This black paint coated copper tube is covered with glass tube (Fig.5.2) to reduce heat loss from the surface of the absorber.

#### 5.2.3 Arrangement for circulating water through the receiver:

Water was used as the working fluid in the receiver. A water tank has been used to supply water to the receiver. The natural circulation type arrangement was made to <sup>make</sup> water <sup>flow</sup> through the receiver. Gate valves were used at the inlet and outlet to control the flow rate of water through the receiver.

#### 5.2.4 Measuring instruments :

periments

Following measuring devices were used for

##### i) Thermometers:

Six thermometers were used to measure the temperature of the working fluid along the length of the receiver. They were placed at different points along the length of the receiver.

##### ii) Measuring cylinder and stop watch:

A measuring cylinder and a stop watch were used to measure the flow rate of water through the receiver. The measuring cylinder was used to collect the hot water and the stop watch was used to note time of hot water collected.

##### iii) Solar intensity meter:

A pyranometer was used to measure the intensity of solar radiation during the day. It is connected to a recorder through a sensor. The recorder recorded the variation of the intensity of solar radiation during the day.

##### iv) Anemometer:

It was used to measure the speed of the wind so that the effect of the wind on the heat loss from the surface of the receiver could be studied. It was connected through the sensor to the same recorder to which the pyranometer was connected.

#### 5.3 TEST PROCEDURE:

The schematic diagram of the arrangement for the test setup of the prototype solar concentrator and receiver system is shown in Fig. 5.1

The following steps were followed to conduct the experiments on the test setup having a fixed length of the receiver.

i) In the first experiment, the flow rate of water was kept constant. This was done by keeping the gate valve  $G_3$  at a fixed position and the other gate valves  $G_1$  and  $G_2$  fully open. At this position of the outlet gate valve  $G_3$  of the receiver, the flow rate of water was measured using measuring cylinder and the stop watch.

At a particular value of the solar concentration ratio, the readings of six thermometers, placed at different positions of the receiver, were noted. The initial temperature of water and the ambient temperature were also noted. The readings of the wind speed meter and the solar intensity meter were noted. The above procedures were followed at various solar concentration ratios of the concentrator (by changing the number of mirror strips).

ii) In the second experiment, the solar concentration ratio of the concentrator was kept fixed. At different flow rates of water (by changing the position of the gate valve  $G_3$ ), the readings of six thermometers were noted. The speed of the wind and the intensity of the solar radiation were also noted from the recorder.

iii) In the third experiment, the flow rate of water and the solar concentration ratio were kept constant. The readings of the thermometers were noted at different hours of the day (ie, with the change of the intensity of solar radiation).

iv) In the fourth experiment, the flow rate of water and the solar concentration ratio were kept constant and at a fixed value of the intensity of the solar radiation the readings of the thermometers were noted for the various values of the speed of the wind.

The observations of the above four experiments have been shown in Table-I, Table-II, Table-III and Table-IV.

#### 5.4 RESULTS AND DISCUSSIONS:

The data obtained from the observations are shown in Table-I, Table-II, Table-III and Table-IV and have also been graphically plotted to study the temperature variation along the length of the receiver.

Figure 5.3 shows the variation of the temperature along the length of the receiver with the solar concentration ratio.

It may be observed that the rate of rise in temperature of the water along the length of the receiver is more at higher concentration ratio than that of at lower concentration ratio for mass flow rate of water. It is due to the fact that the receiver absorbs more heat at higher concentration ratio than that of at lower concentration ratio.

Figure 5.4 shows the variation of the temperature along the length of the receiver with the mass flow rate of water. It may be seen that the rate of rise in temperature of water along the length of the receiver is less at higher mass flow rate of water than that at lower mass flow rate. It may be due to the fact that at same intensity of solar radiation and solar



concentration ratio, the heat absorbed by the receiver is fixed. It is, however obvious that at higher mass flow rate of water the rise in temperature of water is less than that of at lower mass flow rate of water.

Figure 5.5 shows the variation of the temperature along the length of the receiver with the intensity of the solar radiation.

It may be indicated that at higher intensity of solar radiation, the rate of rise in temperature of water is more than that at lower intensity of solar radiation. It is due to the fact that at higher intensity of solar radiation, the heat received by the receiver is comparatively more than that at lower intensity of solar radiation for fixed solar concentration ratio and the mass flow rate of water.

Figure 5.6 shows the variation of the temperature along the length of the receiver with the speed of the wind.

It may be observed that there is more fall in temperature of water along the length of the receiver at higher wind speed than that at lower wind speed. It is due to the fact that at higher wind speed the heat loss from the surface of the receiver is more than that at lower wind speed.

Figure 5.6 shows the variation of the water temperature along the length of the receiver for theoretical as well as experimental results. It may be observed that the rate of rise in temperature is more in case of theoretical results due to obvious reasons for the simplified assumptions made. The experimental results, however show good agreement with theoretical results.

TABLE -I

| Intensity of solar radiation, $I$ ( $KW/m^2$ ) | Wind speed, $V_w$ ( m/s) | Solar concentration ratio, $R$ | Mass flow rate of water, $m_w$ (kg/s) | Ambient temperature, $T_a$ ( $^{\circ}C$ ) | Initial temperature of water, $T_i$ ( $^{\circ}C$ ) |
|--|--------------------------|--------------------------------|---------------------------------------|--|---|
| 0.1030   | 2.6                      | 5                              | 0.003                                 | 30   | 37  |
|  | 2.7                      | 10                             | 0.003                                 | 40   | 37.5  |
|  | 2.6                      | 15                             |                                       | 40.5                                       | 38  |

---

Temperatures of the water in the receiver at the length of

| 0.20<br>(m)     | 0.40<br>(m)     | 0.60<br>(m)     | 0.80<br>(m)     | 0.100<br>(m)    | 0.120<br>(m)    |
|-----------------|-----------------|-----------------|-----------------|-----------------|-----------------|
| $T_1$           | $T_2$           | $T_3$           | $T_4$           | $T_5$           | $T_6$           |
| ( $^{\circ}$ C) | ( $^{\circ}$ C) | ( $^{\circ}$ C) | ( $^{\circ}$ C) | ( $^{\circ}$ C) | ( $^{\circ}$ C) |

---

44      53      62      67      76      83

48      59      67      77      84      89

50      64      75      84      90      96

---

TABLE-II

| intensity of solar radiation, $I$ ( $KW/m^2$ ) | Wind speed, $V_w$ ( $m/s$ ) | solar concentration ratio, $R$ | Mass flow rate of water, $\dot{m}_w$ ( $kg/s$ ) | Ambient temperature, $T_a$ ( $^{\circ}C$ ) | Initial temperature of receiver at the length of 0.20, 0.40, 0.60, 0.80 & 1.00 Cm | Temperature of the water in the receiver at the length of 0.20, 0.40, 0.60, 0.80 & 1.00 Cm |                       |                       |                       |    |    |
|--|-----------------------------|--------------------------------|---|--|---|--|-----------------------|-----------------------|-----------------------|----|----|
|  |                             |                                |   | $T_1$ ( $^{\circ}C$ )                      | $T_2$ ( $^{\circ}C$ )   | $T_3$ ( $^{\circ}C$ )  | $T_4$ ( $^{\circ}C$ ) | $T_5$ ( $^{\circ}C$ ) | $T_6$ ( $^{\circ}C$ ) |    |    |
| 0.900  | 3.0                         |                                |   | 33   | 29  | 33.5   | 43                    | 50                    | 57                    | 54 | 55 |
| 0.930  | 3.1                         | 2.0                            | 0.004   | 32   | 30  | 37   | 47                    | 52                    | 60                    | 69 | 74 |
| 0.960  | 3.2                         |                                |   | 33   | 35  | 42   | 54                    | 60                    | 70                    | 77 | 82 |

TABLE III

| Intensity of solar radiation, $\dot{I}$ ( $\text{KJ}/\text{m}^2$ ) | Wind speed, $v_w$ (m/s) | Solar concentration R | Mass flow rate of water, $\dot{m}_w$ (Kg/s) | Ambient temperature $T_a$ ( $^{\circ}\text{C}$ ) | Initial temperature $T_1$ ( $^{\circ}\text{C}$ ) | Temperature of the water in the receiver at the length of |          |          |          |          |          |
|--|-------------------------|-----------------------|---|--|--|---|----------|----------|----------|----------|----------|
|  |                         |                       |   |  |  | 0.20 (m)  | 0.40 (m) | 0.60 (m) | 0.80 (m) | 1.00 (m) | 1.20 (m) |
| 0.350  | 4.0                     | 10                    | 0.002                                       | 41   | 40   | 53  | 62       | 68       | 72       | 75       | 79.5     |
|  | 4.0                     | 10                    | 0.003                                       | 41   | 40   | 50  | 58       | 64       | 68       | 72       | 75       |
|  | 4.1                     |                       | 0.004                                       | 41.5   | 40   | 46  | 54       | 60       | 65       | 68       | 70       |

Intensity of solar radiation,  $I_k$  ( $\text{W}/\text{m}^2$ )

Wind speed,  $V_w$  (m/s)

Solar concentration ratio R

Mass flow rate of water,  $\dot{m}_w$  (kg/s)

Ambient temperature,  $T_a$  ( $^{\circ}\text{C}$ )

Initial temperature,  $T_i$  ( $^{\circ}\text{C}$ )

Temperature of the water in the receiver at the length of 0.20 (m), 0.40 (m), 0.60 (m), 0.80 (m), 1.00 (m), 1.20 (m)

$T_1$  ( $^{\circ}\text{C}$ )    $T_2$  ( $^{\circ}\text{C}$ )    $T_3$  ( $^{\circ}\text{C}$ )    $T_4$  ( $^{\circ}\text{C}$ )    $T_5$  ( $^{\circ}\text{C}$ )    $T_6$  ( $^{\circ}\text{C}$ )

---

|       |     |      |    |    |    |      |    |    |    |
|-------|-----|------|----|----|----|------|----|----|----|
| 0.970 | 3.7 | 41   | 39 | 54 | 65 | 75.5 | 80 | 90 | 94 |
|       | 4.0 | 41.5 | 40 | 50 | 60 | 65   | 75 | 80 | 85 |
|       | 4.2 | 42   | 41 | 45 | 55 | 60   | 65 | 74 | 79 |

---

## 5.5 THE LIST OF THE FIGURE CAPTIONS:

- Fig.5.1 : Schematic diagram of an experimental setup of a concentrator and receiver system.
- Fig.5.2 : Details of the receiver.
- Fig.5.3 : Variation of the temperature of the water along the length of the receiver with solar concentration ratio.
- Fig.5.4 : Variation of the water temperature along the length of the receiver with the intensity of solar radiation.
- Fig.5.5 : Variation of the water temperature along the length of the receiver with the mass flow rate of water.
- Fig.5.6 : Variation of the water temperature along the length of the receiver with the wind speed.
- Fig.5.7 : Comparison between theoretical and experimental results for the variation of the water temperature along the length of the receiver with solar concentration ratio.

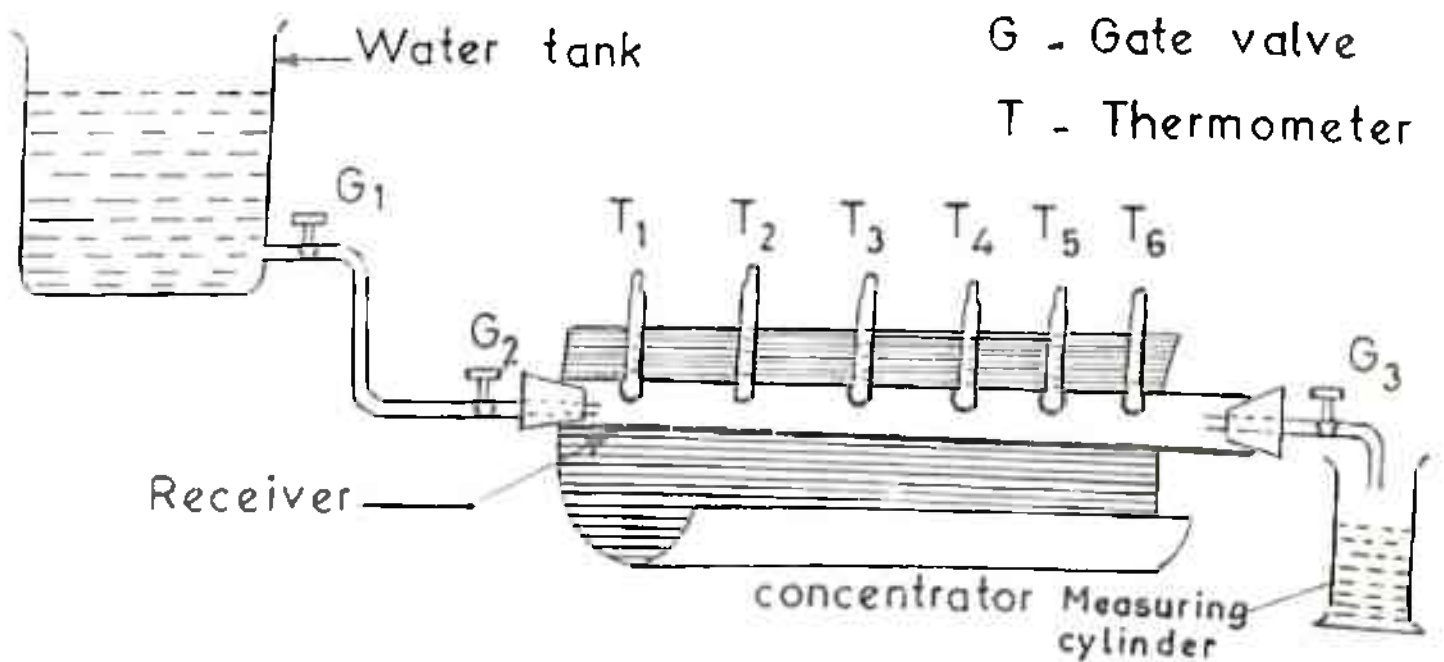


Fig. 5.1 Schematic diagram of an experimental setup of a concentrator and receiver system.

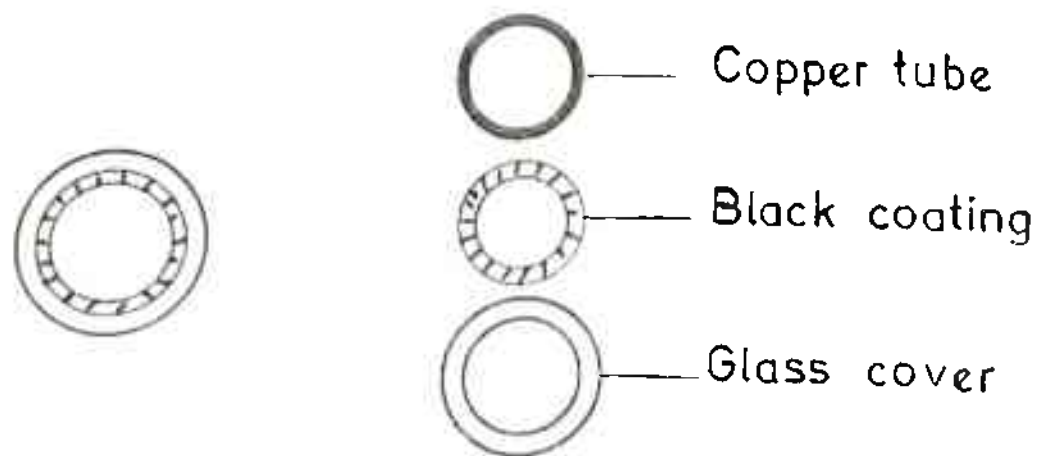
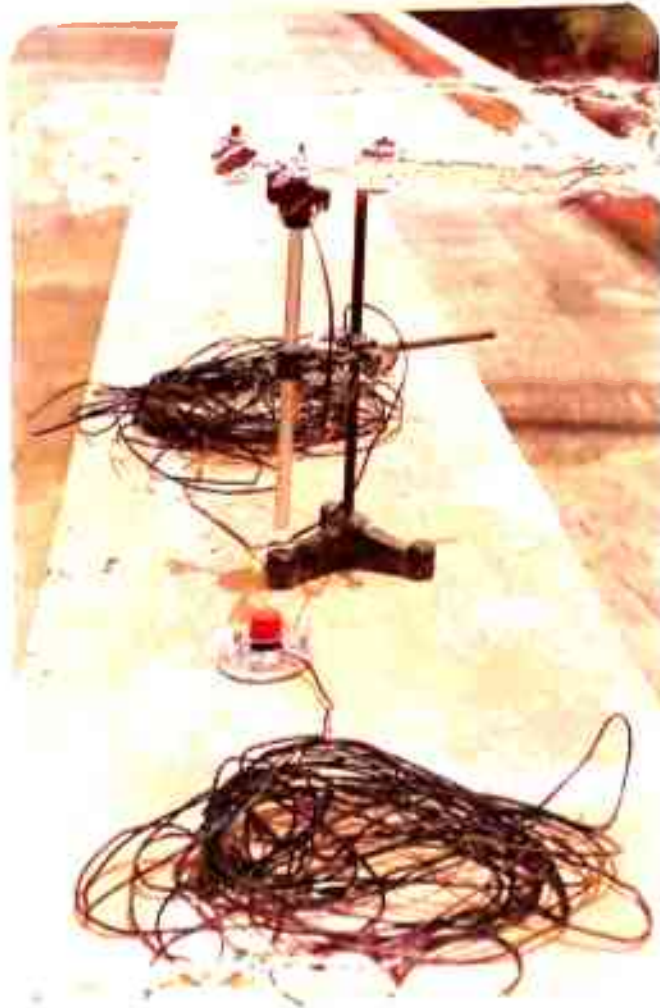


Fig. 5.2 Details of the receiver.









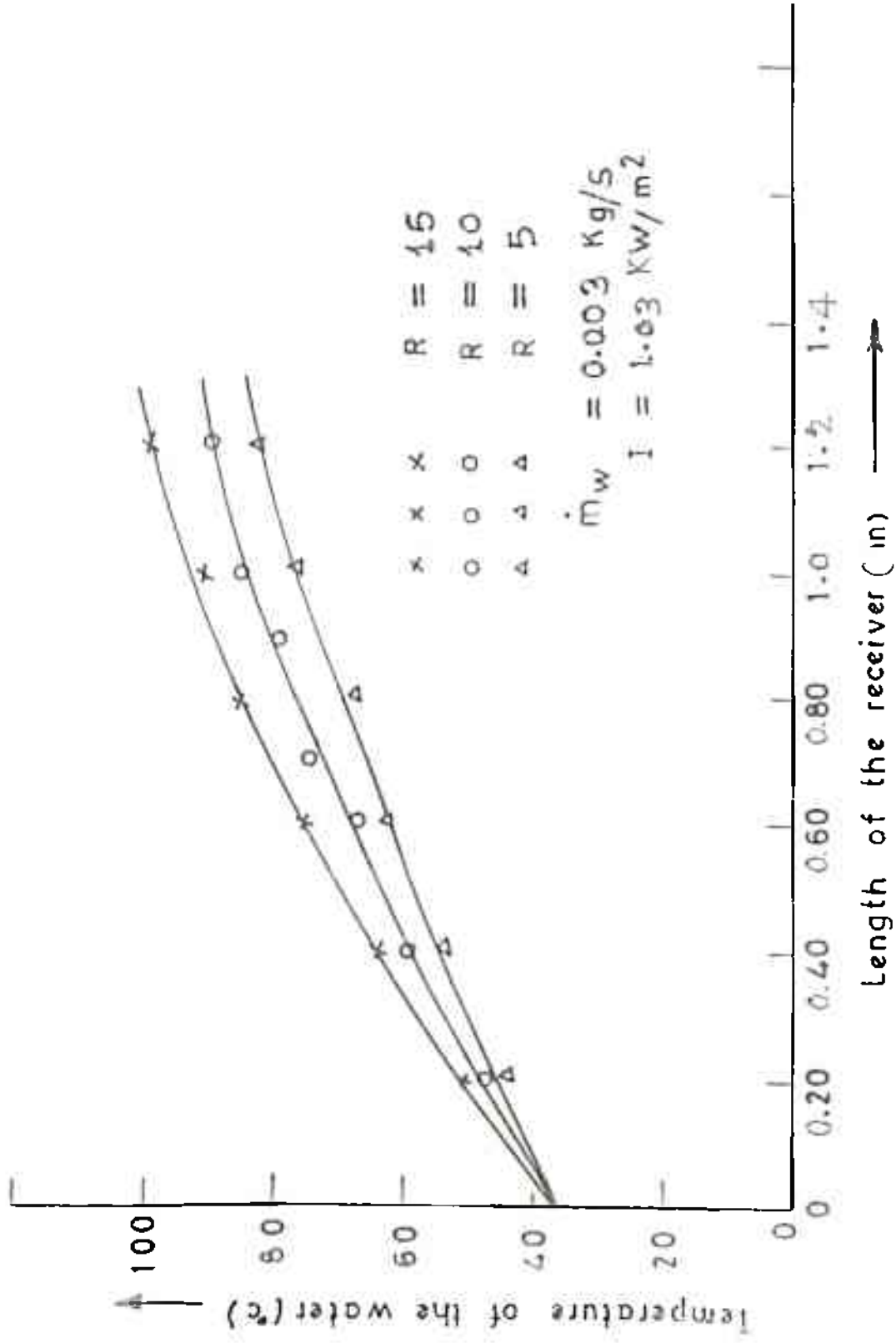


Fig. 5.3 Variation of the temperature of water along the length of the receiver with solar concentration ratio .

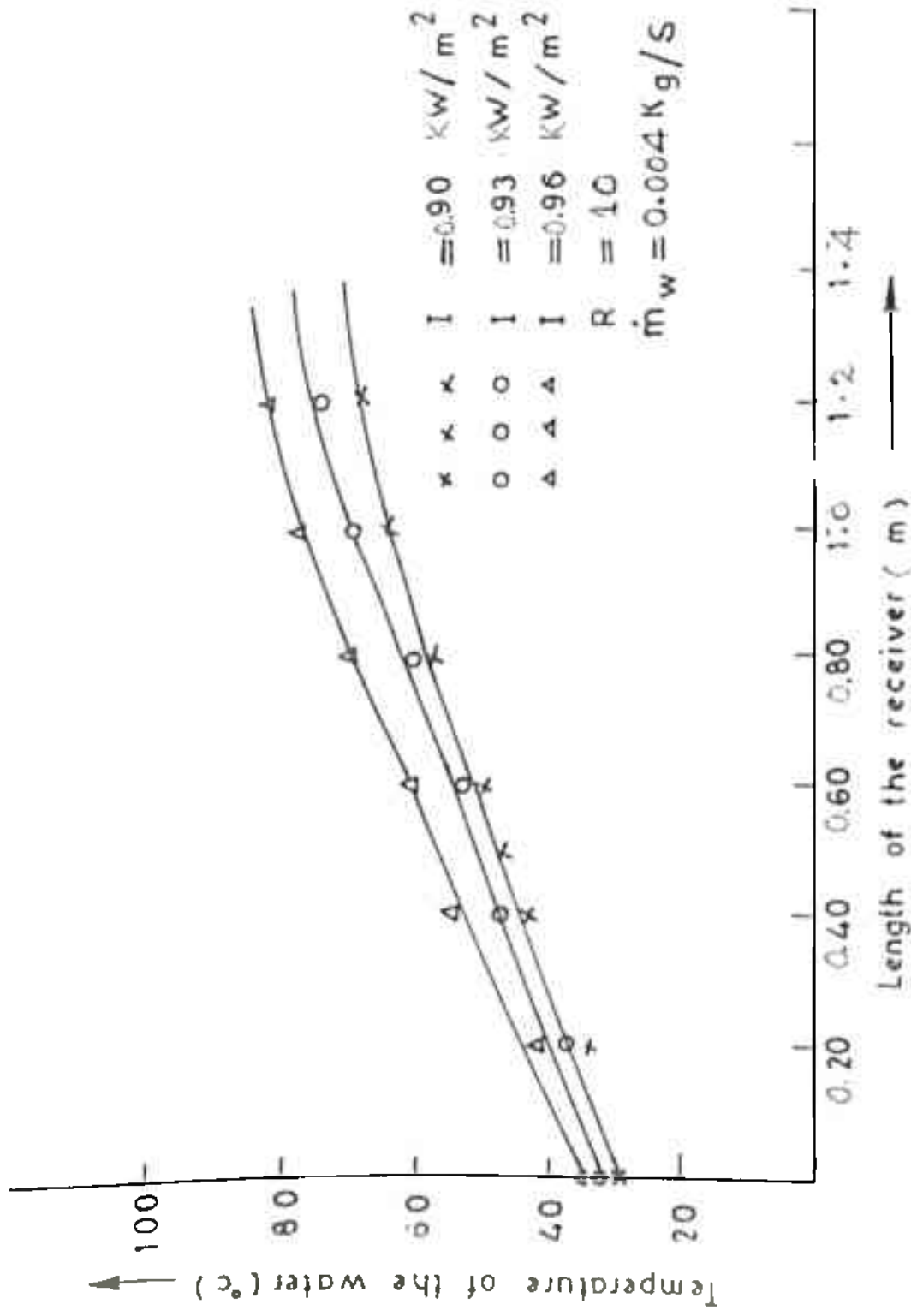


Fig. 5.4 Variation of the temperature at the water along the length of receiver with the intensity of solar radiation

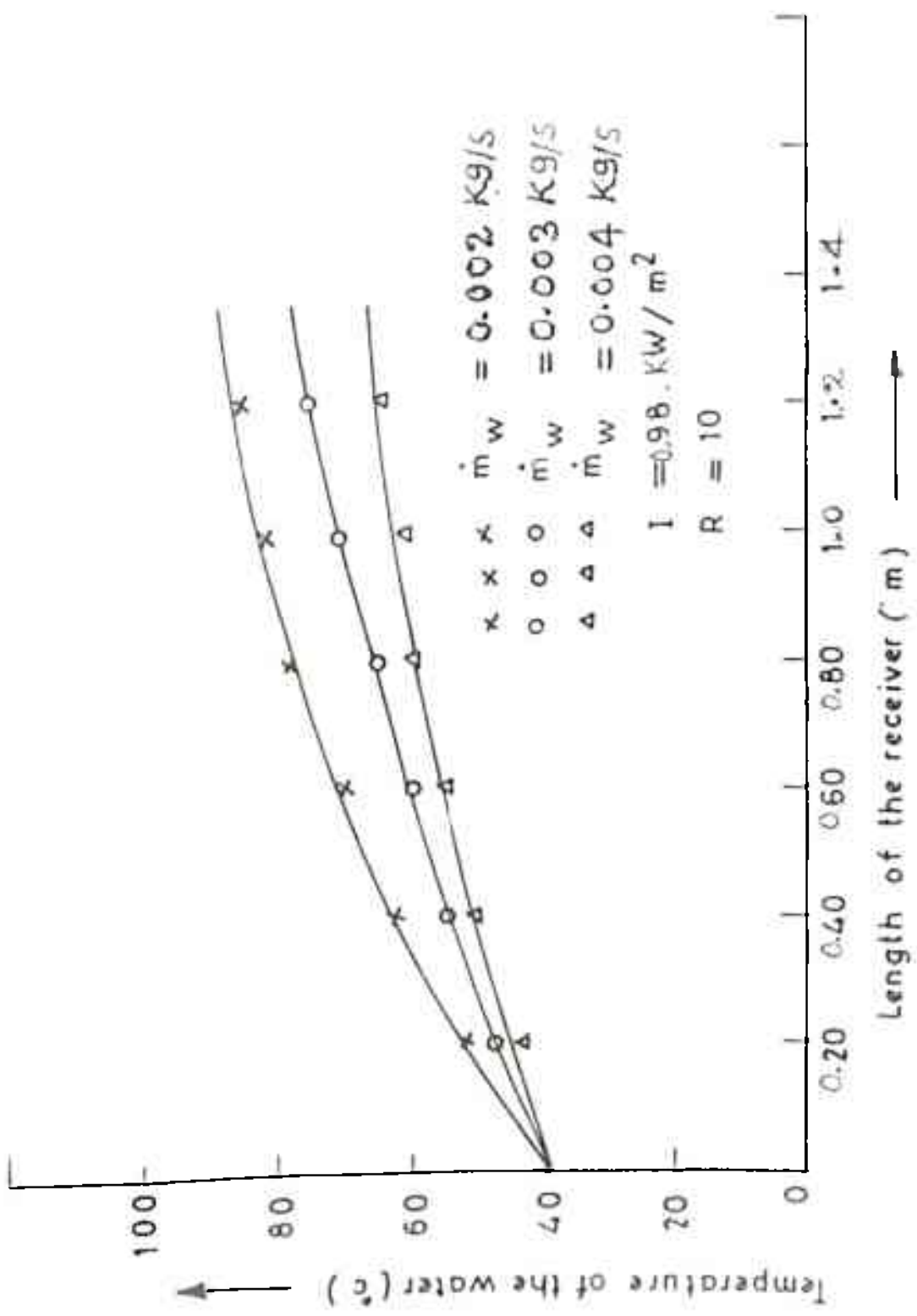


Fig. 5.5 Variation of the temperature along the length of the receiver with mass flow rate of water .

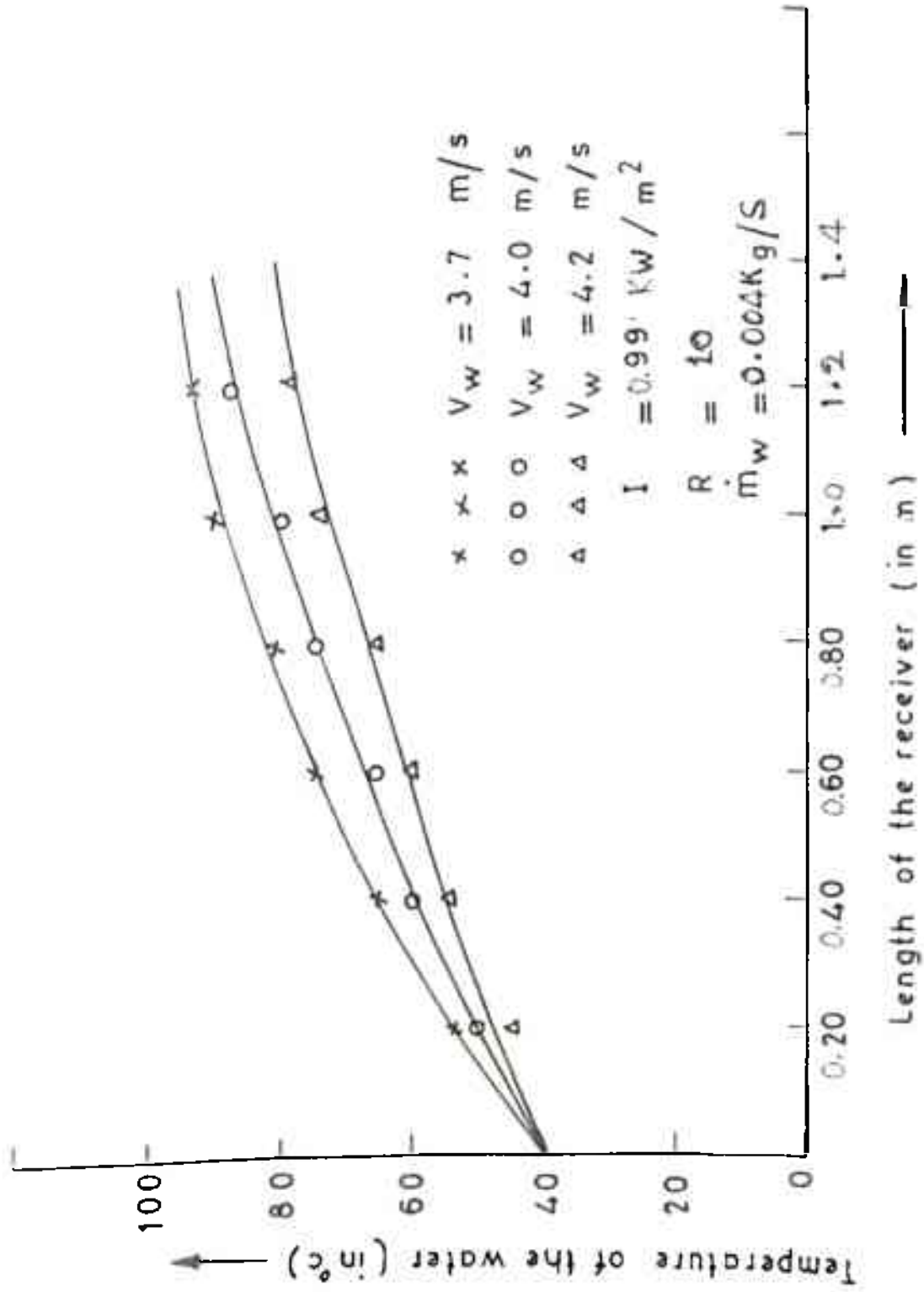


Fig. 5.6 Variation of the temperature of the water along the length of the receiver with the wind speed

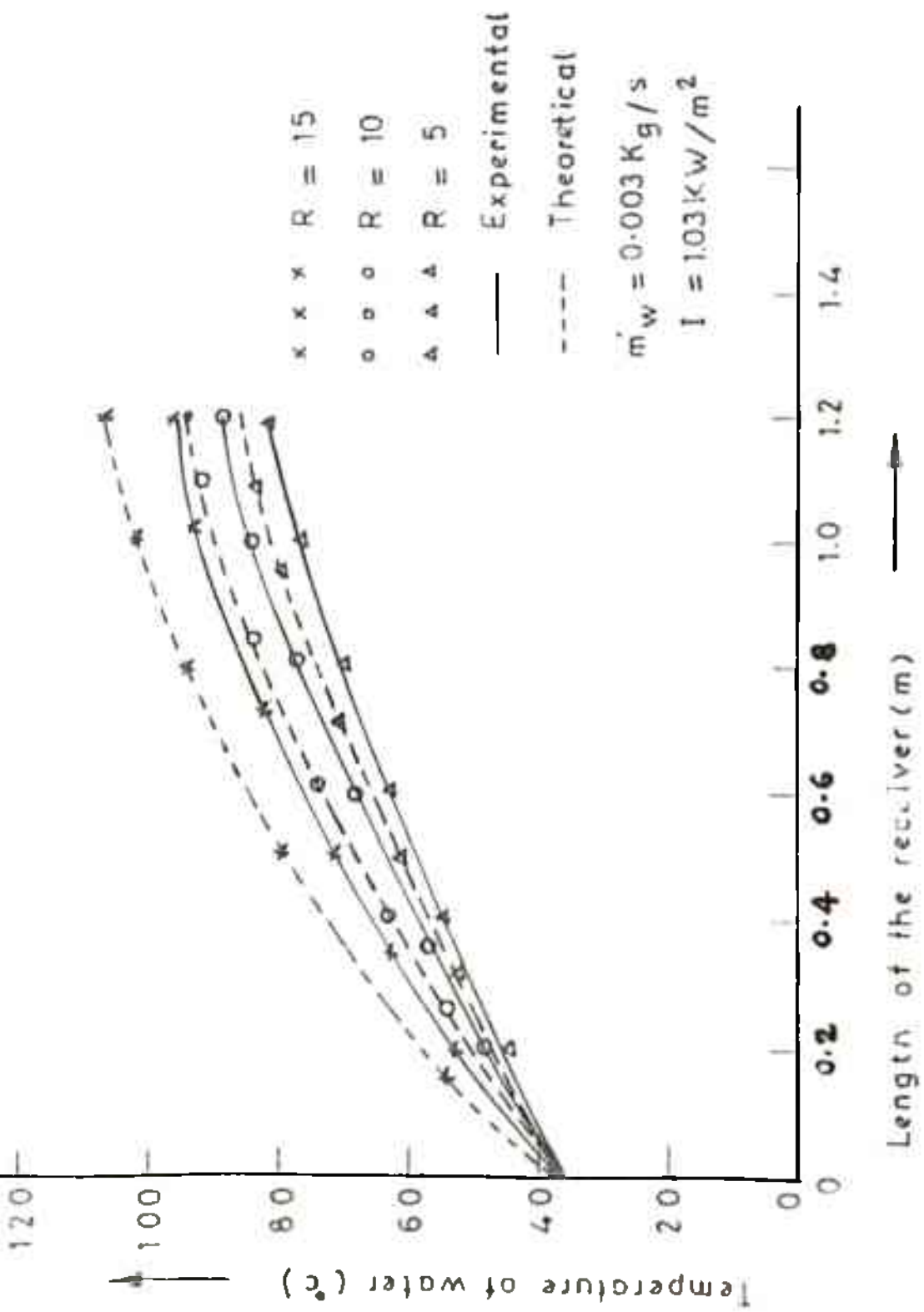


Fig. 5.7 Variation of water temperature along the length of the receiver with solar concentration ratio for theoretical and experimental results.



CHAPTER -VI

Conclusion

## CHAPTER VI : Conclusion

In this thesis, an effort has been made to present the results of the studies on the linear solar concentrator - receiver systems and its applications in electrical power generating system and irrigational water pumping system. It should, however, be mentioned that though for the last two decades or so several efforts have been made to design and implement solar water pumping system and solar energy based electric power systems but, there is hardly any literature available that describe as to how to design a solar concentrator-receiver system which could deliver specified input power to the the pumps or electric generator.

In the second chapter of this thesis, an analysis has been presented to study the input - output behaviour of the concentrator - receiver system. In this analysis, it has been assumed that concentrator which is used for the collection of solar radiation belongs to the class of linear concentrators and also are fully tracked. On the basis of the analysis, expressions for the temperature of water along the length of the receiver as functions of mass flow rate of water and intensity of solar radiation has been obtained. As expected, with the increase in the concentration factor the output temperature of the steam increases with the increase in the concentration ratio if one keeps flow rate constant. But, if one increases the flow rate while maintaining the concentration factor at the same level as described above, the temperature of the steam goes down. According to an interesting study, it has been found that if one maintains the steam temperature and pressure at certain desired level, then the requirement of the length of the receiver changes inversely with the change

in the concentration factor. In other words, if one increases concentration factor and maintain the output at the same level then the requirement of the length of the receiver is decreased. This, however, is achieved at certain cost. That is, the decrease in the length of the receiver leads to an increase in the requirements of the reflecting or refracting surface of the linear concentrator. It should, however, be emphasized here that using the analytical expressions presented in this thesis, one can easily arrive at an optimized length of the receiver taking into account the price rate of the material of both the concentrator as well as the receiver.

The results presented in chapters 3 and 4 are essentially based on the analysis presented in the second chapter where the concentrator-receiver, in fact, act as the input device to the electric power system and the irrigational pumping system respectively.

In the chapter five, results of the experiments conducted on a prototype linear solar concentrator-receiver system have been presented and discussed. These results to a great extent conform to the theoretical results presented in Chapter 2. It must, however, be pointed out that the experimental setup used for conducting experiments were made locally and hence, there may be certain amount of error in the results.

The analytical results obtained for the solar steam generating system and other combined systems, such as solar thermal electric power generating system and solar steam generator coupled to a water lifting system for irrigation, are based on the -

mathematical models obtained by making some assumptions. Actual results can be obtained by performing some experiments on the above systems. For this the experimental setups for the above systems are required to be designed. The above models are applicable for the low capacity systems. For higher capacity systems, some modifications are required. The experimental setup for the solar concentrator-receiver system has been fabricated using locally available materials. It has been tracked manually when the experiments were performed. Arrangement for natural circulation of water through the receiver has been made. A low capacity pump may be used for force circulation. The performance of the above system may be improved by using automatic tracking system and proper arrangement to reduce heat loss from the surface of the receiver.

Finally, it must be mentioned that the analysis and the results presented are only applicable to linear solar concentrator-receiver system and to arrive at an optimized design, some other concentrator-receiver configurations have to be studied in terms of their efficiency, fabrication cost, aspects related to their operation and maintenance, etc.

## R E F E R E N C E S

1. Moustaf S., Hoefler W., Mansy H. E., Hoppman H., Jarrar D. and Zewen H., Design specification and application of a 100 KWe ( 700 Kwth.) co-generation solar power plant, Solar Energy: 32(2), 263 - 269 (1984).
2. Hoefler W., Design specification and application of a 100 KW co-generation solar power plant, Solar Energy: 32, 263 ( 1984 ).
3. Tanka T., Solar thermal electric power system in Japan, Solar Energy: 25, 97 -104 ( 1980 ).
4. Vojdani S., Woolham V. J., Solar Thermal electric power plants for Iran, Solar Energy: 22, 205 -210 ( 1979 ).
5. Pytlinski J. T., Solar Energy installations for pumping irrigation water, Solar Energy: 28 (2), 67( 1982 ).
6. Bahadori M. N., Solar water pumping, Solar Energy: 21, 307 - 316 ( 1978 ).
7. Rabl A., Comparison on solar concentrator, Solar Energy: 18, 93 - 111 ( 1976 ).
8. Willis W. S. and Duff W. S., Solar thermal electric power system; Comparison of line focus collector, Solar Energy: 22, 49 - 61 ( 1978 ).
9. Jafee L. D., Test results on Parabolic Dish concentrators for solar power system, Solar Energy: 42(2 ); 173 -187 (1989 ).
10. Hsieh C. K., Thermal analysis of a compound parabolic concentrating collectors, Solar Energy: 27, 19 -29 ( 1981 ).

11. Kritchman E. M., Friesem A. A., and Yekutieli G.; Efficient Fresnel lens for solar collectors, Solar Energy: 22, 119 - 123 ( 1979 ).
12. Nelson D. T., Evans D. L., and Bansal R. K.; Linear Fresnel lens concentrators, Solar Energy: 17 , 285 - 289 ( 1975 ).
13. Sakurai T., Theoretical concentration of solar radiation by central receiver system, Solar Energy: 31.(3 ), 261 -270 ( 1983 ).
14. Lippe F. W., and Van-hull L. L., A cellwise method for the Optimization of large central receiver system, Solar Energy 2, 505 -516 ( 1978 ).
15. Sobin A., Wagner W. and Easton C. R., Central collector solar energy receivers, Solar Energy: 18, 21 - 30 ( 1976 ).
16. Gerwin H. L., A minimized low cost Heliostat system, Solar Energy: 36(1), 3 -9 ( 1986 ).
17. Rabl A.; Tower reflector for solar power plant, Solar Energy: 18, 269 - 271 ( 1976 ).
18. Heiti R. V. and Thodes G., An experimental parabolic cylindrical concentrator: Its construction and thermal performance, Solar Energy: 30 (5), 483 - 485 ( 1983 ).
19. Cachorro V.E. and Casanova J. L., Optical efficiency of a semistatic cylindrical parabolic concentrator, Solar Energy: 36 (2), 147 - 149 ( 1986 ).

20. Singh S. N., Mathur S. S. and Singhal A. K., Optical performance of a composite parabolic concentrator, Applied Energy: 6 (1980 ).
21. Kandpal T. C., Mathur S. S., and Singhal A. K., Optical performance of a composite parabolic trough, Applied Energy: 19 ( 1985 ).
22. Rapp Donald, Solar Energy, Prentice Hall of Inc., London, New Delhi, Sydney ( 1981 ).
23. James A. Harris and Terry G. Lenz, Thermal performance of a solar concentrator / cavity receiver system, Solar Energy: 34 (2), 135 - 142 ( 1985 );
24. Francis S. G., Pilot plant of solar steam generating stations, Solar Energy: 12(2) , (1968 -69).
25. Roy A., Non-linear dynamic model of a solar steam generator Solar Energy: 26, 297 -306 ( 1981 ).
26. Pargi F., Dynamic analysis and control of a solar power plant, Solar Energy: 28, 105 .( 1982 );
27. Monstrap S. M. A., Operation strategies for Kuwait's 100 KW solar power plant, Solar Energy : 28, 105 ( 1982 );
28. Hollman J. P., Heat transfer ( 1988 ): MCGRAW-HILL BOOK COMPANY, LONDON, NEW DELHI
29. Rao D.P. and Rao K.S., Solar water pump for lift irrigation, Solar Energy: 18, 405 -411 ( 1976 ).
30. Hicks and Edwards, Pump application Engineering, McGraw Hill Book Company, Newyork, London ( 1971 );
31. Peters Max. S. and Timmerhaus K. D., Plant Design and Economics for Chemical Engineers, 2nd Edition, McGraw Hill Ltd. (1971).

32. Sayigh A.A.M, Renewable Energy: Technology and Environment, Vol.2, PP 944-948, Pergamon Press, New York (1992).
33. Bansal, N. K., New Dimensions in Renewable Energy, Tata McGraw Hill Publishing Company Limited, New Delhi (1992).
34. Singhal, A.K and Philip, S.K., Installation and Start up of a Multipurpose 5KW Solar Thermal Power Generation system, Journal of Solar Energy Society of India (SESI), PP.9-18 (1987).
35. Khan, K.A and Khan, A.J., Performance Evaluation Study of a Linear Solar Concentrator with Reverse Flat-Plate Absorber, Proc. of the 2nd World Renewable Energy Congress, Reading, U.K., PP.858-861(1992).
36. Petrenko V.A. and Goubano, V.A., An Autonomous Combined Solar System for Heating, Cooling and Water supply, Proc. of the 2nd World Renewable Energy Congress, Reading, U.K. PP. 1175 - 1179 (1992).



## LIST OF THE PUBLICATIONS

1. Mandal N.K. and Sharan S.N., 'Analysis of a steam generating system, using linear solar concentrator for generation of electrical power', Renewable Energy : Technology and the Environment (U.K.) Vol. 3, PP 944 - 948 (1992).
2. Mandal N.K. and Sharan S.N., 'Analysis of a steam generating system, using linear solar concentrator', Proc. National Solar Energy convention, New Delhi, PP ST-29 (1992).
3. Mandal N.K. and Sharan S.N., ' Analysis of a solar steam generating system using linear solar concentrator', International Journal of Energy, USA (1993) (in press).
4. Mandal N.K. and Mandal T., 'Analysis of a combined system, consisting of a solar steam generator and a water pumping system for irrigation', Proc. of ISES Solar world congress, Hungary (1993) (in press).
5. Mandal N.K., Mandal T. and Rao V.S., 'Solar steam heating of biomass before gasification: An analysis, 'New dimensions in solar energy, PP 411 - 416 (1992).
6. Mandal N.K. and Mandal T., 'Role of some Non-Conventional energy systems in environmental pollution control,' Proc. Ninth National Convention of Environmental Engineers, Jaipur, PP 46 - 52 (1992).

7. Mandal N.K. and Mandal T., 'Solar steam drying of pulp in paper industry: An analysis', Proc. Ninth National Convention of Mechanical Engineers on 'Alternative Energy Resources', IIT, Kanpur (1993) (in press).
  
8. Mandal N.K., ' Design and performance testing of a concentrator - receiver system', Proc. National Solar Energy Convention, Gujrat (1993) (in press).

APPENDIX  
-----

A.1: Evaluation of overall heat transfer coefficient (U):

To evaluate the over all heat transfer coefficient, let us consider, the receiver as shown in the Fig.A1. Let us assume that the temperature of the working fluid is  $T_w$  and the surface temperature is  $T_s$ , then, the heat transfer can be expressed as

$$T_s = T_w$$

$$q = \frac{1}{\frac{1}{h_w A_i} + \frac{\ln(r_o/r_i)}{2\pi KL}} \quad (2.22)$$

If 'U' is taken as over all heat transfer coefficient, then the heat transfer can be expressed as

$$q = U A_o (T_s - T_w) \quad (2.23)$$

From equation (2.3) and (2.4), we get,

$$U = \frac{1}{\frac{A_o}{A_i h_w} + \frac{A_o \ln(r_o/r_i)}{2\pi KL}} \quad (2.23)$$

Where,  $h_w$  = Convective heat transfer coefficient from the inner surface of the receiver to the water  
 $(\text{KW/m}^2 \text{ } ^\circ\text{C})$

$K$  = Thermal conductivity of receiver material  
 $(\text{KW/m } ^\circ\text{C})$

$r_i$  = Inner radius of the receiver (m)

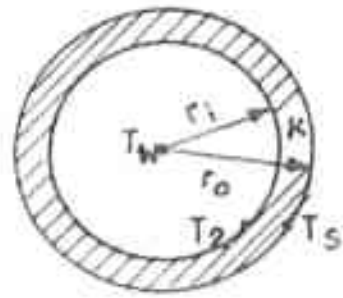
$r_o$  = Outer radius of the receiver (m)

$A_o$  = Outer surface area of the receiver ( $m^2$ )

$A_i$  = Inner surface area of the receiver ( $m^2$ ).

A2 : Linearized heat transfer coefficient for convection and radiation.

Heat flow from the surface of the receiver to glass and from glass to ambient has two terms- one being linear in a temperature difference and other depending on the fourth powers of temperature. The surface of the receiver is uniformly heated (illuminated) for a particular value of intensity of solar radiation. If the total heat flow is plotted VS. temperature difference as shown in Fig. A2, it is found that the heat flow rate is sum of linear and curve functions. A linear function may be made to approximate the total heat flow curve. Thus one can approximate the function by linear term  $C(T_1 - T_2)$  at equilibrium condition, where C is the linearized heat transfer coefficient for convection and radiation expressed as  $C = h_a + h_r$



$$\frac{A_o}{h_w A_i} \quad \frac{A_o \ln(r_o/r_i)}{2 \pi K L} \quad T_w \quad T_2 \quad T_s$$

Fig. A1 : Overall heat flow through a pipe

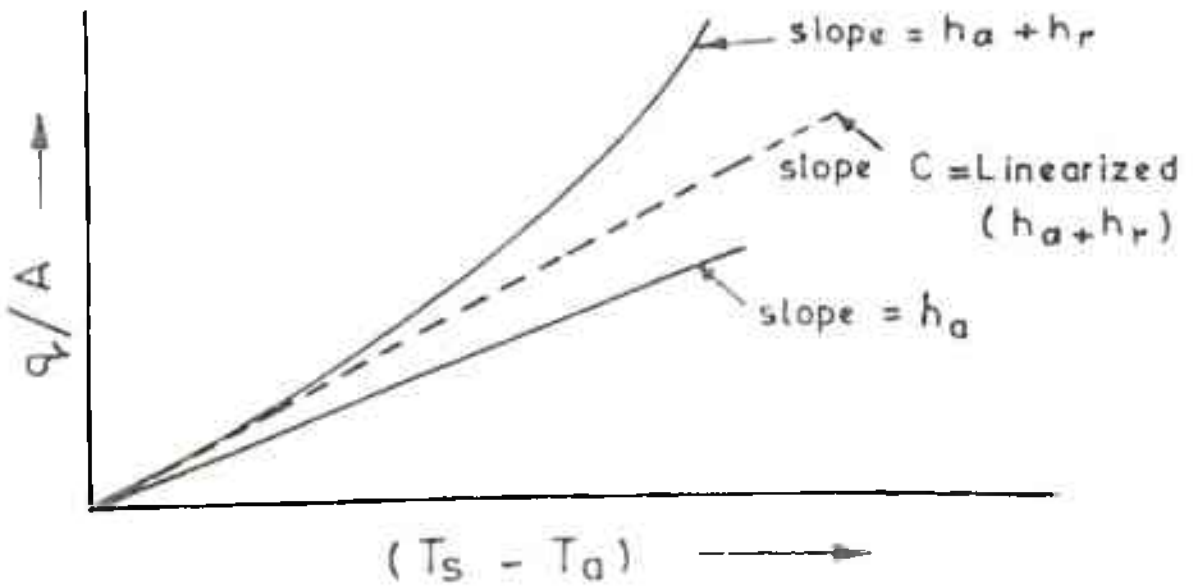


Fig. A2 : Linearized heat transfer coefficient for convection and radiation

A3 : Computer Programming and results for the Chapters  
II - V.





1. 计算  $\int_0^1 x^2 dx$  的近似值，取  $n=10$ ， $\epsilon=0.001$ 。  
 2. 计算  $\int_0^1 \sin(x) dx$  的近似值，取  $n=10$ ， $\epsilon=0.001$ 。  
 3. 计算  $\int_0^1 e^{-x} dx$  的近似值，取  $n=10$ ， $\epsilon=0.001$ 。

| 函数        | 积分值      | 误差     |
|-----------|----------|--------|
| $x^2$     | 0.333333 | 0.0001 |
| $\sin(x)$ | 0.785398 | 0.0001 |
| $e^{-x}$  | 0.718282 | 0.0001 |

For  $i = 100$ ,  $r = 10$ ,  $m = 0.001$ ,  $x_1 = 1.06$ ,  $x_2 = 3.42$ ,  $y_1 = 0.30$ ,  $x = 4.78$   
 For  $i = 500$ ,  $r = 20$ ,  $m = 0.001$ ,  $x_1 = 0.50$ ,  $x_2 = 1.50$ ,  $x_3 = 0.92$ ,  $x = 2.44$   
 For  $i = 1000$ ,  $r = 30$ ,  $m = 0.001$ ,  $x_1 = 0.30$ ,  $x_2 = 1.34$ ,  $y_1 = 0.04$ ,  $x = 1.67$

```

#include <stdio.h>
#define pi 3.1415926535
#include <math.h>
main()

double x=1,r=0.05,c=10,u=5.73,if[3],n=0.8,r[10],ta=52,ti=30,tb=193.4;
double tv=290,hg=2789000,hl=822600,cs=1199;
double num,den,cw=4180;
int k, d;
double val1,val2;
FILE *fp;
float vid,vin,v2d,v2n,mtn,mtd;
fp=fopen("proj.dat","w");
for(k=0;k<9;k++)
    r[k]=10+10*k;
for(k=0;k<2;k++)
    i[k]=500+200*k;
for(k=0;k<2;l++){
    for(d=0;d<=7;d++){
        vid = i[k] * n * r[d] + c * ( ta - tb ) ;
        vin = i[k] * n * r[d] + c * ( ta - ti ) ;
        v2n = i[k] * n * r[d] + c * ( ta - tv ) ;
        v2d = i[k] * n * r[d] + c * ( ta - tv ) ;
        val1 = ( double ) ( vin / vid ) ;
        val2 = ( double ) ( v2n / v2d ) ;
        printf ( "val1 = %ld and val2 = %ld \n" , val1 , val2 ) ;*/
        mtn = c * ( hg - hl ) ;
        mtd = i[l] * n * r[d] + c * ( tb - ta ) ;
        printf("vid= %f vin= %f v2n= %f\n",vid,vin,v2n);
        printf("v2d= %f mtn= %f mtd= %f\n",v2d,mtn,mtd);
        den = ( 1/c + 1/u ) * ( cw * log ( val1 ) + mtn/mtd + cs * log ( val2 ) ) ;
        num = 2 * pi * r0 * x ;
        fprintf(fp,"%f is m for r = %f and i = %f \n", num/den,r[d],i[k]);
    }
}
fclose(fp);

```



The first part of the document discusses the general principles of the system, including the role of the control unit and the various components involved in the process. It mentions that the system is designed to be flexible and adaptable to different operating conditions.

The second part of the document provides a detailed description of the hardware and software components. It lists the various modules and their functions, as well as the software routines that control the system's operation. This section is crucial for understanding the technical details of the system.

The third part of the document describes the experimental setup and the results of the tests. It includes data tables and graphs that show the system's performance under various conditions. The results indicate that the system is capable of operating efficiently and reliably over a wide range of parameters.

The fourth part of the document discusses the future work and the potential applications of the system. It mentions that further research is needed to optimize the system's performance and to explore new applications in different fields. The authors express their confidence that the system will have a significant impact on the industry.

The fifth part of the document is a conclusion that summarizes the main findings of the study. It reiterates the key points of the document and emphasizes the importance of the system's design and implementation. The authors thank the funding agencies and the colleagues who assisted them during the project.

The sixth part of the document is a list of references that cites the works of other researchers in the field. This list provides a comprehensive overview of the current state of the art and identifies the sources of the information used in the document.

The seventh part of the document is an appendix that contains additional information that is not included in the main text. This may include detailed diagrams, tables of data, or other technical details that are relevant to the system's operation.

\*\*\*\*\*FDR I = 600 W/eq.m \*\*\*\*\*

FOR R = 10

THE MASS FLOW RATE IS: 0.000119 Kg/second  
X1 = 0.341328 metres, X2 = 0.400136 metres, X3 = 0.260703 metres  
A1 = 0.152505 , A3 = 0.532112 , P = 5375.000000  
ALPHA = 0.000493 BETA = 2420.659930  
MECHANICAL POWER OUTPUT Pm = 517.88800  
ELECTRICAL POWER OUTPUT Pe = 466.09920 Watts  
CAPACITY OF THE PUMP Cp = 0.112417 cubic m/second  
Length = 0.001228 metres  
Height = 0.368549 metres

\*\*\*\*\*next\*\*\*\*\*

FOR R = 20

THE MASS FLOW RATE IS: 0.000290 Kg/second  
X1 = 0.727300 metres, X2 = 0.600870 metres, X3 = 0.076517 metres  
A1 = 0.062580 , A3 = 0.218349 , P = 10176.000000  
ALPHA = 0.001201 BETA = 3928.624378  
MECHANICAL POWER OUTPUT Pm = 1262.00000  
ELECTRICAL POWER OUTPUT Pe = 1135.87200 Watts  
CAPACITY OF THE PUMP Cp = 0.112417 cubic m/second  
Length = 0.002991 metres  
Height = 0.898144 metres

\*\*\*\*\*next\*\*\*\*\*

FOR R = 30

THE MASS FLOW RATE IS: 0.000428 Kg/second  
X1 = 0.298505 metres, X2 = 0.640784 metres, X3 = 0.061588 metres  
A1 = 0.042402 , A3 = 0.147947 , P = 14976.000000  
ALPHA = 0.001773 BETA = 5436.588826  
MECHANICAL POWER OUTPUT Pm = 1862.65600  
ELECTRICAL POWER OUTPUT Pe = 1676.39040 Watts  
CAPACITY OF THE PUMP Cp = 0.112417 cubic m/second  
Length = 0.004418 metres  
Height = 1.325537 metres

\*\*\*\*\*next\*\*\*\*\*

FOR R = 40

THE MASS FLOW RATE IS: 0.000562 Kg/second  
X1 = 0.285481 metres, X2 = 0.658698 metres, X3 = 0.055640 metres  
A1 = 0.032292 , A3 = 0.112671 , P = 19776.000000  
ALPHA = 0.002327 BETA = 6944.553274  
MECHANICAL POWER OUTPUT Pm = 2465.82100  
ELECTRICAL POWER OUTPUT Pe = 2201.24150 Watts  
CAPACITY OF THE PUMP Cp = 0.112417 cubic m/second  
Length = 0.005802 metres  
Height = 1.740542 metres

\*\*\*\*\*next\*\*\*\*\*

FOR R = 50

THE MASS FLOW RATE IS: 0.000695 Kg/second  
X1 = 0.277702 metres, X2 = 0.669257 metres, X3 = 0.052454 metres  
A1 = 0.026112 , A3 = 0.091110 , P = 24776.000000  
ALPHA = 0.002878 BETA = 8452.517722  
MECHANICAL POWER OUTPUT Pm = 3024.64000  
ELECTRICAL POWER OUTPUT Pe = 2722.17000 Watts  
CAPACITY OF THE PUMP Cp = 0.112417 cubic m/second  
Length = 0.007175 metres  
Height = 2.152449 metres

\*\*\*\*\*next\*\*\*\*\*

FOR R = 60

THE MASS FLOW RATE IS: 0.000828 Kg/second  
X1 = 0.272690 metres, X2 = 0.676619 metres, X3 = 0.050495 metres  
A1 = 0.021918 , A3 = 0.075475 , P = 29376.000000  
ALPHA = 0.003429 BETA = 9960.482170  
MECHANICAL POWER OUTPUT Pm = 3603.45600  
ELECTRICAL POWER OUTPUT Pe = 3243.11110 Watts  
CAPACITY OF THE PUMP Cp = 0.112417 cubic m/second  
Length = 0.008548 metres  
Height = 2.564157 metres

\*\*\*\*\*LINE\*\*\*\*\*

FOR R = 70

THE MASS FLOW RATE IS: 0.000961 Kg/second  
X1 = 0.269190 metres, X2 = 0.652045 metres,  
A1 = 0.018285 , A3 = 0.065891 , P = 3476.000000  
ALPHA = 0.003900 BETA = 11469.443618  
MECHANICAL POWER OUTPUT Pm = 4182.27200  
ELECTRICAL POWER OUTPUT Pe = 3764.4480 Watts  
CAPACITY OF THE PUMP Cp = 0.112417 cubic m/second  
Length = 0.009921 metres  
Height = 2.976265 metres

X3 = 0.048169 metres

FOR R = 80

THE MASS FLOW RATE IS: 0.001093 Kg/second  
X1 = 0.266364 metres, X2 = 0.685592 metres,  
A1 = 0.016604 , A3 = 0.057934 , P = 3976.000000  
ALPHA = 0.004527 BETA = 12976.411066  
MECHANICAL POWER OUTPUT Pm = 4756.73600  
ELECTRICAL POWER OUTPUT Pe = 4281.06240 Watts  
CAPACITY OF THE PUMP Cp = 0.112417 cubic m/second  
Length = 0.011294 metres  
Height = 3.385075 metres

X3 = 0.048166 metres

THE MASS FLOW RATE IS: 0.001225 Kg/second

X1 = 0.264193 metres, X2 = 0.688383 metres,  
A1 = 0.014815 , A3 = 0.051691 , P = 4376.000000  
ALPHA = 0.005073 BETA = 14484.375514  
MECHANICAL POWER OUTPUT Pm = 5331.20000  
ELECTRICAL POWER OUTPUT Pe = 4798.08000 Watts  
CAPACITY OF THE PUMP Cp = 0.112417 cubic m/second  
Length = 0.012646 metres  
Height = 3.793886 metres

X3 = 0.047409 metres

FOR R = 100

THE MASS FLOW RATE IS: 0.001357 Kg/second  
X1 = 0.242472 metres, X2 = 0.690656 metres,  
A1 = 0.013374 , A3 = 0.046663 , P = 4876.000000  
ALPHA = 0.005620 BETA = 15992.339962  
MECHANICAL POWER OUTPUT Pm = 5905.66400  
ELECTRICAL POWER OUTPUT Pe = 5315.09760 Watts  
CAPACITY OF THE PUMP Cp = 0.112417 cubic m/second  
Length = 0.014009 metres  
Height = 4.202496 metres

X3 = 0.046816 metres

\*\*\*\*\*next\*\*\*\*\*

\*\*\*\*\*FOR I = 500 W/m \*\*\*\*\*

FOR R = 10

THE MASS FLOW RATE IS: 0.000170 Kg/second  
X1 = 0.355184 metres, X2 = 0.529020 metres,  
A1 = 0.093516 , A3 = 0.333270 , P = 5976.000000  
ALPHA = 0.000787 BETA = 2923.314745  
MECHANICAL POWER OUTPUT Pm = 826.88000  
ELECTRICAL POWER OUTPUT Pe = 744.19200 Watts  
CAPACITY OF THE PUMP Cp = 0.112417 cubic m/second  
Length = 0.001761 metres  
Height = 0.588139 metres

X3 = 0.124000 metres

THE MASS FLOW RATE IS: 0.000302 Kg/second

X1 = 0.304322 metres, X2 = 0.430178 metres,  
A1 = 0.047508 , A3 = 0.165763 , P = 13776.000000  
ALPHA = 0.001582 BETA = 4873.750010  
MECHANICAL POWER OUTPUT Pm = 1662.46400  
ELECTRICAL POWER OUTPUT Pe = 1496.21760 Watts  
CAPACITY OF THE PUMP Cp = 0.112417 cubic m/second  
Length = 0.007045 metres

X3 = 0.124000 metres

Height= 1.183073 metres

FOR R = 30

THE MASS FLOW RATE IS: 0.002540 Kg/second

X1 = 0.295451 metres, X2= 0.658493 metres, X3= 0.055640

A1= 0.032292 ,A3= 0.112671 ,P= 1977.000000

ALPHA= 0.002707 BETA= 8744.000000

MECHANICAL POWER OUTPUT Pm= 2445.82600

ELECTRICAL POWER OUTPUT Pe= 2201.26150

CAPACITY OF THE PUMP Cp= 0.112417 cubic m

Length= 0.005902 metres

Height= 1.740342 metres

\*\*\*\*\*next\*\*\*\*\*

FOR R = 40

THE MASS FLOW RATE IS: 0.002710 Kg/second

X1 = 0.276055 metres, X2= 0.672582 metres, X3= 0.051752

A1= 0.124324 ,A3= 0.085569 ,P= 26176.000000

ALPHA= 0.003065 BETA= 8955.172538

MECHANICAL POWER OUTPUT Pm= 3220.48000

ELECTRICAL POWER OUTPUT Pe= 2898.43200

CAPACITY OF THE PUMP Cp= 0.112417 cubic m

Length= 0.007632 metres

Height= 2.291817 metres

\*\*\*\*\*next\*\*\*\*\*

FOR R = 50

THE MASS FLOW RATE IS: 0.000911 Kg/second

X1 = 0.270034 metres, X2= 0.672307 metres, X3= 0.049522

A1= 0.019317 ,A3= 0.069128 ,P= 32571.000000

ALPHA= 0.003793 BETA= 10965.791802

MECHANICAL POWER OUTPUT Pm= 3986.43200

ELECTRICAL POWER OUTPUT Pe= 3587.78880

CAPACITY OF THE PUMP Cp= 0.112417 cubic m

Length= 0.009456 metres

Height= 2.836897 metres

\*\*\*\*\*next\*\*\*\*\*

FOR R = 60

THE MASS FLOW RATE IS: 0.001093 Kg/second

X1 = 0.266364 metres, X2= 0.685582 metres, X3= 0.048166

A1= 0.016604 ,A3= 0.057934 ,P= 38976.000000

ALPHA= 0.004527 BETA= 12976.411066

MECHANICAL POWER OUTPUT Pm= 4756.73600

ELECTRICAL POWER OUTPUT Pe= 4201.52400

CAPACITY OF THE PUMP Cp= 0.112417 cubic m

Length= 0.011284 metres

Height= 3.385075 metres

\*\*\*\*\*next\*\*\*\*\*

FOR R = 70

THE MASS FLOW RATE IS: 0.001217 Kg/second

X1 = 0.265074 metres, X2= 0.688182 metres, X3= 0.047196

A1= 0.014501 ,A3= 0.049899 ,P= 43276.000000

ALPHA= 0.005075 BETA= 14987.000000

MECHANICAL POWER OUTPUT Pm= 5320.6

ELECTRICAL POWER OUTPUT Pe= 4970.61

CAPACITY OF THE PUMP Cp= 0.112417 cubic m

Length= 0.013101 metres

Height= 3.930253 metres

\*\*\*\*\*next\*\*\*\*\*

FOR R = 80

THE MASS FLOW RATE IS: 0.001465 Kg/second

X1 = 0.241510 metres, X2= 0.691282 metres, X3= 0.046487

A1= 0.012559 ,A3= 0.043821 ,P= 51776.000000

ALPHA= 0.005984 BETA= 17007.640000

MECHANICAL POWER OUTPUT Pm= 6060.64

ELECTRICAL POWER OUTPUT Pe= 5659.7300

CAPACITY OF THE PUMP Cp= 0.112417 cubic m

Length= 0.015005 metres

Height= 4.475431 metres

Height= 4.475117 metres  
\*\*\*\*\*next\*\*\*\*\*

IR R = 90

IE MASS FLOW RATE IS: 0.011196 Kg/second  
L = 0.011196 metres, X2 = 0.007905 metres  
PHI = 0.006713 BETA = 1000.000000  
MECHANICAL POWER OUTPUT Pm = 7051.59200  
ELECTRICAL POWER OUTPUT Pe = 2010.13200 Watts  
CAPACITY OF THE PUMP Cp = 0.112417 cubic m/second  
Length = 0.46774 metres  
Height = 5.020317 metres  
\*\*\*\*\*next\*\*\*\*\*

IR R = 100

IE MASS FLOW RATE IS: 0.010099 Kg/second  
L = 0.010099 metres, X2 = 0.007442 metres  
PHI = 0.007442 BETA = 1000.000000  
MECHANICAL POWER OUTPUT Pm = 7820.54400  
ELECTRICAL POWER OUTPUT Pe = 2038.40260 Watts  
CAPACITY OF THE PUMP Cp = 0.112417 cubic m/second  
Length = 0.46774 metres  
Height = 5.020317 metres  
\*\*\*\*\*next\*\*\*\*\*

\*\*\*\*\*next\*\*\*\*\* FOR I = 1000 W/m^2 \*\*\*\*\*next\*\*\*\*\*

IR R = 10

IE MASS FLOW RATE IS: 0.000242 Kg/second  
L = 0.000242 metres, X2 = 0.007442 metres  
PHI = 0.007442 BETA = 3425.269562  
MECHANICAL POWER OUTPUT Pm = 1053.18400  
ELECTRICAL POWER OUTPUT Pe = 947.86540 Watts  
CAPACITY OF THE PUMP Cp = 0.112417 cubic m/second  
Length = 0.002498 metres  
Height = 0.747486 metres  
\*\*\*\*\*next\*\*\*\*\*

X3 = 0.088438

IR R = 20

IE MASS FLOW RATE IS: 0.000473 Kg/second  
L = 0.000473 metres, X2 = 0.007442 metres  
PHI = 0.007442 BETA = 5939.243642  
MECHANICAL POWER OUTPUT Pm = 2058.49600  
ELECTRICAL POWER OUTPUT Pe = 1852.64460 Watts  
CAPACITY OF THE PUMP Cp = 0.112417 cubic m/second  
Length = 0.004883 metres  
Height = 1.464904 metres  
\*\*\*\*\*next\*\*\*\*\*

X3 = 0.059122

IR R = 30

IE MASS FLOW RATE IS: 0.000695 Kg/second  
L = 0.000695 metres, X2 = 0.007442 metres  
PHI = 0.007442 BETA = 8452.517722  
MECHANICAL POWER OUTPUT Pm = 3024.64000  
ELECTRICAL POWER OUTPUT Pe = 2700.07000 Watts  
CAPACITY OF THE PUMP Cp = 0.112417 cubic m/second  
Length = 0.007175 metres  
Height = 2.152404 metres  
\*\*\*\*\*next\*\*\*\*\*

X3 = 0.052054

IR R = 40

IE MASS FLOW RATE IS: 0.000916 Kg/second  
L = 0.000916 metres, X2 = 0.007442 metres  
PHI = 0.007442 BETA = 10265.791200  
MECHANICAL POWER OUTPUT Pm = 3985.43200  
ELECTRICAL POWER OUTPUT Pe = 3567.78880 Watts  
CAPACITY OF THE PUMP Cp = 0.112417 cubic m/second  
Length = 0.009467 metres  
Height = 2.840004 metres  
\*\*\*\*\*next\*\*\*\*\*

X3 = 0.049524



Length = 0 metres

Height = 2.521715 metres

\*\*\*\*\*next\*\*\*\*\*

FOR R = 50

THE MASS FLOW RATE IS: 0.001137 Kg/second

X1 = 0.265580 metres, X2 = 0.686586 metres

X3 = 0.046798 metres

A1 = 0.015961, A3 = 0.055692, P = 40576.000000

ALPHA = 0.004709 BETA = 13479.063985

MECHANICAL POWER OUTPUT Pm = 4948.001

ELECTRICAL POWER OUTPUT Pe = 4453.40120 Watts

CAPACITY OF THE PUMP Cp = 0.112417 cubic m/second

Length = 0.011738 metres

Height = 3.521715 metres

\*\*\*\*\*next\*\*\*\*\*

FOR R = 60

THE MASS FLOW RATE IS: 0.001757 Kg/second

X1 = 0.262472 metres, X2 = 0.690656 metres

X3 = 0.046816 metres

A1 = 0.013374, A3 = 0.046663, P = 48576.000000

ALPHA = 0.005620 BETA = 15992.339962

MECHANICAL POWER OUTPUT Pm = 5905.66400

ELECTRICAL POWER OUTPUT Pe = 5315.09760 Watts

CAPACITY OF THE PUMP Cp = 0.112417 cubic m/second

Length = 0.013007 metres

Height = 4.521715 metres

\*\*\*\*\*next\*\*\*\*\*

FOR R = 70

THE MASS FLOW RATE IS: 0.001577 Kg/second

X1 = 0.261208 metres, X2 = 0.693671 metres

X3 = 0.046070 metres

A1 = 0.011508, A3 = 0.040153, P = 56576.000000

ALPHA = 0.006531 BETA = 18505.614042

MECHANICAL POWER OUTPUT Pm = 6863.10400

ELECTRICAL POWER OUTPUT Pe = 6175.79560 Watts

CAPACITY OF THE PUMP Cp = 0.112417 cubic m/second

Length = 0.016280 metres

Height = 4.894047 metres

\*\*\*\*\*next\*\*\*\*\*

FOR R = 80

THE MASS FLOW RATE IS: 0.001777 Kg/second

X1 = 0.258653 metres, X2 = 0.695877 metres

X3 = 0.045822 metres

A1 = 0.010099, A3 = 0.035237, P = 64576.000000

ALPHA = 0.007442 BETA = 21018.989122

MECHANICAL POWER OUTPUT Pm = 7820.54400

ELECTRICAL POWER OUTPUT Pe = 7038.48560 Watts

CAPACITY OF THE PUMP Cp = 0.112417 cubic m/second

Length = 0.018551 metres

Height = 5.565398 metres

\*\*\*\*\*next\*\*\*\*\*

FOR R = 90

THE MASS FLOW RATE IS: 0.002017 Kg/second

X1 = 0.257374 metres, X2 = 0.697651 metres

X3 = 0.045104 metres

A1 = 0.008790, A3 = 0.031071, P = 72576.000000

ALPHA = 0.008303 BETA = 23532.162202

MECHANICAL POWER OUTPUT Pm = 8777.98400

ELECTRICAL POWER OUTPUT Pe = 7900.18560 Watts

CAPACITY OF THE PUMP Cp = 0.112417 cubic m/second

Length = 0.020822 metres

Height = 6.245749 metres

\*\*\*\*\*next\*\*\*\*\*

FOR R = 100

THE MASS FLOW RATE IS: 0.002203 Kg/second

X1 = 0.256279 metres, X2 = 0.699770 metres

X3 = 0.044707 metres

A1 = 0.008110, A3 = 0.028319, P = 80576.000000

ALPHA = 0.009260 BETA = 26045.436282

MECHANICAL POWER OUTPUT Pm = 9731.07400

ELECTRICAL POWER OUTPUT Pe = 8757.96480 Watts

CAPACITY OF THE PUMP Cp = 0.112417 cubic m/second

1000  
1000  
1000



#####

#####

Tue Sep 14 12:19:17 IST 1993

#####

file printed below is -> /final/usr0777/z

|   |
|---|
| For I = 1030 , R = 5 , c = 18 , x = 0.20 , t = 45.210   |
| For I = 1030 , R = 10 , c = 18 , x = 0.20 , t = 51.251  |
| For I = 1030 , R = 15 , c = 18 , x = 0.20 , t = 59.041  |
| For I = 1030 , R = 5 , c = 18 , x = 0.40 , t = 57.547   |
| For I = 1030 , R = 10 , c = 18 , x = 0.40 , t = 64.015  |
| For I = 1030 , R = 15 , c = 18 , x = 0.40 , t = 72.115  |
| For I = 1030 , R = 5 , c = 18 , x = 0.60 , t = 65.153   |
| For I = 1030 , R = 10 , c = 18 , x = 0.60 , t = 73.171  |
| For I = 1030 , R = 15 , c = 18 , x = 0.60 , t = 85.234  |
| For I = 1030 , R = 5 , c = 18 , x = 0.80 , t = 74.022   |
| For I = 1030 , R = 10 , c = 18 , x = 0.80 , t = 82.532  |
| For I = 1030 , R = 15 , c = 18 , x = 0.80 , t = 94.674  |
| For I = 1030 , R = 5 , c = 18 , x = 1.00 , t = 81.155   |
| For I = 1030 , R = 10 , c = 18 , x = 1.00 , t = 90.267  |
| For I = 1030 , R = 15 , c = 18 , x = 1.00 , t = 102.15  |
| For I = 1030 , R = 5 , c = 18 , x = 1.20 , t = 85.114   |
| For I = 1030 , R = 10 , c = 18 , x = 1.20 , t = 94.875  |
| For I = 1030 , R = 15 , c = 18 , x = 1.20 , t = 107.62  |
| For I = 1030 , R = 5 , c = 18 , x = 1.40 , t = 88.021   |
| For I = 1030 , R = 10 , c = 18 , x = 1.40 , t = 97.045  |
| For I = 1030 , R = 15 , c = 18 , x = 1.40 , t = 109.458 |